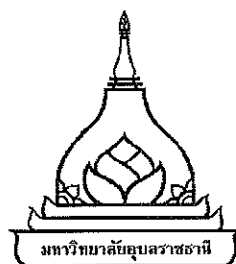


**DEVELOPMENT OF LOW SPEED WATER TURBINE FOR  
GENERATING ELECTRICITY OF 200 WATTS**

**PALAPUM KHUNTHONGJAN**

**A THESIS SUBMITTED IN PARTIAL FULFILLMENT OF THE REQUIREMENTS  
FOR THE DEGREE OF DOCTOR OF PHILOSOPHY  
MAJOR IN MECHANICAL ENGINEERING  
FACULTY OF ENGINEERING  
UBON RACHATHANI UNIVERSITY  
YEAR 2012**

**COPYRIGHT OF UBON RACHATHANI UNIVERSITY**



**THESIS APPROVAL**

**UBON RATCHATHANI UNIVERSITY**

**DOCTOR OF PHILOSOPHY**

**MAJOR IN MECHANICAL ENGINEERING FACULTY OF ENGINEERING**

**TITLE** DEVELOPMENT OF LOW SPEED WATER TURBINE FOR  
GENERATING ELECTRICITY OF 200 WATTS

**NAME** MR.PALAPUM KHUNTHONGJAN

**THIS THESIS HAS BEEN ACCEPTED BY**

..... CHAIR  
(ASST.PROF.DR.ADUN JANYALERTADUN)

..... COMMITTEE  
(ASSOC.PROF.DR.RATCHAPHON SUNTIVARAKORN)

..... COMMITTEE  
(ASST.PROF.DR.CHAWALIT THINVONGPITAK)

..... DEAN  
(ASST.PROF.DR.NOTE SANGTIAN)

**APPROVAL BY UBON RATCHATHANI UNIVERSITY**

.....  
(ASST.PROF.DR.UTITH INPRASIT)

**VICE PRESIDENT FOR ACADEMIC AFFAIRS**

**FOR THE PRESIDENT OF UBON RATCHATHANI UNIVERSITY**

**ACADEMIC YEAR 2012**

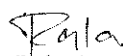
## ACKNOWLEDGEMENT

I would like to express my gratefulness to Asst. Prof. Dr. Adun Janyalertadun, my advisor, who has strongly supported me in my dissertation work. I truly appreciate his long-term patience, energy, and concerns for me during the years of my Ph studies. His excellent guidance, very helpful comments, and valuable advice have widened my knowledge and helped this dissertation reach its final shape.

I am deeply thankful to Electricity Generating Authority of Thailand (EGAT), Department of Research and Development, who supported and provided grant funding for this study.

I also would like to knowledge Asst. Prof. Dr. Umpaisak Teeboonma as well as all of my instructors in the Department of Mechanical Engineering, Ubon Ratchathani University who played an important role in completing this dissertation.

My profound gratitude is extended to my father, my mother, and my all first teachers for their empathy, patience, unfailing, and precious support, and encouragement. This dissertation would not have been accomplished without them by my side.

  
(Mr. Palaphum Khunthongjan)

Researcher

### บทคัดย่อ

ชื่อเรื่อง : การพัฒนากังหันกระแสความเร็วต่ำ เพื่อผลิตกระแสไฟฟ้าขนาด 200 วัตต์  
 โดย : พลภูมิ ขุนทองจันทร์  
 ชื่อปริญญา : ปรัชญาคุณภิวัฒน์  
 สาขาวิชา : วิศวกรรมเครื่องกล  
 ประธานกรรมการที่ปรึกษา : ผู้ช่วยศาสตราจารย์ ดร.อดุลย์ จรรยาเลิศอดุลย์

ศัพท์สำคัญ : กังหันกระแส น้ำ ผลิตไฟฟ้า เพิ่มความเร็วกระแส น้ำ  
 ทฤษฎี blade element momentum การจำลองการไหล

ปัจจุบันการแสวงหาพลังงานทดแทนเป็นเรื่องที่มีความสำคัญและเร่งด่วนเป็นอย่างยิ่ง พลังน้ำนับเป็นทางเลือกหนึ่ง อย่างไรก็ตามการสร้างเขื่อนขนาดใหญ่ในประเทศไทยเป็นเรื่องที่เป็นไปได้ยาก สืบเนื่องมาจากกระแสการอนุรักษ์และทรัพยากรที่มีอย่างจำกัด การสร้างกังหันน้ำขนาดเล็กซึ่งต้องการแรงดันน้ำสถิตยต่ำ หรือมีเฉพาะแรงดันอันเนื่องมาจากความเร็วของน้ำเพื่อการผลิตกระแสไฟฟ้า จึงน่าจะเป็นทางออกที่ดีและมีความเป็นไปได้ ซึ่งแนวคิดในการออกแบบกังหันชนิดนี้คือกังหันจะถูกวางในกระแสน้ำซึ่งมีความเร็ว กระแสน้ำจะขับกังหันให้หมุนและส่งต่อกำลังไปยังเพลลาซึ่งติดอยู่กับเครื่องผลิตกระแสไฟฟ้า เช่นเดียวกับกังหันลม ในการออกแบบกังหันจะใช้ทฤษฎี Blade element momentum theory การออกแบบdiffuser จะใช้การคำนวณเชิงตัวเลข โดยผู้ศึกษาได้เลือกกังหันแบบแกนนอน จำนวน 3 ใบพัด เส้นผ่าศูนย์กลาง 1.1 เมตร และติดตั้ง diffuser เพื่อเพิ่มความเร็วกระแสน้ำเข้าสู่กังหัน จากการศึกษารูปแบบของ diffuser 2 รูปแบบ คือ diffuser แบบ 2 ชั้น (Two shell diffuser) มีพื้นผิวที่ทางเข้าโค้งภายใน และ diffuser แบบธรรมดา (simple diffuser) ซึ่งทางเข้าเป็นทางเรียบ พบว่า ความเร็วของกระแสน้ำภายใน diffuser แบบ 2 ชั้น สามารถให้ความเร็วกระแสน้ำสูงสุด 2.0 เท่าของความเร็วน้ำขาเข้า ขณะที่ diffuser แบบธรรมดาทำได้ 1.7 เท่า อย่างไรก็ตาม diffuser แบบธรรมดาสามารถสร้างได้ง่ายกว่า จึงถูกเลือกเพื่อก่อสร้างและในการศึกษาถึงผลของมุมของ simple diffuser พบว่า ความสามารถในการเพิ่มความเร็วของกระแสน้ำ ( $\beta\gamma$ ) จะเพิ่มตามมุมที่เพิ่มขึ้น โดยที่ความเร็วสูงสุดที่สามารถเพิ่มได้เป็น 3.5 เท่าของกระแสน้ำขาเข้าที่มุม 90 องศา โดยพบว่า ความเร็วที่เพิ่มขึ้นมีความสัมพันธ์กับปัจจัยดังนี้ (1) Back pressure velocity ratio ( $\gamma$ ) หรือ อัตราส่วนความเร็วที่ทางออกและความเร็วของน้ำด้านหน้า diffuser โดยพบว่า ในช่วง 0-70 องศา  $\gamma$  จะมีค่าเพิ่มขึ้นตามมุม และคงที่เมื่อมุมอยู่ระหว่าง 70-90 องศา โดย

เมื่อมีการไหลและเกิดการหมุนวนบริเวณใกล้ผนังทางออก มีผลให้ static pressure บริเวณทางออกต่ำ ซึ่งจะช่วยให้ของไหลที่อยู่ด้านหน้าของ diffuser เข้ามาภายในมากขึ้น เป็นผลให้ความเร็วภายในและความเร็วตามแนวแกนที่ทางออกของ diffuser มีค่าสูงขึ้น (2) diffuser area ratio ( $\beta$ ) หรืออัตราส่วนความเร็วที่ภายในและทางออกของ diffuser ซึ่งมีค่าเพิ่มขึ้นในช่วง 0 ถึง 20 องศา และลดลงจนกระทั่งที่มุม 50 ถึง 90 องศา ซึ่งพบว่า ในช่วง 0-20 องศา ไม่มีการแยกไหล การกระจายตัวของของไหลภายในจะมีรูปแบบใกล้เคียงกับ diffuser ในอุดมคติ แต่ในช่วงมุม 50-90 องศา มีการแยกไหลเกิดขึ้น การกระจายตัวของของไหลไม่สม่ำเสมอ และมีรูปแบบที่คล้ายกันทำให้ค่า  $\beta$  ไม่เปลี่ยนแปลง และเมื่อพิจารณาถึง power coefficient ของกังหัน ( $C_{P,R}$ ) พบว่า มีค่าสูงสุดที่มุม 90 องศา เท่ากับ 2.14, power coefficient ของ DAWT ( $C_{P,DAWT}$ ) มีค่าไม่เกิน 0.59 ซึ่งเป็นไปตาม Betz limits และ  $C_{P,DAWT}$  จะขึ้นกับ  $C_{P,R}$  เป็นสำคัญ เมื่อติดตั้ง simple diffuser มุม 20 องศา เข้ากับกังหันซึ่งค่า ( $\gamma$ ) ( $\beta$ ) ( $\gamma\beta$ ) ของ diffuser เท่ากับ 1.2 , 1.5, 1.86 ตามลำดับ พบว่า สามารถเพิ่มกำลังที่ได้ 53.4% เทียบกับเมื่อไม่ได้ติดตั้ง diffuser และจากการทดสอบ สามารถผลิตกระแสไฟฟ้าได้ 301 วัตต์ ที่ความเร็วน้ำเข้า 1.8 m/s

## ABSTRACT

**TITLE** : DEVELOPMENT OF LOW SPEED WATER TURBINE FOR  
GENERATING ELECTRICITY OF 200 WATTS

**BY** : PALAPUM KHUNTHONGJAN

**DEGREE** : DOCTOR OF PHILOSOPHY

**MAJOR** : MECHANICAL ENGINEERING

**CHAIR** : ASST.PROF.ADUN JANYALERTADUN, Ph.D.

**KEYWORDS** : FLOW WATER TURBINE / ELECTRICITY GENERATING / WATER  
VELOCITY ADDITION / BLADE ELEMENT MOMMENTUM THEORY /  
FLOW SIMULATION

Nowadays, searching for alternative energy is really urgent and important. Hydro power is the one to be considered first. Regarding the strict natural reservation and bounded resource it is not easy to construct such a huge dam in Thailand. Creating either low-hydrostatic pressure turbine or turbine from the velocity head in order to generate electricity would be possible way or a better choice. Concepts of the design are to place turbine into flow water stream, turbine blades will be rotated and transmit its power to the shaft that coupled with the electricity generator as same was the wind turbine. Blade element momentum theory was applied in designing of turbine and computational fluid dynamics for diffuser studying. The researcher studied three blades that was 1.1 in diameter of horizontal axis turbine and to increase water velocity diffuser was installed with. In numerical calculation two types of diffuser were studied (1) two shell diffuser with the curved surface at the inlet and (2) simple diffuser with the flat space at the inlet. The study found that the two shell diffuser would be able to generate the maximum flow water at 2.0 times at the inlet and the simple diffuser would merely generate the flow water at 1.7 times of the inlet. But the latter type of diffuser was chosen to build because it more easy. In the studying the effect of diffuser angle. The results revealed that the capacity of flow water would be higher regarding the widened angle. At 90 degree the flow water reached the maximum rate at 3.5 times. The influential factor to the velocity addition are (1) back pressure velocity ratio ( $\gamma$ ) or the ratio

of outlet velocity and in front velocity of diffuser it found that in between 0-70 degree  $\gamma$  would be increasing regarding it widened angle and would be constant when the angle was between 70-90 degree. When it flowed and recirculated near outlet surface static pressure at the outlet would be low that helped draw outside fluid to come greater inside diffuser. As a result, inner velocity and axial velocity at the outlet of diffuser would be higher (2) diffuser area ratio ( $\beta$ ) or ratio of inner velocity and at outlet of diffuser that would be increased when angle was between 0 – 20 and kept constantly when angle was between 50-90 degree. It found that there was no flow separation when angle was between 0-20 degrees and fluid distribution was similar to bare ideal diffuser. But, in between 50-90 degree of angle there found similarly flow separation and inconstant fluid distribution that caused unchanging of  $\beta$ . Considered power coefficient of turbine ( $C_{P,R}$ ), it found to reach the maximum rate 2.14 at 90 degree of angle, power coefficient of DAWT ( $C_{P,DAWT}$ ) was not more than 0.59 regarding Betz limits and  $C_{P,DAWT}$  would significantly depend on  $C_{P,R}$ . When the 20 degree of simple diffuser was installed, ( $\gamma$ ) ( $\beta$ ) ( $\gamma\beta$ ) are equal to 1.2, 1.5, 1.86 respectively. It revealed that it was able to raise 53.4% of power when compared to non-diffuser installation and generate the electricity 301 watts at the inlet velocity 1.8 m/s.

## CONTENTS

	PAGE
<b>ACKNOWLEDGEMENTS</b>	<b>I</b>
<b>THAI ABSTRACT</b>	<b>II</b>
<b>ENGLISH ABSTRACT</b>	<b>IV</b>
<b>CONTENTS</b>	<b>VI</b>
<b>LIST OF TABLES</b>	<b>VIII</b>
<b>LIST OF FIGURES</b>	<b>IX</b>
<b>LIST OF ABBREVIATION SYMBOLS</b>	<b>X</b>
<b>CHAPTER</b>	
<b>1 INTRODUCTION</b>	
1.1 Background of the research	1
1.2 Research Objectives	5
1.3 Research Goals	5
1.4 Expected outcome	5
<b>2 THE CONCERNED THEORY</b>	
2.1 Blade element momentum theory (BEM)	6
2.2 The equation of flow conduction of fluid	12
2.3 The model of fluid turbulence	15
2.4 Continuity equation in an uninstalled air-propeller diffuser	19
2.5 Continuity equation inside Diffuser augmented wind turbine (DAWT)	21
<b>3 LITERARY OVERVIEW</b>	
3.1 Diffusers and windmills	25
3.2 A diffuser and a water current turbine	28
3.3 The particular study of diffuser	29
3.4 The particular study of a horizontal axis water current turbine	30



## CONTENTS (CONTINUED)

	PAGE
<b>4 RESEARCH METHODOLOGY</b>	
4.1 Research Methodology	33
4.2 Computational Fluid Dynamics (CFD)	34
4.3 Blade element momentum theory (BEM)	46
4.4 Experimental set up	48
4.5 Summary and Report	49
4.6 Required tools and appliances for research	49
<b>5 RESULTS AND DISCUSSIONS</b>	
5.1 2 Dimensional simulation results of diffuser	50
5.2 Design results of turbine blade	67
5.3 Simulation results of a diffuser augmented water current turbine	68
5.4 Examination of generating power	70
<b>6 CONCLUSION</b>	
6.1 Result of design and examination of diffuser	73
6.2 Electricity generating test	74
6.3 Application	75
6.4 Suggestions	76
<b>REFERENCES</b>	77
<b>APPENDIX</b>	
A: Publication	83
B: Presentations	91
C: Test results	98
<b>VITAE</b>	132

**LIST OF TABLES**

<b>TABLE</b>	<b>PAGE</b>
4.1    Fluent set up for 2D diffuser simulation.	41
4.2    Fluent set up for 3D diffuser simulation..	43
4.3    Fluent set up for DAWT Simulation.	46
5.1    Blade design results based on blade element momentum theory.	67
5.2    Simulation results with the turbine installed inside the diffuser.	70

## LIST OF FIGURES

FIGURE	PAGE
2.1 Axial stream tube around turbine.	7
2.2 Annular rotating stream tube.	7
2.3 Velocity and the force on chord of windmill.	8
2.4 Mass forms through a small frame.	12
2.5 The force effects mass of small fluid.	13
2.6 Disordered changes of variation fluid.	15
2.7 The relations between the pressure and the velocity inside diffuser.	20
3.1 Hydro turbine under the concept of David L. et al. (2008).	28
3.2 F1-UBA Vertical axis water current turbines by Ponta and Dutt.	29
3.3 The 35-kW hydro turbine of Danny Sale et al. (2009).	31
4.1 Research methodology.	33
4.2 Finite volume methods in one dimension.	35
4.3 The Segregated solver computation graph.	36
4.4 Coupled solver graphs of computational method.	37
4.5 Domain of 2 D problems.	39
4.6 Diffuser angle.	40
4.7 Domain of 3 D problem.	42
4.8 Domain of DAWT Simulation.	45
4.9 Lift and drag coefficient of FX 63-317.	47
4.10 The ratio of lift to drag coefficient and moment coefficient of the FX 63-317.	47
5.1 Velocity contour of 2 shell diffuser.	50
5.2 Velocity vector of 2 shell diffuser.	51
5.3 Velocity contour of simple diffuser.	51
5.4 Velocity vector of simple diffuser.	52
5.5 Pressure coefficients comparative.	52
5.6 Showed ratio diffuser velocity to free water velocity on the axis of simple and 2 shell diffuser.	53

# LIST OF FIGURES (CONTINUED)

FIGURE	PAGE
5.7 CFD and testing velocity of 2 shell diffuser.	53
5.8 $Y^+$ of simple diffuser wall values from 26 to 398.	54
5.9 Shows $V/V_0$ on the diffuser axis.	55
5.10 Shows $C_p$ on the diffuser axis.	55
5.11 (a) Results of the 2D simulation showing the pressure contour, (b) showing the velocity contour when the diffuser angle was at 0, 20, 40, 60, and 80 degrees.	56
5.12 The relation between $V1/V0$ at different point on x-axis direction to angle of empty diffuser.	57
5.13 The relationships of the diffuser area ratio ( $\beta$ ), back pressure velocity ratio ( $\gamma$ ), and the diffuser augmentation factor ( $\beta\gamma$ ) to the diffuser angle.	57
5.14 The relation of the back pressure velocity ratio ( $\gamma$ ) and the exit pressure coefficient $C_{p,Exit}$ to the diffuser angle.	58
5.15 The comparison of velocity contours between (a) an empty diffuser and (b) a diffuser with a 0.59 $C_p$ rotor.	58
5.16 Water streamlines of diffuser (a) without and (b) with 0.59 $C_p$ of rotor turbine at 0, 20, 80 degrees.	59
5.17 (a) Velocity and (b) Pressure coefficients at the axis of the diffuser with and without the rotor turbine at 0, 20, 80 degree diffuser angles.	60
5.18 Relationship of the disk loading coefficient, $C_{T,Total}$ , $C_{T,D}$ , $C_{T,R}$ , and $\beta\gamma$ to diffuser angle in degrees.	61
5.19 Flow fields regions (P.M. Jamieson, 2009).	61
5.20 Axial induction factor ( $b$ ) at reference plane of system, of turbine ( $a$ ), of turbine at the maximum power coefficient ( $a_{max}$ ), and of non-turbine diffuser ( $a_0$ ) respectively.	62
5.21 Indicates Power coefficient ( $C_p$ ) and Diffuser augmentation factor ( $\beta\gamma$ ).	63
5.22 The contour of the water velocity in the 3D Diffuser.	64

**LIST OF FIGURES (CONTINUED)**

<b>FIGURE</b>	<b>PAGE</b>
5.23 Velocity contour inside the diffuser at different points.	64
5.24 (a) 3D water velocity on the diffuser axis; mesh 400,000; 600,000; and 800,000; and 2D axisymmetric respectively, (b) Static pressure on the diffuser axis in 3D; mesh 400,000; 600,000; 800,000; and 2D axisymmetric.	65
5.25 The diffuser without the rotor turbine test results..	66
5.26 Design result for the turbine blade based on blade element momentum theory.	67
5.27 Water flows via turbine blade.	68
5.28 The velocity contour on the turbine blade.	68
5.29 Pressure contour (1).	69
5.30 Pressure contour (2).	69
5.31 Power (watts) vs velocity (m/s).	70
5.32 Power coefficients at different velocities.	71
5.33 Power coefficients as a function of variable TSR.	71
5.34 Comparison of power before and after installing diffuser.	72

## LIST OF ABBREVIATION SYMBOLS

SYMBOLS	MEAN
$A$	Turbine rotation sweep area
$a, b,$	Axial induction factor
$a_0$	Axial induction factor without energy extraction
$\alpha_k, \alpha_\varepsilon$	Inverse effective Prandtl numbers of $k$ and $\varepsilon$ consequently.
$\alpha$	The permeability of the medium
BET	Blade Element Theory
BEM	Blade Element-Momentum Theory
$\beta$	Diffuser area ratio
$\beta\gamma$	Diffuser augmentation factor
$C_2$	The pressure-jump coefficient
$C_L$	Lifting force coefficient
$C_p$	Pressure coefficient, Power coefficient
$C_{Pi}$	Pressure coefficient at location $i$
$C_{P,R}$	Rotor power coefficient
$C_{P, exit}$	Power coefficient at diffuser exit
$C_{P, DAWT}$	Power coefficient of diffuser augmentation water turbine
$C_{T,D}$	Thrust coefficient of diffuse
$C_{T, Total}$	Total thrust coefficient of diffuser plus rotor
$C_{T,R}$	Thrust coefficient of rotor
$C_{1\theta}, C_{2\theta}, C_{3\theta}$	The constant values
$c$	Chord length
DAWT	Diffuser Augmented Wind or (water)Turbine
$\varepsilon$	Dissipation rate

## LIST OF ABBREVIATION SYMBOLS (CONTINUED)

SYMBOLS	MEAN
$G_k$	Kinematic energy of mean velocity flow
$G_b$	Kinematic energy of buoyancy flow
$\gamma$	Back pressure velocity ratio
$k$	Turbulence kinetic energy
$\lambda$	Tip speed ratio
MT	Momentum Theory
$U$	The velocity normal to the porous face
$\eta$	The energy released per energy of fluid before letting into turbine
$\Omega$	Angled velocity of the blades
$\omega$	Angled velocity of the wake at the turbine blades
$\phi$	Relative velocity
$P_i$	Pressure at location $i$
$\rho$	Density
TSR	Tip speed ratio
$\mu$	Molecular viscosity, the laminar fluid viscosity
$\mu_t$	Virtual viscosity
$U_0$	Velocity at the inlet
$U_d$	Velocity at the blades
$U_{rel}$	Relative velocity
$V_i$	Velocity at location $i$
$\bar{x}$	Mean of $x$
$Y_M$	The contribution of the fluctuating dilatation in compressible turbulence to the overall dissipation rate

## CHAPTER 1

### INTRODUCTION

#### 1.1 Background of the research

While the connection of humans rapidly expands in this globalization period, man's life and business operations have always been based on the competition for the energy to support and the drive business. Energy comes from natural resources and can be found in some form in almost all kinds of environment on earth. The more humans, the higher the energy usage requirements but the natural resources are still without any substitution. So, the rapid depletion of natural resources and energy is happening.

Information on global energy usage shows that fossil fuel (hydrocarbons-- petrol, natural gas, and coal) are most used representing 95% of usage. Another 2% is from nuclear power and another 3% is from other sources. Examples of these other energy sources include but are not limited to hydropower from dams, solar energy, biomass, waves, and underground thermal. Only in 1997 energy equivalent to 9,371 billion liters of crude oil were used or almost 10,000 billion liters, nuclear energy 2%, water; wind; waves; biomass 3%, natural gas 25%, coal 28%, crude oil 42%. (Energy Policy and Planning Office, 2011: website)

Electrical energy is a major factor in building the economy in a developing country like Thailand. Requirements for electrical power in Thailand are increasing. The appropriate way of using the energy is to be careful about it (which will help lessen the national electrical usage and individual expenses) and acquirement of additional natural resources. Saving the energy effectively; moreover, will reduce the investment cost for new energy resources that strengthens the competition competency in the world market and foreign currency in such period of economic crisis. However, a measure on cost to encourage men using energy efficiently is the first one need to be operated with energy conservation that are composed of encouragement, building conscious mind, and giving support for domestic production activity in order to compete with the world market, such as supporting investment and making improvements and exceptions on the concerned regulations; so that, the electrical production business will be able to change its administration



form in order to reduce operation costs and enhance the competition competency. Besides, to be the fundamental components of the electrical business e.g. using alternative energy by cooperation of the neighbors, should be supported, since not much reserved energy in Thailand were found. After surveying energy brought into our country until 1998 was 60% import. By geologist's report if there's no more reserved energy resources and the usage amount is equal to the present, we will have reserved crude oil 17 billion liters, which certainly are not enough. Natural gas 357 billion liters (equiv. to crude oil) will be gone within 22 years. Coal (lignite) is left only 1,676 billion liters (equiv. to crude oil) and will be gone away within 62 years. (Energy Policy and Planning Office, 2011: website) Therefore alternative energy/ water power are the best choice at present, since the clean energy with non-toxic release, water power, help decrease production cost. The electricity is often generated by water power by letting water flows through turbine, which is similar to cycling generator. After cycling a dynamo attached with the wheel will be charged, then we can turn on the headlight. The strengthen of hydropower is whenever water flows through turbine then electric power will immediately be released that is opposite to fuel power plant, burning fuel at the appropriate temperature first and wait until the generator gets ready to produce the power. Hydropower plant, thus, suits the electrical requirements during prime time from midday to midnight. But the power plant from fossil fuel (coal, natural gas, crude oil) cannot be interrupted because it takes time to restart the generator. As such, there's leftover electrical power after the power plant continues operating. The left ones are conversely pumped to the reservoir. When the prime time comes again water from the reservoir is let to generate the electricity. Such methodology 'Reverse Hydropower production' is now found in Thailand e.g. at Lam Taklong Dam and Bhumipol Dam. Other positive point of hydropower is a long-lived circulating energy, it's not only to generate the electricity but the agriculture and rain for regenerating also. Somehow, it occupied big space of forest to build the dam for generating hydropower, which numbers of forest spaces and wild animals are getting small. Those creatures leave their place before it is flooded and some of them already extinct from earth. Indigenous people's life is also changed. Mainly, fuels for electricity production are from natural gas, coal, co energy, crude oil, water power, diesel, etc. Though most coal is lignite produced by EGAT, there's still wasteful production costs. There are many concerned points need to be considered well before choosing the energy;

1.1.1 Fuel resources: numbers of reserved energy; it shouldn't be chosen if it is not adequate for the forthcoming future. Once it's gone the power plant will stop.

1.1.2 Stability is to be able to manage or procure from different places. If it comes from single or few locations, it unsecured situation because its cost might be put up unreasonably.

1.1.3 Reasonable price; too expensive price is not worth investing. It should comes along with least environmental effects concerning to poisonous gas or forest intrusion.

1.1.4 Type of power plant: we sometimes need the power urgently. Hydropower is the best choice. But, if we want to continue generating power without interruption, the electricity from coal; natural gas; or crude oil are reasonable. So, the organization in charge of electricity production should rather be aware and make a capacity survey of water power seriously than any other resources because it's last-long energy.

If the EGAT, large organization implementing electricity production activity, bring the alternative energy (Hydropower) to generate the electricity, production costs and natural resources will be down. Also, making environmental conservation and be responsible for society will be key factors supporting the organization as the leader of electricity production in the South East Asia Region with the adequate competency to compete in the foreign market. As aforementioned, the researcher rather realizes the capability of electricity from water power as the alternative energy and reserved power of the nation than any others.

Nowadays, the discovery of alternative energy is so important and urgent. Through the study the documentation there are many capable water resources to be used for electricity production. It is not easy, anyway, to build huge dam in Thailand, since there's strong stream of environmental conservation and finite resources. It'd better if a small hydro turbine is built with low pressure water or pressure from water velocity to produce the electricity. Design of this turbine is the turbine will be put down into the flowing water. Turbines will spin around by the force of water current that give energy to the generator via the connected shaft; as same as the windmill put it the wind current. This concept was studied and applied with the high-speed sea current. S. Kiho et al. (1996) studied the electrical generating by Vertical Darrieus Turbine and found the turbine energy when the water velocity is up to 1 m/s with 56% effectiveness. It's so useful for shipping, fishing and environmental works. Anyway, released energy depends on the landscape. Other one L.B. Wang et al. (2007) applied the turbine in such similar way via a

1.1.1 Fuel resources: numbers of reserved energy; it shouldn't be chosen if it is not adequate for the forthcoming future. Once it's gone the power plant will stop.

1.1.2 Stability is to be able to manage or procure from different places. If it comes from single or few locations, it unsecured situation because its cost might be put up unreasonably.

1.1.3 Reasonable price; too expensive price is not worth investing. It should comes along with least environmental effects concerning to poisonous gas or forest intrusion.

1.1.4 Type of power plant: we sometimes need the power urgently. Hydropower is the best choice. But, if we want to continue generating power without interruption, the electricity from coal; natural gas; or crude oil are reasonable. So, the organization in charge of electricity production should rather be aware and make a capacity survey of water power seriously than any other resources because it's last-long energy.

If the EGAT, large organization implementing electricity production activity, bring the alternative energy (Hydropower) to generate the electricity, production costs and natural resources will be down. Also, making environmental conservation and be responsible for society will be key factors supporting the organization as the leader of electricity production in the South East Asia Region with the adequate competency to compete in the foreign market. As aforementioned, the researcher rather realizes the capability of electricity from water power as the alternative energy and reserved power of the nation than any others.

Nowadays, the discovery of alternative energy is so important and urgent. Through the study the documentation there are many capable water resources to be used for electricity production. It is not easy, anyway, to build huge dam in Thailand, since there's strong stream of environmental conservation and finite resources. It'd better if a small hydro turbine is built with low pressure water or pressure from water velocity to produce the electricity. Design of this turbine is the turbine will be put down into the flowing water. Turbines will spin around by the force of water current that give energy to the generator via the connected shaft; as same as the windmill put it the wind current. This concept was studied and applied with the high-speed sea current. S. Kiho et al. (1996) studied the electrical generating by Vertical Darrieus Turbine and found the turbine energy when the water velocity is up to 1 m/s with 56% effectiveness. It's so useful for shipping, fishing and environmental works. Anyway, released energy depends on the landscape. Other one L.B. Wang et al. (2007) applied the turbine in such similar way via a

potential flow 2-D vortex model and found the accurate result if compared to the outcome of W.M.J. Batten et al. (2006); A.S. Bahaj et al. (2006) studied and designed horizontal axis turbine by the theoretical calculation and set turbine model. To deepen the perception in behavior of turbine happening when it's turning into direction of flowing water, force, thrust coefficient at different level of tip speed ratio and pitch setting were studied thoroughly. Besides, I. G. Bryden et al. (2000) applied the energy storage mechanisms that are composed of flywheels and battery with the horizontal axis tidal turbine. It helps improve the capacity of system. The study of J. VanZieten and Driscoll F. R. (2006) showed design of C-Plane turbine model – y axis tidal turbine set up under the sea with cable and pegs and is able to adjust the level for generating the electricity. Besides, the two turbines mentioned above there are different forms of turbines to be studied; such as Brian Kirke (2005) studied the Ducted Current Turbine, its strengths are high capacity, safe and minimized size of gear box. J. Bayondor et al. (2001) presented the new model of hydro turbine called 'advanced zero-head hydro-propulsion (HYPS)', which consist of set of blades connected with shafts. Under the consideration of aero-hydrodynamics those blades were designed and installed together with different incidence angles; so that, the turbine is able to receive and spread the water power from various water current.

Although there are many concerned studies e.g. windmills, high-speed ship blades and hydro turbine, those three types of technology do not cover all important information of water current turbine and hydro turbine. It, thus, much information is waiting for the study, for example, the analytical equation created from the understandings towards windmill and hydro turbine. Those equations can be revised from the test results by repeating and forwarding the information back for improving the theory. To calculate with Computational Fluid Dynamics (CFD) helps recheck the accuracy of devices before building and cut down the unnecessary expenses. To design the windmills can begin with editing and revising the current ones in order to comply with water qualifications and occurrence. The study should cover cavitations background, level of turbulence, and level of turbine installation. To look for the capacity of the force toward the hydro turbine need to study the force and the moment load as well as different flowing forms concerned to turbine dynamic, gained load comparing to water current and pitch angle change of blade (A.S. Bahaj and L.E. Myers, 2003) and capacity of turbine. The interesting topic is proper location of generator and controlling methodology.

The studies above emphasize on application of high-speed sea current. There's a study report of applied hydro turbine with rivers or other water resources at the low water velocity like to study of Peter Fraekel (2006). He studied the Vertical Darrieus water turbine to pump water from Nile with the most pumping capacity at 2,000 l/h with 5 meters pressure and water velocity at 1 m/s. Later on, it's improved to be the y axis turbine for pumping water generating electricity.

This research aims to study the building and the experiment of hydro turbine installed inside the Duct to be used in the low water velocity areas, such as Mun River north east of Thailand that will be able to generate the electricity for either small villages or irrigation.

## **1.2 Research Objectives**

- 1.2.1 To build and test the water duct model in water flume.
- 1.2.2 To design Duct augmented water turbine.
- 1.2.3 To build and test the capacity of water current turbine in real situation.

## **1.3 Research Goals**

- 1.3.1 There's water duct model with up water speed not less than 50%.
- 1.3.2 There's design of Duct augmented water turbine with its estimated capacity 200W and velocity at 1.0 m/s.
- 1.3.3 There's hardware of Duct augmented water turbine and test result with its estimated capacity 200W at water speed 1.0 m/s. Power coefficient of the system is not less than 2 times of water turbine without duct.

## **1.4 Expected outcome**

- 1.4.1 There will be appropriate design of water turbine with diameter about 1.2 meters 3 blades and tip speed ratio approximate 5 with efficiency of turbine not less than 25%.
- 1.4.2 There will be appropriate design of water duct.
- 1.4.3 An expected ratio of maximum water speed in duct model to free stream not less than 1.5.

## CHAPTER 2

### THE CONCERNED THEORY

Water current turbines differ from hydro turbines that require the potential energy. Water current turbines use the kinetic energy of the water current. As mentioned in Betz theory that power extraction from the fluid will be a function of efficiency of turbine and the cube of the velocity. That is if we need more power we have to get more speed of current. The two dimensional analysis by Gorlov and Silantyev (2001) presented the turbine energy as the equation 2.1.

$$P = \int_{\partial \omega} [p] V \cdot n \quad (2.1)$$

or

$$P = \frac{1}{2} \eta A \rho V_0^3 \quad (2.2)$$

When  $\eta$  is efficiency of the turbine

$A$  is space of the turbine

$\rho$  is the fluid density

$V_0$  is the fluid velocity before flowing into the turbine

#### 2.1 Blade element momentum theory (BEM)

BEM is the combination of momentum theory with blade element theory. The fundamental hypothesis of BEM theory is that the force on the blade is the change of specific momentum of the air flowing throughout the ring, but it does not calculate the fluid result on the radial span or the interaction of fluid in each ring.

##### 2.1.1 Momentum Theory (MT)

It sometimes calls the theory 'Glauert Annulus Momentum Vortex Theory'. It is to separate domain of fluid that are flowing through turbine to be the ring on radiance (Strips or

Annular Stream tube). It, then analyze the transformation and momentum in the ring, which will consist of small theoretical component as below:

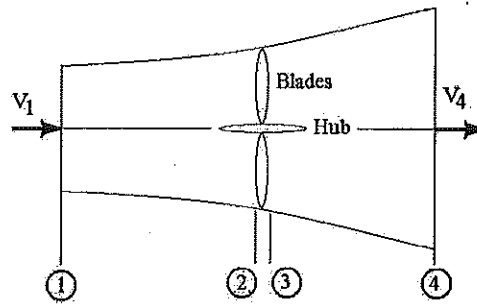


**Figure 2.1** Axial stream tube around turbine.

Consider the stream tube shown around turbine in figure 2.1. From the analytical equation of conservative momentum equation of the ring  $dr$  at density  $\rho$  connection of the force  $F_x$  on axial will be

$$dF_x = 4a(1-a)\rho V_1^2 \pi dr \quad (2.3)$$

When  $a$  is axial induction factor, velocity ratio at the decreasing speed turbine at the inlet per inlet velocity ( $a = (V_1 - V_2)/V_2$ )  $\rho$  is air density,  $V_1$  is air velocity at the inlet and  $V_2$  is the air velocity at the blades.

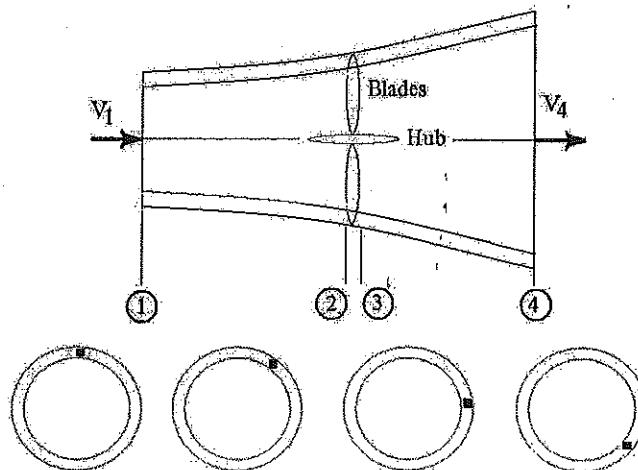


**Figure 2.2** Annular rotating stream tube.

By the analysis of conservative momentum equation at the angled momentum of Annular rotating stream-tube in figure 2.2 the relation of Tangential force  $T$  will be

$$dT = 4a'(1-a)\rho V_1 \pi r^3 \Omega dr \quad (2.4)$$

$\Omega$  is angled velocity of the blades,  $a'$  that was defined as angular induction factor  $a' = \omega / r\Omega$  by  $\omega$  is the angled velocity of wake at the blades turbine.

### 2.1.2 Blade Element Theory (BET)

BET is considerations of the two-dimensional operating force on the blades. The blades are lengthwise separated and calculated it values, such as lifting force and drag force as the results of attack angles. The velocity between each part of blades won't be considered. It means the three-dimensional results are not concerned.

The released velocity were described as the Axial velocity and Tangential Velocity if consider the blade element. The axial velocity on blade element is  $V_2 = V_1(1-a)$  and the Tangential velocity is  $r\Omega + \frac{1}{2}r\omega$ ;  $r\Omega$  is wake velocity

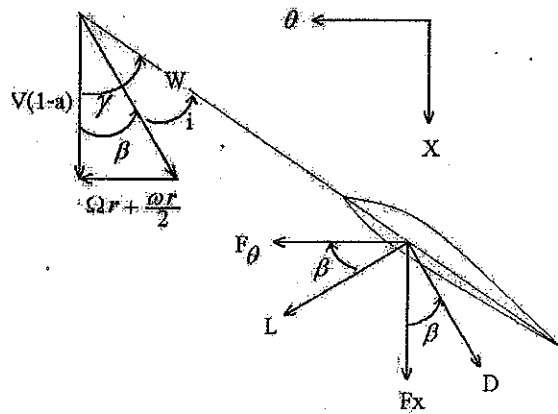


Figure 2.3 Velocity and the force on chord of windmill.

If considered the vectorial velocity as in Figure 2.3, the relation will be

$$\tan \beta = \frac{\lambda_r(1+a')}{(1-a)} \quad (2.5)$$



When  $\lambda_r = \frac{\Omega r}{V}$

From figure 2.3 the follow equation is apparent

$$W = \frac{V(1+a)}{\cos \beta} \quad (2.6)$$

The forces on blade element are show in figure 2.3, not that by definition the lift and drag forces are perpendicular and parallel to the incoming flow. For each blade element one can see

$$dF_x = dL \sin \beta - dD \cos \beta \quad (2.7)$$

$$dF_\theta = dL \cos \beta - dD \sin \beta \quad (2.8)$$

Where  $dL, dD$  are the lift and drag forces on blade element respectively.  $dL, dD$  can be found from definition of the lift and drag coefficient as follow.

$$dL = \frac{1}{2} C_L \rho W^2 c dr \quad (2.9)$$

$$dD = \frac{1}{2} C_D \rho W^2 c dr \quad (2.10)$$

If there are N blades, combining equation (2.7) (2.8) (2.9) and (2.10) it can be shown that

$$dF_x = N \frac{1}{2} \rho W^2 (C_L \sin \beta + C_D \cos \beta) c dr \quad (2.11)$$

$$dF_\theta = N \frac{1}{2} \rho W^2 (C_L \cos \beta - C_D \sin \beta) c dr \quad (2.12)$$

The Torque on an element  $dT$  is simply by the tangential force multiplied by the radius.

$$dT = N \frac{1}{2} \rho W^2 (C_L \cos \beta - C_D \sin \beta) c r dr \quad (2.13)$$

$\beta, W$  can be expressed in term of induction factors etc. (Equation (2.5) (2.6)).

Substituting and carrying out some algebra yields

$$dF_x = \sigma' \pi \rho V^2 \frac{(1-a)^2}{\cos^2 \beta} (C_L \sin \beta + C_D \cos \beta) r dr \quad (2.14)$$

$$dT = \sigma' \pi \rho V^2 \frac{(1-a)^2}{\cos^2 \beta} (C_L \cos \beta - C_D \sin \beta) r^2 dr \quad (2.15)$$

Where  $\sigma'$  is called the local solidity and is defined as

$$\sigma' = \frac{Nc}{2\pi r} \quad (2.16)$$

Define  $Q$  as tip loss correction

$$Q = \frac{2}{\pi} \cos^{-1} \left[ \exp \left( - \left( \frac{N/2(1-r/R)}{(r/R) \cos \beta} \right) \right) \right] \quad (2.17)$$

The tip loss correction is applied to equation 2.3 and equation 2.4 which become

$$dF_x = 4Q \rho V_1^2 a(1-a) \pi r dr \quad (2.18)$$

$$dT = 4Q \rho V a'(1-a) \Omega r^3 \pi dr \quad (2.19)$$

### 2.1.3 Blade Element Momentum Theory (BEM)

We now have four equations; two derived from momentum theory which axial thrust and the torque in terms of flow parameters.

$$dF_x = Q\rho V_1^2 (4a(1-a))\pi r dr \quad (2.20)$$

$$dT = Q\rho V 4a'(1-a)\rho V \Omega r^3 \pi dr \quad (2.21)$$

We also have two equations derived from consideration of blade forces which express the axial force and torque in term of the lift and drag coefficients of the aero foil

$$dF_x = \sigma' \pi \rho V^2 \frac{(1-a)^2}{\cos^2 \beta} (C_L \sin \beta + C_D \cos \beta) r dr \quad (2.22)$$

$$dT = \sigma' \pi \rho V^2 \frac{(1-a)^2}{\cos^2 \beta} (C_L \cos \beta - C_D \sin \beta) r^2 dr \quad (2.23)$$

To calculation rotor performance equation and from a momentum balance are equate with equation. This is done the following useful relationships arise

$$\frac{a}{1-a} = \frac{\sigma' (C_L \sin \beta + C_D \cos \beta)}{4Q \cos^2 \beta} \quad (2.24)$$

$$\frac{a'}{1-a} = \frac{\sigma' (C_L \cos \beta - C_D \sin \beta)}{4Q \lambda_r \cos^2 \beta} \quad (2.25)$$

Two equation above are used in blade design procedure

Power output from each annulus is

$$dP = \Omega dT \quad (2.26)$$

The total power from the rotor is

$$P = \int_{r_h}^R \Omega dT dr \quad (2.27)$$

$r_h$  is the hub radius, The power coefficient  $C_p$  is calculated from:

$$C_p = \frac{P}{P_{wind}} = \frac{\int_{r_h}^R \Omega dT}{0.5 \rho \pi R^2 V^3} \quad (2.28)$$

Using equation it is possible to develop and integral for power coefficient directly. After some algebra:

$$C_p = \frac{8}{\lambda^2} \int_{r_h}^R Q \lambda_r^3 a' (1-a) \left[ 1 - \frac{C_D \tan \beta}{C_L} \right] d\lambda_r \quad (2.29)$$

## 2.2 The equation of flow conduction of fluid

The conduction of fluid flow can be explained by mathematical equation that consist of the equation of mass conservation, momentum conservation, the model of turbulence, and the Computational Fluid Dynamics (CFD) to be used as the study tools water fluid through the hydro turbines. The conservative equation of fluid: The fluid equation is the relation of fluid flow that can be figured out in differential equation, in terms of any quality changes of the fluid. Those equations are from the rules of mass and momentum conservation as explained below.

### 2.2.1 The equation of mass conservation

It's considered when the fluid gets through a small frame at  $dx$  and  $dy$  dimension as in figure 2.4. By the fact that mass can't be vanished; so, both inletting mass and out letting mass at the ratio area will not be different.

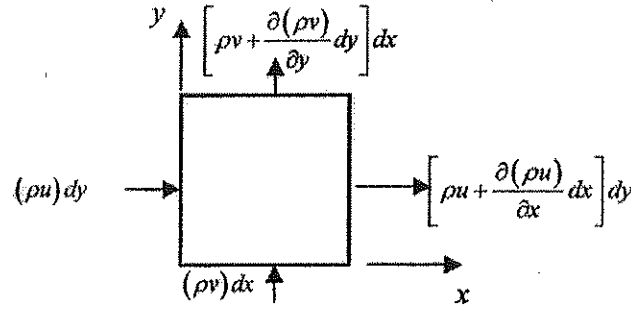


**Figure 2.4** Mass forms through a small frame.

$$\text{X:} \quad \left[ \rho u + \frac{\partial(\rho u)}{\partial x} dx \right] dy - [\rho u] dy = \frac{\partial(\rho u)}{\partial(x)} dx dy \quad (2.30)$$

$$\text{Y:} \quad \left[ \rho v + \frac{\partial(\rho v)}{\partial y} dy \right] dx - [\rho v] dx = \frac{\partial(\rho v)}{\partial(y)} dx dy \quad (2.31)$$

$u$  and  $v$  respectively are the subordinate velocity in  $x$  and  $y$ , which will depend on location of  $x$  and  $y$ . That is  $u = u(x, y, t)$  and  $v = v(x, y, t)$ , as the mass inside a small frame is  $\rho dx dy$ . So, the ration of reduced variable mass is  $-\frac{\partial \rho}{\partial t} dx dy$ ; the increasing mass equals the decreasing ones inside a small frame. The equation 2.32 is the mass conservation equation explaining the first equation.

$$\frac{\partial \rho}{\partial t} + \left[ \frac{\partial(\rho u)}{\partial x} + \frac{\partial(\rho v)}{\partial y} \right] = 0 \quad (2.32)$$

$$\text{or} \quad \frac{\partial \rho}{\partial t} + \text{div}(\rho \bar{V}) = 0 \quad (2.33)$$

### 2.2.2 The equation of momentum conservation

Considering the mass of little fluid with  $dx$  and  $dy$  dimension as in figure 2.5.

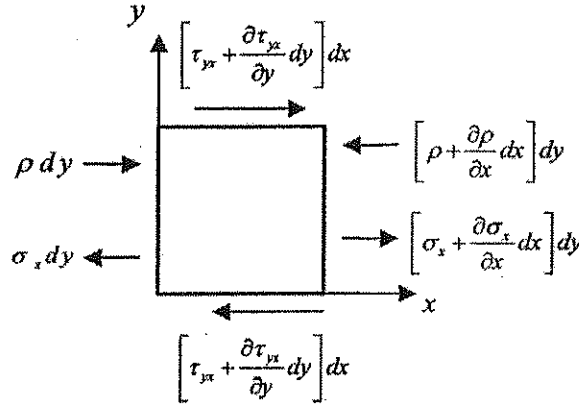


**Figure 2.5** The force effects mass of small fluid.

From the 2<sup>nd</sup> rules of Newton  $F = ma$  when it considered the cooperative force on X the result will be

$$F_x = \left[ -\frac{\partial p}{\partial x} + \frac{\partial \sigma_x}{\partial x} + \frac{\partial \tau_{yx}}{\partial y} \right] dx dy + \rho f_x dx dy \quad (2.34)$$

The mass of this fluid is  $m = \rho(dx dy)$  and the acceleration force on X is  $a_x = \frac{Du}{Dt}$ , if m and  $a_x$  were substituted in the second rules of Newton, the equation 2.34 will be

$$\rho \frac{Du}{Dt} = -\frac{\partial p}{\partial x} + \frac{\partial \sigma_x}{\partial x} + \frac{\partial \tau_{yx}}{\partial y} + \rho f_x \quad (2.35)$$

Whereas the acceleration force on y will be

$$\rho \frac{Dv}{Dt} = \frac{\partial p}{\partial y} + \frac{\partial \sigma_y}{\partial y} + \frac{\partial \tau_{xy}}{\partial x} + \rho f_y \quad (2.36)$$

By equation 2.35 and 2.36 are the absolute value of the differential equation that can be arranged in simple differential equation as in (2.37) and (2.38).

On X axis

$$\frac{\partial(\rho u)}{\partial t} + \frac{\partial(\rho u^2)}{\partial x} + \frac{\partial(\rho uv)}{\partial y} = -\frac{\partial p}{\partial x} + \frac{\partial}{\partial x} \left( \lambda \operatorname{div}(\bar{V}) + 2\mu \frac{\partial u}{\partial x} \right) + \frac{\partial}{\partial y} \left[ u \left( \frac{\partial v}{\partial x} + \frac{\partial u}{\partial y} \right) \right] + \rho f_x \quad (2.37)$$

On Y axis

$$\frac{\partial(\rho v)}{\partial t} + \frac{\partial(\rho v^2)}{\partial y} + \frac{\partial(\rho uv)}{\partial x} = -\frac{\partial p}{\partial y} + \frac{\partial}{\partial y} \left( \lambda \operatorname{div} \bar{V} + 2\mu \frac{\partial v}{\partial y} \right) + \frac{\partial}{\partial x} \left[ u \left( \frac{\partial v}{\partial x} + \frac{\partial u}{\partial y} \right) \right] + \rho f_y \quad (2.38)$$

(2.37) and (2.38) show the conservative momentum equation of the fluid mass.

### 2.3 The model of fluid turbulence

The fluid at high Reynolds's number will be in turbulent form, which the quality of fluid will not in order. To find solutions of fluid mathematical problem, thus, will be digit methods that take times and is uneasy. Some people try to set the disorderliness model of fluid due to be used for calculate the fluid mass. Before that it needs to know the turbulent conduction of fluid and the average equation of Reynolds, as it's the fundamental concept based on turbulent fluid model.

#### 2.3.1 The average equation of Reynolds:

The velocity and all qualities of turbulent fluid disorderly will depend on time as in figure 2.6;  $u = u(x, y, z, t)$  is the quality of fluid and the function of location and time.

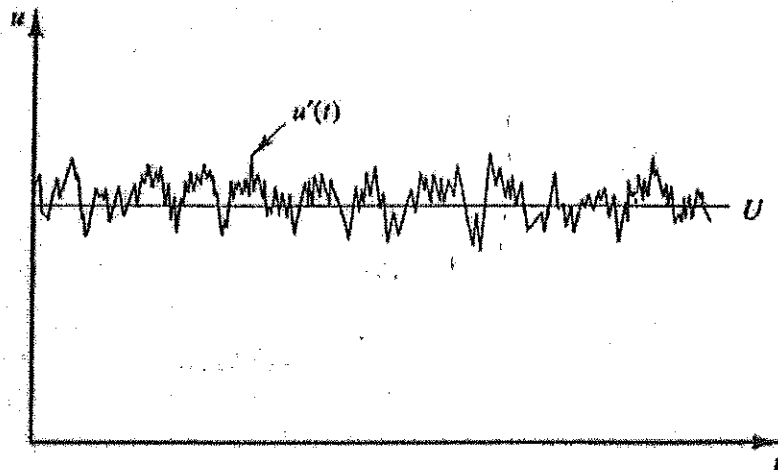


Figure 2.6 Disordered changes of variation fluid.

To be easier to solve the system of Navier-Stokes, Osborne Reynolds the average  $\bar{u}$  is set from

$$\bar{u} = \frac{1}{\Delta t} \int_0^{\Delta t} u dt \quad (2.39)$$

$\Delta t$  is the average of time. The wider space is the more accurate value. Mostly, its set  $\Delta t \rightarrow \infty$ , with quality of fluid will be  $u_i = \bar{u}_i + u'_i$   $U = \bar{U} + U'$  as in the vector form and will be replaced in Navier-Stokes equation.

Mass conservation equation

$$\frac{\partial \rho}{\partial t} + \text{div}(\rho \bar{U}) = 0 \quad (2.40)$$

The equation of three dimensional momentums

$$\frac{\partial(\rho \bar{u})}{\partial t} + \text{div}(\rho \bar{u} \bar{U}) = -\frac{\partial P}{\partial x} + \text{div}(\mu \text{grad} \bar{u}) + \left[ -\frac{\partial(\rho \bar{u}^2)}{\partial x} - \frac{\partial(\rho \bar{u}' v')}{\partial y} - \frac{\partial(\rho \bar{u}' w')}{\partial z} \right] + \rho f_x \quad (2.41)$$

$$\frac{\partial(\rho \bar{v})}{\partial t} + \text{div}(\rho \bar{v} \bar{U}) = -\frac{\partial P}{\partial y} + \text{div}(\mu \text{grad} \bar{v}) + \left[ -\frac{\partial(\rho \bar{u}' v')}{\partial x} - \frac{\partial(\rho \bar{v}^2)}{\partial y} - \frac{\partial(\rho \bar{v}' w')}{\partial z} \right] + \rho f_y \quad (2.42)$$

$$\frac{\partial(\rho \bar{w})}{\partial t} + \text{div}(\rho \bar{w} \bar{U}) = -\frac{\partial P}{\partial z} + \text{div}(\mu \text{grad} \bar{w}) + \left[ -\frac{\partial(\rho \bar{u}' w')}{\partial x} - \frac{\partial(\rho \bar{v}' w')}{\partial y} - \frac{\partial(\rho \bar{w}^2)}{\partial z} \right] + \rho f_z \quad (2.43)$$

Above equations called Reynolds's or Reynolds-Average Navier-Stokes equation (RANS). Those are similar to the former Navier-Stokes equation, but the stress on the right hand side parenthesis is added. All three dimensions will be six terms all together. Those stresses are called Reynolds stresses. By the experiment of Boussineq presented the relation of stress towards the average velocity of fluid by the transformation ratio of fluid element as:



Reynolds stresses, 
$$-\overline{p u_i u_j} = \mu_t \left( \frac{\partial u_i}{\partial z_j} + \frac{\partial u_j}{\partial x_i} \right) - \frac{2}{3} \left( \rho k + \mu_t \frac{\partial u_i}{\partial x_i} \right) \delta_{ij} \quad (2.44)$$

$\mu_t$  is Turbulent viscosity; a necessary variation that needs additional equation in order to enable the equation solves the problem. This equation is the model of turbulent fluid.

### 2.3.2 Standard $k - \varepsilon$ turbulent model

Standard  $k - \varepsilon$  turbulent model is what the turbulent viscosity works as the function of turbulent kinetic energy,  $k$ , and the dissipation of turbulent kinetic energy,  $\varepsilon$  with the two set of transferring equation of  $k$  and  $\varepsilon$  each

$$\frac{\partial(\rho k)}{\partial t} + \text{div}(\rho k \bar{U}) = \text{div} \left[ \left( \mu + \frac{\mu_t}{\sigma_k} \right) \text{grad} k \right] + G_k + G_b + \rho \varepsilon - Y_M + S_k \quad (2.45)$$

$$\frac{\partial(\rho \varepsilon)}{\partial t} + \text{div}(\rho \varepsilon \bar{U}) = \text{div} \left[ \left( \mu + \frac{\mu_t}{\sigma_\varepsilon} \right) \text{grad} \varepsilon \right] + C_{1k} \frac{\varepsilon}{k} + (G_k + C_{3\varepsilon} G_b) - C_{2\varepsilon} \rho \frac{\varepsilon^2}{k} + S_k \quad (2.46)$$

$G_k$  is the befallen kinetic energy. The average velocity  $G_b$  is the kinetic energy from the reaction of Buoyancy;  $Y_M$  is the reaction of the compress per the fluid turbulent viscosity ( $C_{1\varepsilon} + C_{2\varepsilon} + C_{3\varepsilon}$ ),  $\sigma_k$  and  $\sigma_\varepsilon$  respectively is the Prandtl number of  $k$  and  $\varepsilon$ .

Turbulent viscosity Model or  $\mu_t$  is

$$\mu_t = \rho C_\mu \frac{k^2}{\varepsilon} \quad (2.47)$$

When  $C_{1\varepsilon} = 1.44$ ,  $C_{2\varepsilon} = 1.92$ ,  $C_\mu = 0.09$ ,  $\sigma_k = 1.0$ ,  $\sigma_\varepsilon = 1.3$

### 2.3.3 $k - \varepsilon$ RNG turbulent Model:

$k - \varepsilon$  RNG is the invented turbulent model from the Navier-Stokes equation with the methodology called 'Renormalization Group' (RNG). Its turbulent viscosity is different and some terms are added from Standard  $k - \varepsilon$  model. The transferring equation is;

$$\frac{\partial(\rho k)}{\partial t} + \text{div}(\rho k \bar{U}) = \text{div} \left[ \alpha_k \mu_{\text{eff}} \text{grad} k \right] + G_k + G_b + \rho \varepsilon - Y_M + S_k \quad (2.48)$$

$$\frac{\partial(\rho\varepsilon)}{\partial t} + \text{div}(\rho\varepsilon\bar{U}) = \text{div}[\alpha_\varepsilon\mu_{eff}\text{grad}\varepsilon] + G_{1\varepsilon}\frac{\varepsilon}{k} + (G_k + C_{3\varepsilon}G_b) - C_{2\varepsilon}P\frac{\varepsilon^2}{k} - R_\varepsilon + S_\varepsilon \quad (2.49)$$

$G_k, G_b$  and  $Y_M$  similarly mean standard  $k - \varepsilon$  transferring equation; while  $a_k$  and  $a_\varepsilon$  respectively are the verse effective Prandtl numbers of  $k$  and  $\varepsilon$ . Through the differential equation of the turbulent viscosity of RNG  $k - \varepsilon$  model is

$$d\left(\frac{\rho^2 k}{\sqrt{\varepsilon\mu}}\right) = 1.72 \frac{\hat{v}}{\sqrt{\hat{v}^3 - 1 + C_v}} \quad (2.50)$$

$$\hat{v} = \mu_{eff} / \mu \text{ and } C_v \approx 100$$

By the equation 2.50 it will work well when the fluid is at low Reynolds number. If the fluid conducts at high Reynolds number, the equation 2.48 will be replaced with  $C_u = 0.0845$ . The calculation for  $\alpha_k$  and  $\alpha_\varepsilon$  solution is as below

$$\left| \frac{\alpha - 1.3929}{\alpha_0 - 1.3929} \right|^{0.6321} \left| \frac{\alpha - 2.3929}{\alpha_0 - 2.3929} \right|^{0.3679} = \frac{\mu_{mol}}{\mu_{eff}} \quad (2.51)$$

$R_\varepsilon$  in equation 2.49 can be solved from the relation blow; in case the high Reynolds number  $\alpha_k$  and  $\alpha_3 \approx 1.393$

$$Re = \frac{C_u \rho \eta^3 (1 - \eta/\eta_0) \cdot \varepsilon^2}{1 + \beta \eta^3} \cdot \frac{\varepsilon^2}{k} \quad (2.53)$$

The viscosity of equation 2.48 and 2.49 will be  $C_{1\varepsilon} = 1.42$ ,  $C_{2\varepsilon} = 1.68$

### 2.3.4 $k - \varepsilon$ Realizable turbulent model

Realizable turbulent model is invented by the Shih research group. It dissimilar from the two models mentioned above. The eddy-viscosity relation is invented in equation 3.18 by solving  $C_\mu$  as recommended by Reynolds's and build the equation of  $\varepsilon$  from dynamics equation model. The transferring equation of Realizable  $k - \varepsilon$  model is

$$\frac{\partial(\rho k)}{\partial t} + \text{div}(\rho k \bar{U}) = \text{div}\left[\left(u + \frac{\mu_t}{\sigma_k}\right) \text{grad} k\right] + G_k + G_b - p_\varepsilon - Y_M + S_k \quad (2.54)$$

$$\frac{\partial(\rho\varepsilon)}{\partial t} + \text{div}(\rho\varepsilon\bar{U}) = \text{div}\left[\left(\mu + \frac{\mu_1}{\sigma_k}\right)\text{grad}\varepsilon\right] + \rho C_1 S_\varepsilon - \rho C_2 \frac{\varepsilon^2}{k + \sqrt{\nu\varepsilon}} + C_{1\varepsilon} \frac{\varepsilon}{k} C_{3\varepsilon} G_b S_\varepsilon \quad (2.55)$$

when

$$C_1 = \max\left[0.43 \frac{\eta}{\eta + 5}\right] \quad (2.56)$$

$$\eta = S \frac{k}{\varepsilon} \quad (2.57)$$

As same as standard  $k - \varepsilon$  model the relation used for turbulent viscosity is from equation 2.49, but  $C_\mu$  will be used from

$$C_\mu = \frac{1}{A_0 + A_s \frac{kU^*}{\varepsilon}} \quad (2.58)$$

$$\text{Here } U^* \text{ is from } U^* \equiv \sqrt{S_{ij}S_{ij} + \bar{\Omega}_{ij}\bar{\Omega}_{ij}} \quad (2.59)$$

$$\text{An } \bar{\Omega}_{ij} = \Omega_{ij} - 2\varepsilon_{ijk}\omega_k \quad (2.60)$$

$$\Omega_{ij} = \bar{\Omega}_{ij} - \varepsilon_{ijk}\omega_k \quad (2.61)$$

In which  $\bar{\Omega}_{ij}$  definite mean rate-of -rotation tensor with the viscosity value at  $A_0 = 4.04, A_s = \sqrt{6\cos\phi}$ ; anyway

$$\phi = \frac{1}{3} \cos^{-1}(\sqrt{6W}), W = \frac{S_{ij}S_{jk}S_{ki}}{S}, \bar{S} = \sqrt{S_{ij}S_{ij}} \quad (2.62)$$

$$S_{ij} = \frac{1}{2} \left( \frac{\partial\mu_j}{\partial x_i} + \frac{\partial\mu_i}{\partial x_j} \right) \quad (2.63)$$

The viscosity value of transferring equation will be

$$C_{1\epsilon} = 1.44, C_2 = 1.9, \sigma_k = 1.0, \sigma_\epsilon = 1.3$$

#### 2.4 Continuity equation in an uninstalled air-propeller diffuser

According to momentum theory, the pressure and the velocity will be concerned to diffuser figure that will be changed as per space of the surface. In figure 2.7, the reference point will be the space at the diffuser outlet. The pressure at the back and the front of the diffuser equals atmospheric pressure,  $P_0$ . Bernoulli's continuity equation shows the total pressure as:

$$P_{tot} = P_0 + \frac{1}{2} \rho V_0^2 = P_1 + \frac{1}{2} \rho V_1^2 = P_3 + \frac{1}{2} \rho V_3^2 = P_0 + \frac{1}{2} \rho V_e^2 \quad (2.64)$$

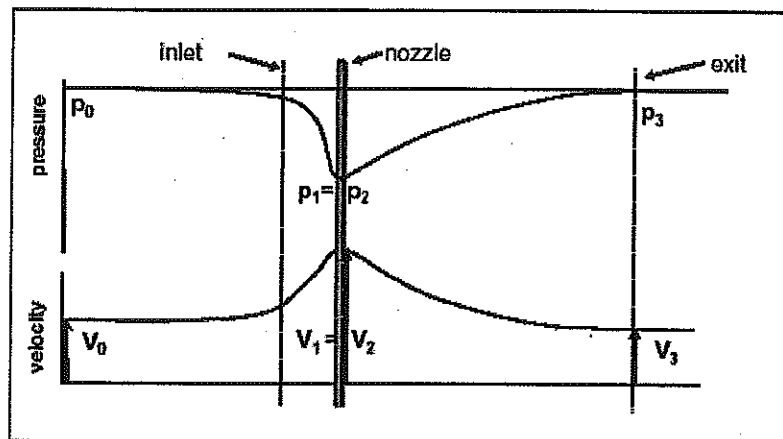


**Figure 2.7** The relations between the pressure and the velocity inside diffuser.

According to the continuity equation, the relationship between the velocity at the nozzle and velocity at the diffuser outlet will be

$$V_1 = \beta V_3 \quad (2.65)$$

$\beta$  is the diffuser area ratio

From equation 2.64, the total pressure at the nozzle equals:

$$P_{tot} = P_1 + \frac{1}{2} \rho (\beta V_0)^2 \quad (2.66)$$

If there is no back pressure at the diffuser outlet ( $P_3 = P_0$  and  $V_0 = V_3$ ), the pressure equation at nozzle will be:

$$P_1 = P_0 + \frac{1}{2} (1 - \beta^2) \rho V_0^2 \quad (2.67)$$

It is obvious that the pressure at the nozzle will be reduced when the diffuser area ratio ( $\beta$ ) is more than 1 and the diffuser outlet pressure will be less than the inlet velocity. The relationship between the inlet and the outlet velocities can be represented as:

$$V_3 = \gamma V_0 \quad (2.68)$$

where  $\gamma$  is the back pressure velocity ratio. The pressure at the nozzle then equals:

$$P_1 = P_0 + \frac{1}{2} (1 - \beta^2 \gamma^2) \rho V_0^2 \quad (2.69)$$

Hence, if the Diffuser area ratio  $\beta$  is more than 1 and back pressure equals naught or less, the pressure at nozzle will be lower than inlet pressure. To calculate the outlet velocity of Diffuser  $V_3$  will be easier if we know the geometric configuration of Diffuser. Also, the velocity at other locations can be calculated with continuity and under the assumption of a uniform velocity distribution at each diffuser section.

Through the force of the axial flow in the uninstalled turbine diffuser, when the conservation of momentum was applied with the circular-pipe shape air inlet, the total axial force on diffuser equals zero. Bernoulli's equation can be applied to all streamlines by using the same calculation. The unchanged velocity and pressure of the streamlines can be shown from the front and the back far away of the diffuser.

Without the turbine, the velocity ratio in the nozzle and the flow velocity before getting to the diffuser ( $V_0$ ) always causes an error in air propeller energy prediction. If equation

2.65 is combined with equation 2.68, the velocity at the nozzle equals  $\beta\gamma V_0$  but the maximum energy is unequally  $\beta^3\gamma^3 C_{p\max}$  where  $C_{p\max}$  defines the coefficient for the maximum energy obtained from the air propeller. If it is without a diffuser, the maximum will be much lower. This will be discussed later on.

## 2.5 Continuity equation inside Diffuser augmented wind turbine (DAWT)

When the diffuser comes with a turbine installed inside, the system study will not be easy. Using the one dimensional theory, the velocity is set from the diffuser configuration, though the configuration at the inlet is flat to protect the separation of fluid flow. The configuration sometimes is not important to be understand process of the DAWT function. Generally, the velocity at the outlet ( $V_3$ ) is lower than at the inlet one that can be lower until reaches the wake velocity ( $V_e$ ) at the atmosphere pressure ( $P_0$ ). The location of the turbine is unimportant to the study of the energy transformation topic in momentum theory. Turbines will lower the total pressure inside the diffuser, which obviously leads to decreasing total pressure at the outlet. The nozzle is the most appropriate location for the turbine because the lowest chord can build the smallest turbine.

Developed by Van Bussel, the one dimensional theory for an air propeller comes with the hypothesis that the wind at the outlet of the diffuser has the same status as the wind from a simple air propeller (without back pressure).

$$V_3 = (1 - a)V_0 \quad (2.70)$$

The axial induction factor ( $a$ ) will be specified for the outlet of diffuser the same as the general air propellers. This induction factor will be half of the one found in the wake of the DAWT ( $V_e = (1 - 2a)V_0$ ). According to the continuity equation, the velocity at the nozzle of the internal turbine equals  $V_1 = \beta V_3$

$$V_1 = (1 - a)\beta V_0 \quad (2.71)$$

For the cases of the velocity at other locations inside a non-turbine diffuser, it can be calculated using the continuity equation, when the back pressure at the outlet of diffuser is present. Then the velocity will equal

$$V_3 = (1-a)\gamma V_0 \quad (2.72)$$

The velocity at the nozzle will equal

$$V_1 = (1-a)\gamma\beta V_0 \quad (2.73)$$

The relationship of the pressure is from Bernoulli's theory when the location of turbine is at nozzle. The front pressure of the turbine equals

$$P_1 = P_0 + \left[1 - \beta^2 \gamma^2 (1-a)^2\right] \frac{1}{2} \rho V_0^2 \quad (2.74)$$

The back pressure of the turbine is

$$P_2 = P_0 + \left[(1-2a)^2 - \beta^2 \gamma^2 (1-a)^2\right] \frac{1}{2} \rho V_0^2 \quad (2.75)$$

The difference in pressure equals

$$P_2 - P_1 = 4a(1-a) \frac{1}{2} \rho V_0^2 \quad (2.76)$$

These are the old equations for straddling pressure of general turbines. On the other hand, the straddling pressure will not depend on the diffuser area ratio and the back pressure ratio. The location in the diffuser means that the gained energy per unit of air volume will equal that in a non-diffuser turbine. If compared to a simple turbine, the air flowing through the turbine in the diffuser case will be increased by a factor of  $\beta\gamma$ .

Force and Trust for a DAWT

From equations 2.73 and 2.67, the power coefficient of the turbine will equal

$$C_{P,rotor} = \beta\gamma 4a(1-a)^2 \quad (2.77)$$

and the power coefficient at the outlet of the diffuser equals

$$C_{P,exit} = \gamma 4a(1-a)^2 \quad (2.78)$$

As mentioned above, the thrust of the turbine in the diffuser will equal the thrust of a non-diffuser turbine. The equation for the conservative of momentum combined with the fluid in a DAWT will be

$$C_{T,Total} = \beta\gamma 4a(1-a) \quad (2.79)$$

Where, for the present purpose, the rotor area is used for non-dimensional the total thrust. This leads to the conclusion that the thrust on the diffuser is dependent upon the thrust of the rotor:

$$C_{T,Diffuser} = C_{T,Total} - C_{T,Rotor} = (\beta\gamma - 1)4a(1-a) \quad (2.80)$$

The diffuser thrust coefficient is non-dimensional with the rotor area. Diffuser thrust coefficient is not concerned to space of turbine. That is the thrust on diffuser will be the proportional of increasing mass in DAWT; whereas, the thrust on turbine is not.



## **CHAPTER 3**

### **LITERARY OVERVIEW**

The DAWT will be installed inside a duct with turbines. Its function is to broaden the air space before it reaches the turbines; this means that much more air will flow through the turbines with less internal pressure and result in a higher energy when compared to non-diffuser turbines. Therefore, there are many people interested in further studying the advantages of a DAWT and the application to a water current turbine that will be discussed later on.

#### **3.1 Diffusers and windmills**

D. G. Phillips et al. (2002) from the University of Auckland, New Zealand studied and developed a DAWT pilot model called Vortec7 using the concepts of Foreman and Grumman (1999). The external air jets are used to prevent fluid separation and control the boundary layer in the diffuser. Through studying an actual built model using CFD and flow visualization techniques, it was shown that there is fluid split at the back of the nacelle, and at the diffuser outlet flange, and there is reverse fluid around the inlet ring that causes a lowering of the effective flow area. It was also discovered that the velocity at the blade plane is changed, depending on blade radiance, and, if the value of disc loading is high, the fluid will be pushed to the diffuser, which causes a lowering on the capacity of the fluid split and the wall decrease, but the unwanted reverse fluid will happen around the nacelle widely. D. G. Philips, therefore, installed an elliptical nosecone with nacelle and bull nose at the inlet slot in order to protect against the fluid reversal. He also improved the diffuser outlet flange and secondary inlet slot in order to improve the flow effectiveness by directing the flow tangentially to the diffuser wall. Moreover, it increases the velocity at the inlet boundary control slot 67%, on the blade plane 10%, and at the blade tip 20%. If it is compared to the former model, it increases the power coefficient factor four times.

D. G. Phillips et al. (2008) also designed a new diffuser using the Vortec7 as the model. The inner inlet and the diffuser exit flange were cut off. He lengthened the primary

diffuser, revised the area ratio, and the diffuser angles such that the effectiveness is two times better than the first revision.

Toshio Matsushima et al. (2006) studied the results of frustum-shaped diffuser that effects to capacity of small air propeller. From the system model by I-DEAS software, he found the more length is the more air velocity at the inlet. The air velocity will increase with the increase in the expansion angle until it reaches  $6^\circ$ . Then the air velocity will be lower and the height of the flange (not over 0.2 m) affects the air velocity. A frustum-shape diffuser will increase the speed 1.7 times if the appropriate diffuser is chosen. The highest velocity at the inlet from the field test showed that the system is able to release the 2.4 times the energy of the equivalent non-diffuser turbine.

Yuji Ohya et al. (2008) studied and developed the installed-diffuser turbine. He has studied nozzle, cylindrical, and diffuser type turbines. The latter model is able to increase the velocity 1.8 times whereas the nozzle type reduces the speed and the cylindrical type maintains the speed. The properly developed diffuser is when  $L/D$  is more than three. In this case the velocity will be faster. In practice, the researcher has replaced  $L/D < 3$  by  $L/D = 2$  because its effectiveness is not significantly different, the diffusers are easy to install, and the diffuser open angle ( $\Phi$ ) is  $4^\circ$ . In addition, the researcher has installed an inlet shroud and ring type flange ( $h/D=0.25$ ) at the outlet of the diffuser, that help augment the air velocity by 1.6-2.4. Installation of a smooth curved inlet shroud helps smooth the fluid and control the fluid split at the inlet.

Setting up the ring type flange at the outlet of the diffuser causes a vortex with less static pressure at the outlet. The base pressure coefficient ( $C_{pb}$ ) at the outlet ( $\frac{x}{L} = 1$ ) = -0.75 and equals -0.2 if the flange is not installed. Vortex and the fluid split at the back of the flange bring more air into diffuser. Ohya then built the turbine and diffuser models and tested them in the lab. The  $L/D$  was overhauled to 1.25 to be a well-proportioned figure. The turbine will resist the air fluid if it is installed inside. Therefore, to control the internal fluid  $\Phi$  was revised to  $12^\circ$  and  $h/D = 0.5$ . Other revised proportions were the hub ratio to  $D_h/D=22$  and the center body length to  $L_s = 0.75L$ . The results show that installing the turbine inside diffuser releases 4-5 times the amount of outlet power over other uninstalled ones.

K. D. Visser (2009) reports on studying the Wind Tamer turbine. The concept of this turbine is to utilize a diffuser to increase the power produced by an open rotor wind turbine. The

configuration combines the concepts into a functionally attractive design that eliminates the need for furling and reduces noise. The WindTamer turbine has produced a power coefficient based on rotor area of twice of current small turbines. Visser also estimates for the WindTamer turbine that span a generator range of 1-15 kW with varying rotor diameters of 52-172 inches. Power ratings are defined at 11 m/s wind speed based on assumptions of an augmentation factor of 2, no furling of turbine, and a maximum continuous generator output at 33% above the stated generator value. It was observed from the numerical estimations that the Wind Tamer can produce approximately twice the annual energy output for a given swept rotor area as a conventional open rotor design.

Juma Yousuf Alaydi (2010) presents a theoretical demonstration of a DAWT. They studied the DAWT using one-dimension analysis, mathematical models, assumptions, estimations, and maximization of power coefficients and augmentation ratios. With momentum theory, it was shown that power augmentation is proportional to the mass flow increased in the throat of the DAWT. He also stated that increasing the diffuser area as well as the negative pressure at the diffuser exit was profitable. The rotor power coefficient values of  $C_{p,rotor} = 2.5$  might be achievable according to theory. An optimal exit-area-ratio depends upon economic arguments however the exit-area-ratio would not likely exceed a value of around three.

Yuji Ohya and Takashi Karasudani (2010) have developed a wind turbine that consists of a diffuser shroud with a broad-ring brim at exit periphery and a wind turbine inside. In a long diffuser (Length =  $1.47 \times$  diameter) the output power of a micro scale wind turbine was increased 4-5 times that of a conventional wind turbine. This was due to the low pressure region created due to a strong vortex that was formed behind the broad brim and caused more mass to pass through the diffuser. At the same rated power, a compact brimmed diffuser wind turbine is two-third the size of a bare turbine.

Ken-ichi Abe and Yuji Ohya (2004) investigated for flow fields around flanged diffusers to develop small-type wind turbines under 1.5 kW. Comparison of the computed results and experimental data shows the performance of a flanged diffuser strongly depends on the loading coefficient as well as the opening angle because it affects the nature of the separation appearing inside the diffuser. The investigation suggests that the loading coefficient for the best performance of a flanged diffuser is considerably smaller than that for a bare wind turbine.

### 3.2 A diffuser and a water current turbine

The results of diffuser per energy obtained from hydro turbine by the system model was studied by D. L.F. Gaden and Eric L. Bibeau (2008) under the steady state, inlet water velocity at 3.0 m/s and 2.4 meters of turbine diameter as fig 3.1

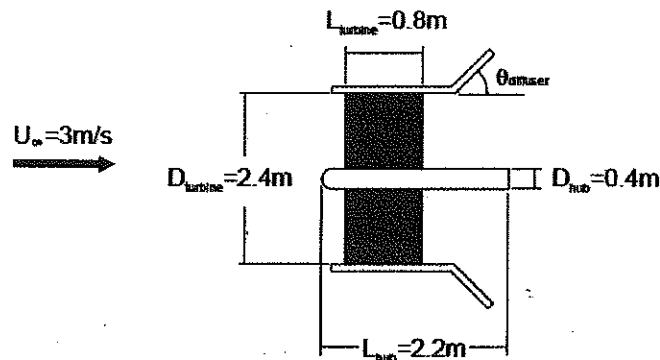


**Figure 3.1** Hydro turbine under the concept of David L. et al. (2008).

If the shroud is installed without the diffuser, the output power will be 16.4 kW when the Betz limit is 34.9 kW (only 46.9% of the maximum theoretical output.)

When the diffuser is installed inside the hydro turbine area ratios  $>1$  and  $<1.56$  will have the effect of augmenting the velocity or increasing the energy generated while the drag force will increase with the area ratio. The net result is that the energy generated will be at its maximum at a diffuser angle of  $20\text{-}30^\circ$  and then will decline. When the diffuser angle on the model was  $45^\circ$  there was a vortex at the outlet of the diffuser. From this study the well proportioned diffuser angle is  $20^\circ$ , with an outlet diameter at 3.0 meters. The generated energy will be 3.1 times that of a turbine with no diffuser installed.

By Brian Kirke (2005) is the study of setting  $1.2 \times 1.2$  meters slot duct that consist of 2-sided airfoil section slats with the cross flow hydro turbine with the velocity test at  $0.5\text{-}0.9\text{ m/s}$ . The capacity of  $C_p$  system will triple increased or be able to augment the water velocity 43% of the uninstalled diffuser ones. Somehow, it doesn't mention any information concerned to diffuser.

The study of F.L. Ponta and G. S. Dutt (2000); F.L. Ponta and P.M. Jacovkis (2008) reported on the development of a hydro turbine using a channeling device as shown in figure 3.2.

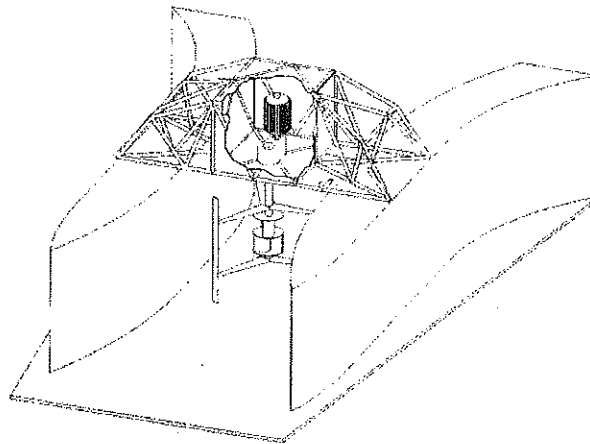


**Figure 3.2** F1-UBA Vertical axis water current turbines by Ponta and Dutt.

In the study of 5 forms of channeling devices, the output velocity was augmented 25-80% over the input velocity. When the external water velocity is higher than 2.0 m/s the channeling device has little effect on the augmentation of water velocity.

### 3.3 The particular study of diffuser

Karanja Kibicho and Anthony Sayers (2008) studied the fluid in wide angle diffuser, since the dispersion of pressure inside wide angle diffuser is irregular. There is a split of the fluid from wall but the fluid remains attached to the other side. This is called stalling. Stalling effects the overall fluid behavior inside the diffuser and makes the flow very inefficient. Kibicho and Sayers measured the complete velocity and static pressure fields and pressure recovery data for diffusers in fully stalled regimes with the Reynolds numbers between  $1.07 \times 10^5$  -  $2.14 \times 10^5$  and diffuser divergence angles between  $30^\circ$  -  $50^\circ$ . The Reynolds number did not significantly effect the velocity and pressure profile but rather effected the pressure recovery when the velocity was increased from 10 m/s to 20 m/s increasing the wall static pressure recovery 8.32%. If the diffuser angle is increased, the percentage of pressure recovery is also raised by a similar increase in the Reynolds number.

R. K. Sullerey et al. (1983) conducted a comparative study between the capacity of straight and curved diffusers at Reynolds numbers between  $7.8 \times 10^5$  -  $1.29 \times 10^6$ . The fluid behavior in the diffuser depends on the divergence angle, the ratio of the wall length to the throat width and

the turbulence of the inlet free stream. The study said that higher pressure coefficients are attainable with straight diffusers. Increasing stream turbulence has a favorable effect on diffuser performance.

### 3.4 The particular study of a horizontal axis water current turbine

In 2006 W. M. J. Batten et al. (2006) presented the methodology for the design of horizontal axis marine current turbines. They investigated the performance of 2D section shapes both experimentally in a cavitation tunnel and with numerical simulations. A numerical model of a typical 3D rotor is used to demonstrate parametric variations of the design parameters and the use of alternative blade sections. The results show that the narrow blades and near 2D flow, the turbine can be modeled successfully using blade element momentum theory. The investigation also demonstrates that the 0 degree pitch angle blades of the NACA 63-2xx and NACA 63-8xx series gave higher performance than the 8 degree pitch angle. It was reported that the NACA 63-2xx section blade at  $0^\circ$  pitch suffered some cavitation on the blade, while the NACA 63-8xx section was cavitation free. The cavitation can be avoided or minimized by suitable pitching of the blades or the use of a section with higher camber.

W. M. J. Batten et al. (2007) reported test results on 1/20th scale model of a 16m diameter horizontal axis tidal turbine. Cavitation tunnel experiments for different blade pitch settings were compared with simulations based on a blade element-momentum theory they developed. The results showed good agreement with theory. Then this numerical method was used as a tool for designing a turbine and optimizing the energy output with tidal data of Portland Bill. The results showed that there was a balance between design loads and energy yields.

D. P. Coiro et al. (2006) presented the numerical and experimental investigations of a scaled model of a horizontal axis turbine which was designed to harness energy from marine tidal currents, based on standard Glauert's blade element theory and modified Prandtl's theory. The scale model turbine was tested in a towing tank reproducing the same cavitation number and tip speed ratio (TSR) expected for the real scale turbine which is expected to produce 300 kW of electrical energy. The experiment data showed 45% efficiency and the turbine has good performance at design TSR and higher.

Danny Sale, Jason Jonkman and Walt Musial (2009) presented the adaptation of a wind turbine performance code for use in the development of a general use design code and optimization method for stall-regulated horizontal-axis hydrokinetic turbine rotors. This code couples a modern genetic algorithm and blade-element momentum performance code. They stated that this method calculates the optimal chord, twist, and hydrofoil distributions and rotor speed which maximize the hydrodynamic efficiency and ensure that the rotor produces an ideal power curve and avoids cavitation. They also verified the hydrodynamic model using an array of 6 35-kW, 5 m diameter turbines in the East River of New York. They found that the errors of prediction of mechanical power were  $\pm 15\%$ .

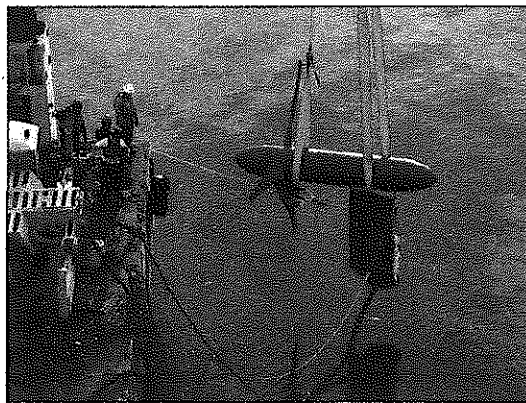


**Figure 3.3** The 35-kW hydro turbine of Danny Sale et al. (2009).

Ju Hyun Lee et al. (2011) reported on studying horizontal axis marine current turbines using computational and experimental methods. For the computational analysis, two methods were utilized: the blade element momentum theory (BEMT) and the computational fluid dynamics (CFD) method, based on the Reynolds-averaged Navier-Stokes equations. For the experimental analysis, open water tests were carried out in a towing tank. The comparison of CFD and experimental results showed that the results of BEMT and CFD were close to each other around the design TSR. The peak power was predicted around the design TSR of 0.46 for both cases. The differences between the experimental and computational results are considered mainly as Reynolds number effects. Due to the friction loss in the gear, the torque was slightly under-measured.

X. Sun, J. P. Chick and I. G. Bryden (2008) reported the establishment of a laboratory-scale model, by using the commercial computational fluid dynamics (CFD) code Fluent, in order to predict local-flow consequences resulting from the extraction of energy in a tidal flow. The CFD model simulates the operational conditions for tidal energy extraction in a channel. A wake region is formed behind the tidal energy converter, which is characterized by reduced velocity due to energy loss. The velocity however, recovers gradually with downstream distance. Since the mean velocity in the wake is lower than the free stream velocity, the velocity outside the wake in the channel must be higher than the free stream in order to maintain continuity of flow rate. Because of the blockage effect, the water speed is accelerated around the tidal energy converter and also along the downstream wake. The CFD results also demonstrated that the distortion of the free water surface will distort the wake and influence the performance of a turbine. Hence, the use of theoretical methods for wind turbines would cause fundamental errors, when applied to tidal current devices.

T. O'Doherty et al. (2009) studied and described in their paper using CFD and laboratory tests undertaken on a 0.5 meter diameter horizontal axial tidal turbine (HATT). The viscous models all performed well at predicting the power characteristics, but the higher order turbulence models captured the full operational range of the measured power and torque curves better, with the Reynolds Stress Model (RSM) being the preferred model. The predicted  $C_p$  for this blade design of  $\sim 0.4$  was confirmed by the experimental study which also confirmed the relative insensitivity to the blade pitch angle within the discussed range of  $3^\circ - 9^\circ$ .

Chris Garret and Patrick Cummins (2007) report on the maximum efficiency of turbines in a tidal channel. In order to achieve the upper limit the turbines should be deployed uniformly across the channel, with all the flow through them. An isolated turbine is more effective in a channel than in an unbounded flow, but the current downstream is non-uniform between the wake and the free stream. Hence some energy is lost when wake and free stream merge as occurs in a long channel. For the ideal turbine, the fractional power loss increases from  $1/3$  to  $2/3$  as the fraction of the channel cross section spanned by the turbine increases from 0 to 1.



## CHAPTER 4

### RESERCH METHODOLOGY

#### 4.1 Research Methodology

In the study the important tool is Computational Fluid Dynamics (CFD) Program that will be able to show the virtual flow that occurred inside diffuser and turbine. The fundamental turbine design was applied with Blade element momentum (BEM), then created the flow simulation by CFD that would probably be revised its design if necessary. Designed by CFD, the authentic.

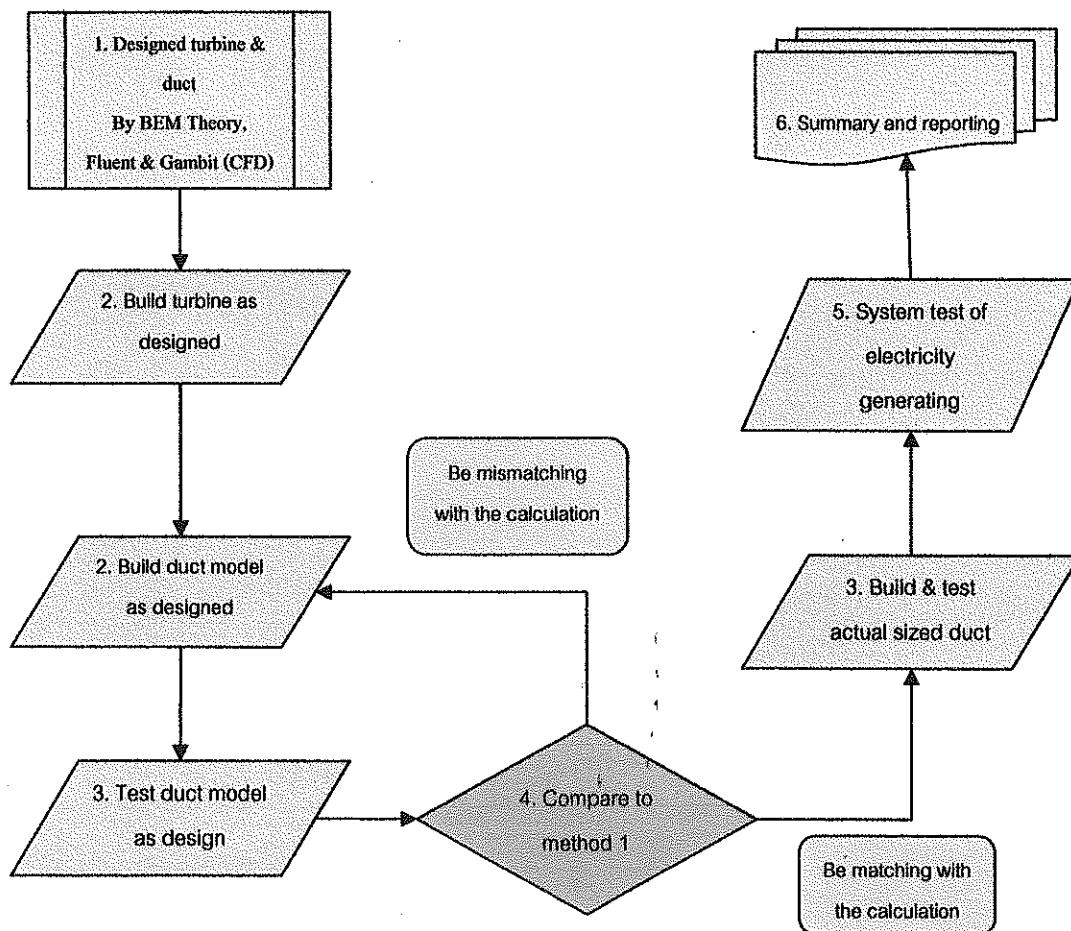


**Figure 4.1** Research methodology

In this study the important tool is the Computational Fluid Dynamics (CFD) Program that will be able to show the virtual flow that occurs inside diffuser and turbine. The fundamental turbine design was applied with Blade Element Momentum (BEM), then the flow simulation was created by CFD that would probably be revised its design if necessary. Designed by CFD, the authentic figure would be simulated to compare its result and chose the proper design to be built in reality. To examine power generating, it would be tested in a current during the last stages Sirindhorn Dam, Ubon Ratchathani.

## **4.2 Computational Fluid Dynamics (CFD)**

CFD (Computational Fluid Dynamics) is the fluid system analysis using numerical methods to determine the solution. In this process, a computer is used to do the calculations by iteration. There are three main processing methodology that consist of

(1) The pre-processor is to define the physical domain, split the domain problem into small cells, and define fluid properties and characteristics of flow such as laminar or turbulent flow and the boundary conditions.

(2) The processor calculation will solve the problem using the numerical method in order to determine the solutions. There are three popular processing methods at present: (1)The finite difference method; (2) The finite element method; and (3) The finite volume method. Their details will be discussed later on.

(3) The post-processor shows the solutions to the problem, which are generally the contour, graph, or vector.

The analysis of fluid dynamics problems will be concerned with partial differential equations that explain the properties of fluid related to mass, momentum, and energy conservation. Their details are 2. The finite volume method will be discussed in the report, since this discretization was applied in the FLUENT 6.3.

### **4.2.1 Finite volume method**

In this case, the technique in the CFD calculation will mainly the finite invent volume method to invent fluid calculation program because it's particularly created for fluid flow. The method will be able to integrate the problem equation throughout the controlled volume, such as setting heat conduction in one dimension as Figure 4.2

$$\frac{df}{dx} \left( K \frac{dT}{dx} \right) + S_x = 0 \quad (4.1)$$

After the integration completes Equation 4.1 throughout, the controlled volume will be

$$\int_{\Delta v} \frac{df}{dx} \left( k \frac{dT}{dx} \right) dV + \int_{\Delta v} S_x dV = \left( KA \frac{dT}{dx} \right)_e + \left( KA \frac{dT}{dx} \right)_w + \bar{S} \Delta V = 0 \quad (4.2)$$

The estimation of linear change (k) will be

$$K_w = \frac{K_w + K_p}{2} \quad \text{and} \quad K_e = \frac{K_e + K_p}{2} \quad (4.3)$$

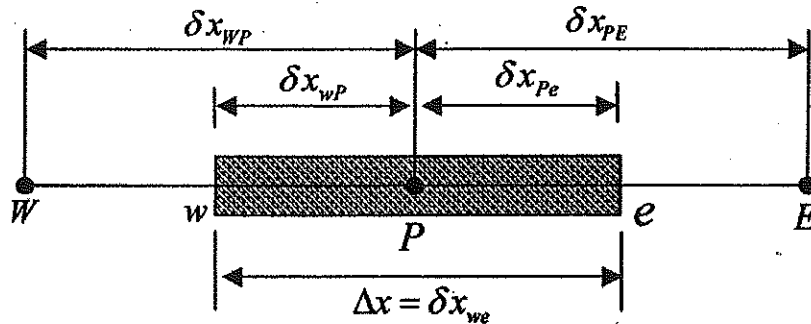


**Figure 4.2** Finite volume methods in 1 dimension.

The heat conduction will be

$$\left( KA \frac{dT}{dx} \right)_e = K_e A_e \left( \frac{T_e - T_p}{\delta x_{pe}} \right) \quad \text{and} \quad \left( KA \frac{dT}{dx} \right)_w = K_w A_w \left( \frac{T_p - T_w}{\delta x_{wp}} \right) \quad (4.4)$$

After combining with Equation 4.2 the value will be

$$\left( \frac{K_e}{\delta x_{pe}} A_e + \frac{K_w}{\delta x_{wp}} A_w - S_p \right) T_p = \left( \frac{K_w}{\delta x_{wp}} A_w \right) T_w + \left( \frac{K_e}{\delta x_{pe}} A_e \right) T_e + S_u \quad (4.5)$$

Equation 4.5 is the estimation equation to solve heat Equation of 4.1 using the finite volume method. Next, it is the mathematical calculation continuously towards circumference areas. At the end of the calculation the residual fraction will be compared to the satisfaction value. If the residual is too large, the iteration needs to be continued until it converge.

As aforementioned, the problems become more complicated when there are more differential equations. It is tough work and needs high accuracy. It's necessary to set the equation process of the finite volume method in order to arrange the priority of the equation sets before being processed computationally.

#### 4.2.2 Solution methods:

The mathematical fluid solution will use all three types of conservation equations and others, such as the turbulent model, the fluid equation (if there are several types of fluid), and other scalar equations. The solution methods of each will affect the keys and average values. Generally, the computation will be comprised of two solution methods, which depends on the type of problem as follows:

4.2.2.1 The methods of solving momentum equation prior to others is to repeat the method of equation sets, as the conservation equation will not be a linear type. So, the segregated solver methods will be as in Figure 4.3

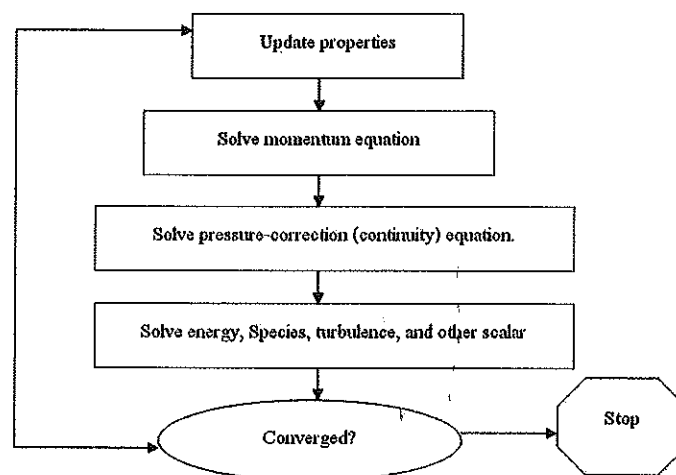


**Figure 4.3** The Segregated solver computation graph.

(1) The updated properties will be input into the equation at the beginning of the method. The update properties will be improved every time when the computation methods start.

(2) All three conservation equations will be computed to find out the pressure and fluid ratio of fluid velocity.

(3) As the fluid velocity in the previous iteration probably doesn't match the conservation of mass equation, in this iteration it needs to be revised by the pressure – correction equation, which is combined from the conservation of mass equation and the momentum; so that, the pressure value, the fluid ratio, and the velocity will be more appropriate.

(4) This iteration is used to solve other additional equations of each problem, such as the energy equation, the turbulence model, and other scalar equations by using the values obtained from previous turbulence model, and other scalar equations by using the values obtained from previous.

(5) The acceptance of computation results from the residual fraction will be set in this iteration. If the obtained value is too high to be accepted, it needs to be recomputed (repeat the iteration) until it will be less than or equal to the acceptable point.

4.2.2.2 The coupled solver method seems to be new for computation. Both conservation equation and the fluid equation (in case there are several fluid types) are operated together before solving other scalar equations. To calculate these equations mathematically needs the circular operation as demonstrated in Figure 4.4

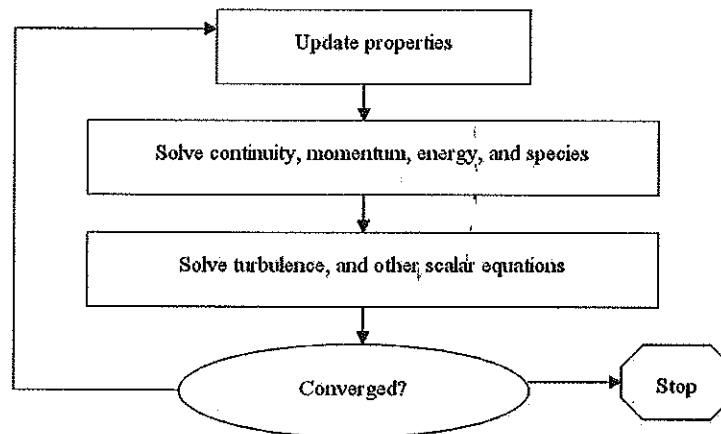


**Figure 4.4** Coupled solver graphs of computational method.

(1) As in the previous method, the updated properties will be input into the equation at the beginning of the method. The updated properties will be improved every time when the computation methods start.

(2) The next step is to calculate the conversation equation and the fluid equation (in case there're several fluid fluid types).

(3) Then, the equation of turbulent model and other scalar equations will be computed the obtained value from previous method.

(4) Last, there's a residual fraction evaluation to determine if the solution is acceptable. If the obtained value is too high to be accepted, it needs to be recomputed (turn back to step 1) until the residual fraction is less than or equal to the acceptable point.

#### **4.2.3 Computation methods:**

There are two methods of solving differential equations in numerical analysis; the explicit method and the implicit method. What makes them different is the way of setting the linear equation of the relation between node and element in order to replace in the relation of differential unknown value. But the implicit method will be used together with segregated solver computation because such calculation type will calculate the single variation of all elements at the same time. The coupled solver method is able to use either the explicit or implicit method or both.

#### **4.2.4 Solution methods of the near-wall model and the near-wall function:**

It's so important to the mathematical fluid model. The wall of fluid velocity will be close to naught or be naught because the fluid viscosity will be so effective. Besides, the wall friction is the key factor that causes circulation and fluid turbulence. Thus, it's necessary to find out the solutions of these problems by mathematical methods.

There are two options in the FLUENT program to solve those two mentioned problems; the near-wall function and near-wall model, with different computation methods. The near-wall model will be in the terms of the turbulent model in order to particularly solve this problem by decreasing the near-wall elements and continue calculating each element until stick the wall. Meanwhile, the near-wall function will set the separating function from the turbulent model to calculate the properties of the fluid at the near-wall element. The standard near-wall function and non-equilibrium near-wall function are the types handled by FLUENT. The limitation of both near-wall functions is that they are not good at calculating the fluid at low Re

value and its hypothesis doesn't cover all problems. As such, to solve the problem of the uncertified near-wall function model, the capable model that can be used with such a turbulence model has been built. It's called the 'enhanced near-wall model'. The concept of function setting is used to improve the turbulence model that brings the effectiveness to the solution of wall function problems and be able to use it widely and thoroughly.

#### 4.2.5 Dimensional simulation setup

Two types of diffuser were studied 1) a 2-shell diffuser with a curved space at the inlet and 2) a simple diffuser with a flat space at the inlet. The boundary of simulation is show in Figure 4.5 and calculation conditions in Table 4.1.

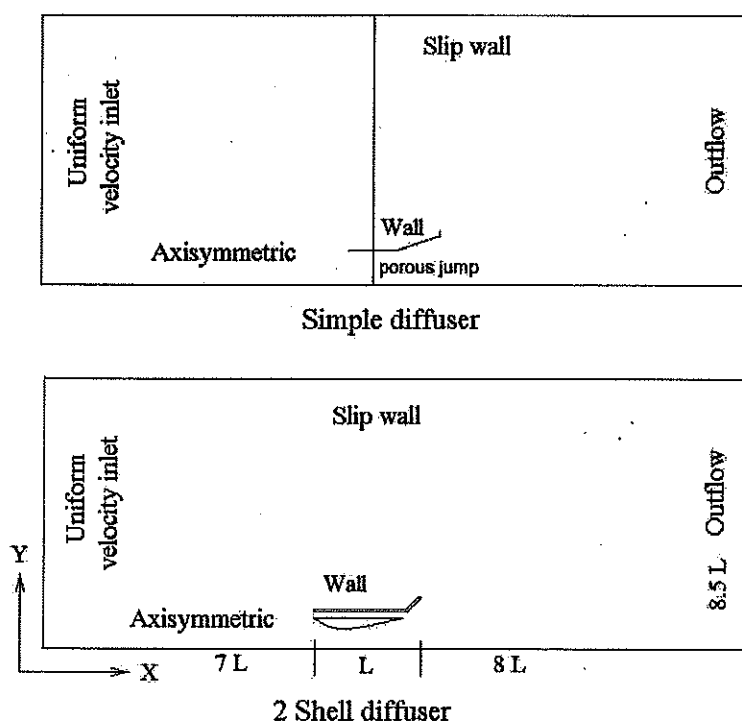
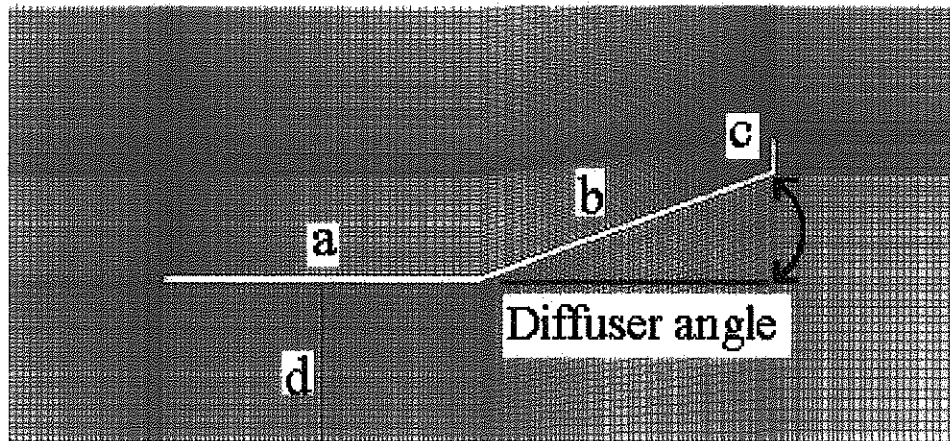


Figure 4.5 Domain the 2 D problems.

The domain of the fluid model problem would include the diffuser and the turbine area which are specified as the wall and the porous jump condition respectively. Inlet boundary use of uniform flow velocity, outlet boundary use of outflow, top wall use of slip wall and bottom wall use of axisymmetric boundary as indicated in Figure 4.5. Figure 4.6 show the dimension and angle a simple diffuser when a, b, equals 0.5 L, c equals 0.05 L and d equals 0.25 L

( $L$  is a total length of diffuser). Before using Fluent 6.3 to solve the problem, the domain would be divided with a quadrilateral grid of approximately 11,000 cells; there was more density in the grid at the diffuser wall and the turbine area.



**Figure 4.6** Diffuser angle.



**Table 4.1** Fluent set up for 2D diffuser simulation.

Condition	Type
Solver	Solver: pressure base Formulation: implicit Space: axisymmetric Time: steady Velocity formulation: absolute Gradient option: green gauss cell based Porous formulation: superficial velocity
Viscous model	Model: K-e epsilon (2 eqn.) K-e epsilon model: RNG Model constant: default Near wall treatment: standard wall functions
Solution controls	Under-relaxation factors: default Pressure- Velocity coupling: simple Discretization, Pressure: standard Momentum: first order upwind Turbulent kinetic energy: first order upwind Turbulent dissipation rate: first order upwind
Convergence criteria	1e-6

In this study the flow was set as axisymmetric steady flow. The segregated solver was employed as the solution method. When the turbulence model was the RNG  $k - \varepsilon$  model, the standard near- wall function was used for the near-wall treatment method with a convergence criterion of  $10^{-6}$ . The size of the diffuser would remain the same, except that the diffuser angle (as shown in figure 4.6) changed from 0-90 degrees, and the pressure of the porous medium could be found from Darcy's Law and an additional inertial loss term as in the equation.

$$\Delta p = \left( \frac{\mu}{\alpha} v + C_2 \frac{1}{2} \rho v^2 \right) \Delta m \quad (4.6)$$

Where  $\mu$  is the laminar fluid viscosity,  $\alpha$  is the permeability of the medium,  $C_2$  is the pressure-jump coefficient,  $v$  is the velocity normal to the porous face, and  $\Delta m$  is the thickness of the medium.

#### 4.2.6 3-Dimensional simulation setup

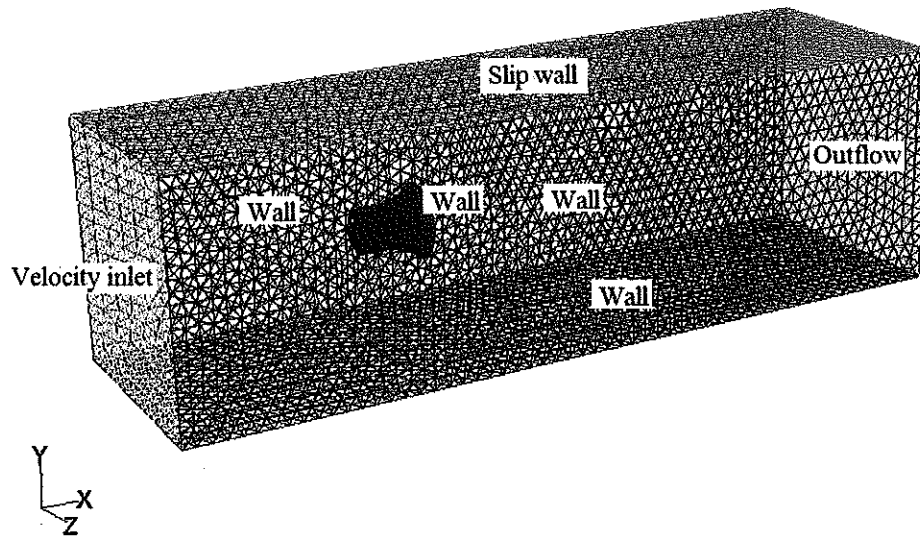


**Figure 4.7** Domain of 3 D problem.

**Table 4.2** Fluent set up for 3D diffuser simulation.

Condition	Type
Solver	Solver: pressure based Formulation: implicit Space: 3D Time: steady Velocity formulation: absolute Gradient option: green gauss cell based Porous formulation: superficial velocity
Viscous model	Model: K-e epsilon (2 eqn.) K-e epsilon model: RNG Model constant: default Near wall treatment: standard wall functions
Solution controls	Under-relaxation factors: default Pressure- Velocity coupling: simple Discretization, Pressure: standard Momentum: first order upwind Turbulent kinetic energy: first order upwind Turbulent dissipation rate: first order upwind
Convergence criteria	1e-5

The fluid model would cover the diffuser and the turbine areas that were specified as wall and porous jump conditions. The inlet boundary was indicated as having uniform flow velocity, the outlet boundary was indicated as outflow, the top wall was indicated as a slip wall, and the bottom was indicated as the wall of both sides of the boundaries as in Figure 4.7. The domain was separated into a quadrilateral grid of 400,000-800,000 cells.

#### 4.2.7 Simulation of a diffuser augmented water current turbine (DAWT)

To be convenient and accurate, the axis would be rotated and the turbine left still, its answer would be proceeded with CFD that would cause relative velocity when facing headwind as same as when the turbine is rotating through fluid. Therefore, the relationship

between relative velocity and absolute speed would be  $U_r = U - (\omega \times r)$  that would cause two terms for acceleration in the momentum equation.

$$\frac{\partial \rho U_r}{\partial t} + \nabla \cdot (\rho U_r U_r) + 2\rho \omega \times U_r + \rho \omega \times (\omega \times r) = \nabla \cdot \sigma \quad (4.7)$$

Conservation of momentum rotated the frame of reference in the form of relative velocity without calculating gravitational force;

Where  $2\rho \omega \times U$  is the Coriolis force and  $\rho \omega \times (\omega \times r)$  is centrifugal force. On the other hand, the momentum equation for the frame of reference would be written in the form of absolute speed as follows:

$$\frac{\partial \rho U}{\partial t} + \nabla \cdot (\rho U U) + \rho (\omega \times U) = \nabla \cdot \sigma \quad (4.8)$$

When  $\sigma$  was the tensor of the Newtonian fluid stress and would be as follows if combined with turbulent fluid simulation by the Eddy viscosity tensor:

When  $\mu_{eff} = \mu + \mu_t$ ; where  $\mu$  is the fluid viscosity and  $\mu_t$  is the virtual viscosity gained from turbulent viscosity simulation (eddy viscosity) which needs to found from the turbulence equation. In the study  $\mu_t$  would be from  $k - \varepsilon$  where  $\mu_t = \rho c_\mu (k / \varepsilon)$ ,  $c_\mu = 0.09$ , and  $k$  and  $\varepsilon$  need to be calculated from the Law of the Conservation of Momentum which was not mentioned here.

#### 4.2.8 Computational conditions

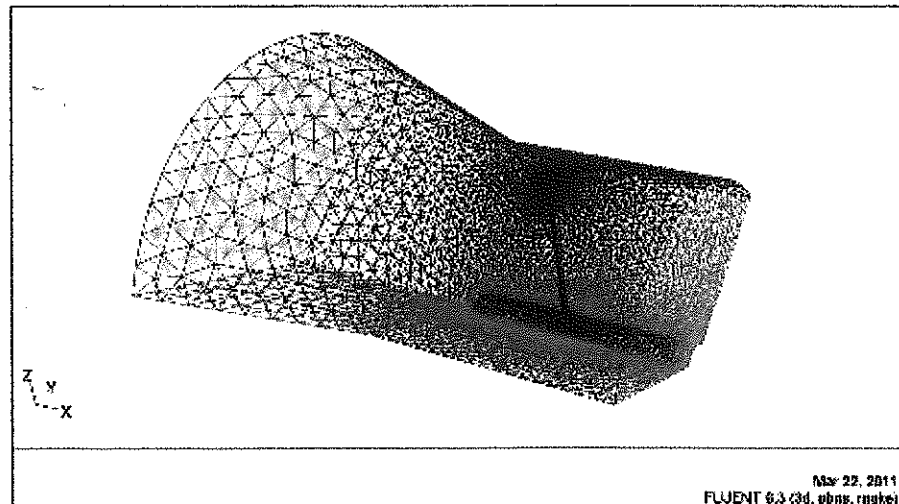


**Figure 4.8** Domain of DAWT Simulation.

The domain be divided into a grid 415,000 and 517,000 cells that covered and set diffuser, turbine blade and. The inlet boundary was specified as having uniform flow velocity and the outlet boundary was specified as outflow, diffuser, turbine blade and hub was set as stationary wall and moving wall respectively. Only one third of all scope would be calculated, since it was period repeating as in Figure 4.8 , the fluid on turbine surface was set to rotate when compared to the absolute axis; the turbine blade was not moved.

**Table 4.3** Fluent set up for DAWT Simulation.

Condition	Type
Solver	Solver: pressure based Formulation: implicit Space: 3D Time: steady Velocity formulation: absolute Gradient option: green gauss cell based Porous formulation: superficial velocity
Viscous model	Model: K-e epsilon (2 eqn.) K-e epsilon model: RNG Model constant: default Near wall treatment: standard wall functions
Solution controls	Under-relaxation factors: default Pressure- Velocity coupling: simple Discretization, Pressure: standard Momentum: first order upwind Turbulent kinetic energy: first order upwind Turbulent dissipation rate: first order upwind
Convergence criteria	1e-5

### 4.3 Blade element momentum theory: BEM

To design a turbine blade, the researcher chose the airfoil model fx63-317 that functioned well in giving a high lift force in low velocity conditions. The attack angle was set at 7 degrees where the ratio of  $C_L/C_D$  force was highest at the Reynolds number 300,000. This was acsimilar Reynolds number as in Figures 4.9 and 4.10.

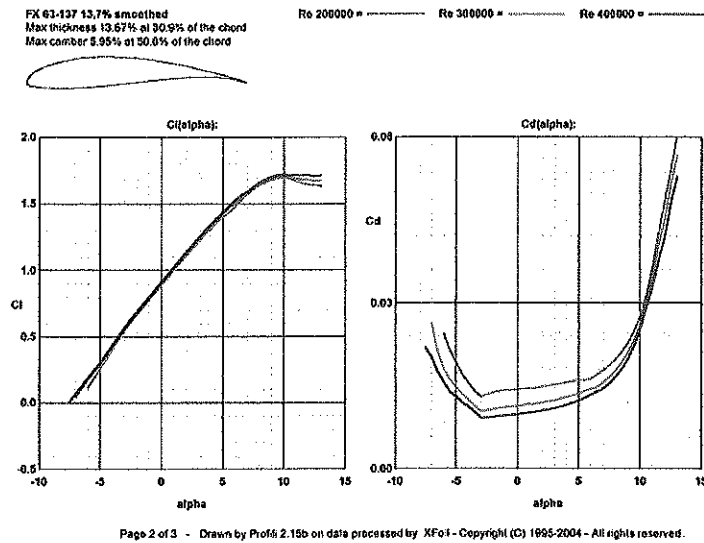


**Figure 4.9** Lift and drag coefficient of the FX 63-317.

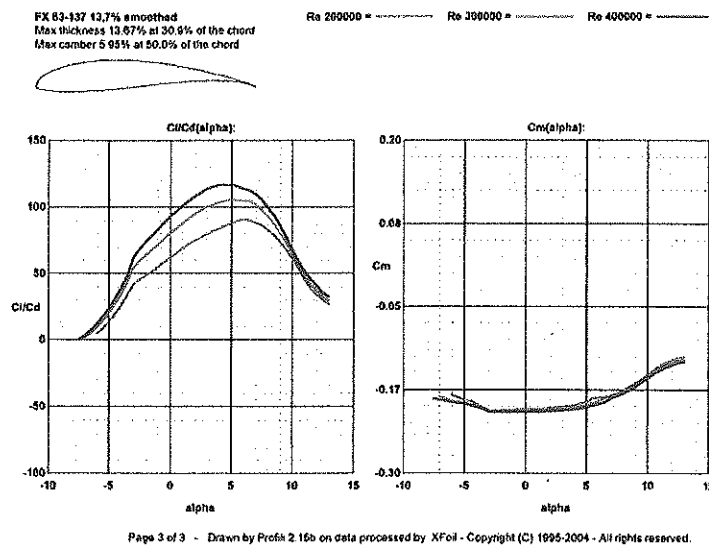


**Figure 4.10** The ratio of lift to drag coefficient and moment coefficient of the FX 63-317.

Designing a turbine blade includes consideration of size, twist angle, and capability. This could be done by iterating until the optimum answer was found. Here, prediction of  $a$  and  $a' - C_D =$  and tip loss correction = 1, would yield the following equations:

$$\tan \beta = \frac{\lambda_r (1 + a')}{(1 - a)} \quad (4.10)$$

$$\frac{a}{1-a} = \frac{\sigma'(C_L \sin \beta)}{4 \cos^2 \beta} \quad (4.11)$$

$$\frac{a'}{1-a} = \frac{\sigma' C_L}{4 \lambda_r \cos \beta} \quad (4.12)$$

The calculation process and iteration were:

- (1) Calculate  $a$  and  $a'$ .
- (2) Calculate  $\lambda_r$  and  $\beta$ .
- (3) Examine  $C_L$  and  $C_D$  to find proper incidence angle.
- (4) Again find  $a$  and  $a'$  by calculating and comparing to 1.

When getting results of the blade size and twist angle, it would be written by Gambit software, then calculated with the Fluent commercial code to find the ability of the turbine and finally examined to generate electricity.

#### 4.4 Experimental set up

##### 4.4.1 Diffuser model test

- 4.4.1.1 Install the diffuser model in the water flume.
- 4.4.1.2 Measure the pressure at difference point of duct and free flow.
- 4.4.1.3 Calculate velocity from at water level.
- 4.4.1.4 Calculate the augmentation factor of the duct model from velocity at the duct throttle divided by inlet free flow.

##### 4.4.2 Diffuser test

- 4.4.2.1 Install the diffuser model in the water flume.
- 4.4.2.2 Measure the water speed in the diffuser and at the free flow inlet.
- 4.4.2.3 Calculate the augmentation factor of the diffuser from the velocity at the duct throttle divided by the inlet free flow.

##### 4.4.3 Electricity generating test

- 4.4.3.1 Assemble and set all systems.
- 4.4.3.2 Test the system.



4.4.3.3 Record the free flow speed and released energy that come from the generator on the Data logger, then transfer it into the laptop computer in order to calculate for the next step.

4.4.3.4 Calculate the power coefficient of the turbine from equation below.

$$C_p = \frac{P}{\frac{1}{2} A \rho V_0^3}$$

When  $P$  is the electric power divide by generator efficiency

$A$  is the swept area of the turbine

$\rho$  is the density of the fluid

$V_0$  is the free flow velocity

## 4.5 Summary and Report

Collecting information/ Information sources

4.5.1 Reference sources: all researches was found in energy journals, papers from meetings or seminars or [www.sciencedirect.com](http://www.sciencedirect.com), [www.google.com](http://www.google.com), [www.eppo.go.th](http://www.eppo.go.th), [www.egat.co.th](http://www.egat.co.th), etc.

4.5.2 Collecting data was from the test will be from the individual or automatically saved with the memory of the measurement tools. After the tests were complete all collected data was transferred into the laptop computer in order to process forwards.

4.5.3 Processing methods / analysis / and synthesis have been computed by the Fluent commercial code program and have been designed and compared to the test results by the Gambit program. The basic design of the water current turbine is from Blade element- Momentum Theory.

## 4.6 Required tools and appliances for research

4.6.1 Fluent commercial code program.

4.6.2 Laptop computer.

4.6.3 Water speedometer.

4.6.4 Digital data logger.

4.6.5 Power meter.

## CHAPTER 5

### RESULTS AND DISCUSSIONS

#### 5.1 2 Dimensional simulation results of the diffuser

##### 5.1.1 2-Shell diffuser simulation results

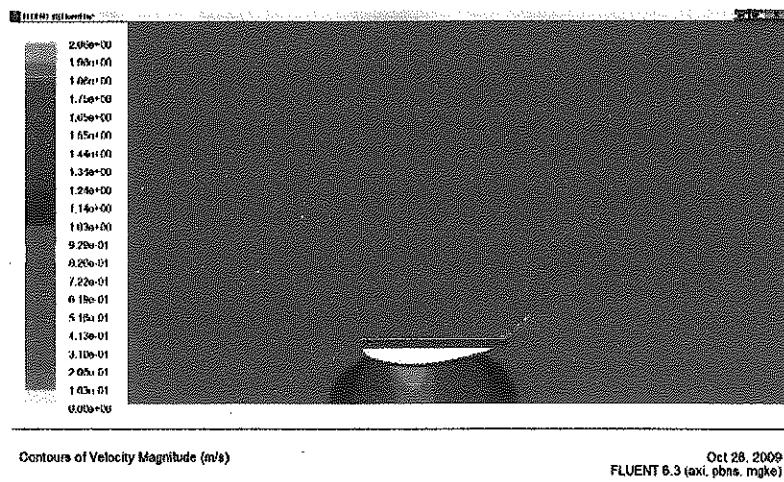


**Figure 5.1** Velocity contour of 2 shell diffuser.

Figure 5.1 shows the velocity contour of 2-shell diffuser simulation. From the figure, the velocity contour was faster at the inlet and reached the maximum rate at the half way point of the diffuser, it then slowed down little by little. The maximum velocity was 1.98 m/s; while the water velocity at the inlet was 0.9 m/s or the water velocity at the inlet was increased 2.2 times by the 2-shell diffuser. In addition, it found that there was a swirl flow at the outlet as can be seen in Figure 5.2 when static pressure was getting down while the velocity inside the diffuser increased.

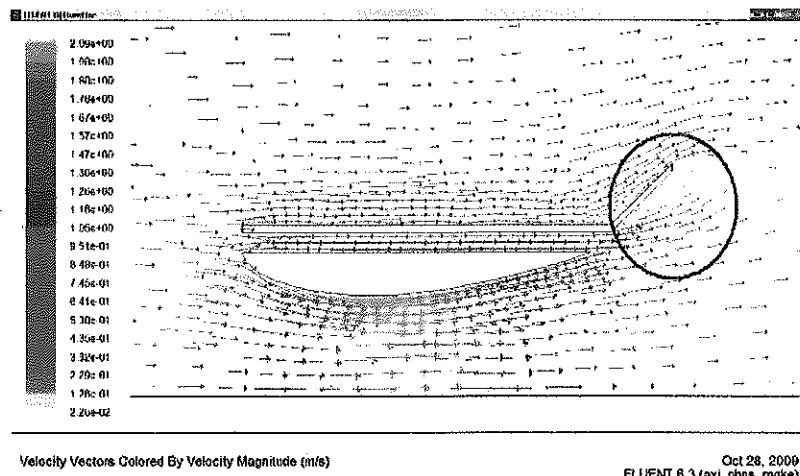


**Figure 5.2** Velocity vector of 2 -shell diffuser.

### 5.1.2 Simple diffuser simulation results

Regarding the study of flow in the simple diffuser at the steady state as in Figure 5.3, the velocity contour was faster at the inlet and reached the maximum rate at the half way point of the diffuser. Initially, the water velocity at the inlet was high and changed from 1.0 m/s to 1.9 m/s. This was lower increase when compared to the 2-shell diffuser in Figure 5.1.

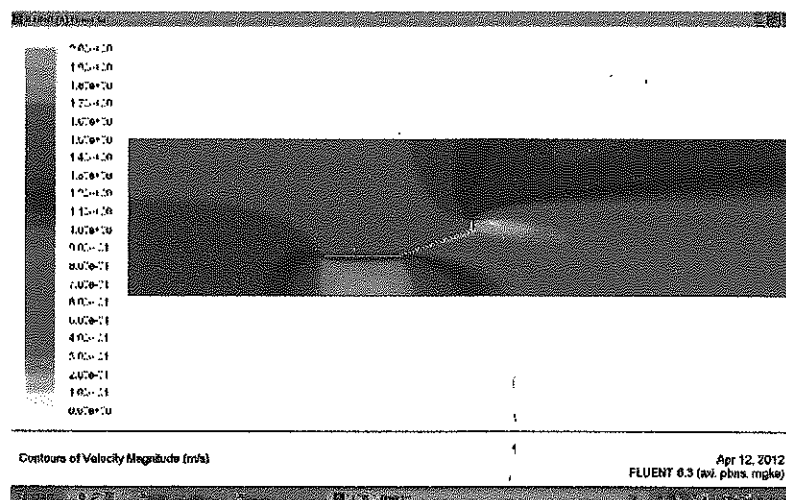


**Figure 5.3** Velocity contour of simple diffuser.

Figure 5.4 shows the velocity vector of the simple diffuser that was recognized regarding the color of water velocity. It resulted that water direction swayed at the inlet to diffuser

as indicated in the black line that caused the velocity inside diffuser higher. Then, at the outlet of diffuser water direction swayed out of the line, velocity was getting slow, while the pressure was higher.

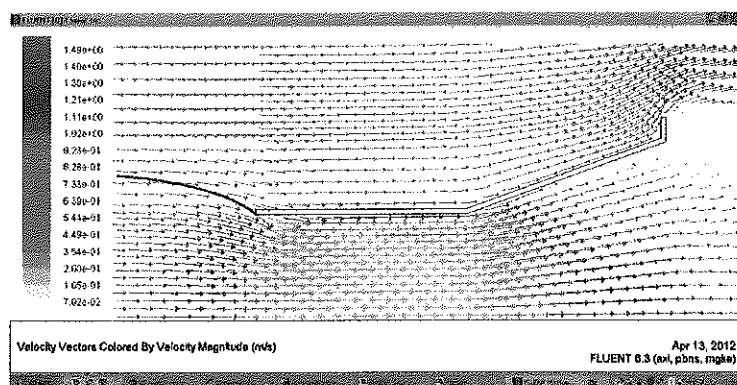


Figure 5.4 Velocity vector of the simple diffuser.

### 5.1.3 The comparative of simulation results of simple diffuser and 2 shell diffuser

Figure 5.5 compared the pressure coefficients between the 2-shell diffuser and the simple diffuser. The pressure of both types of diffuser was similar but the minimum pressure. The 2-shell diffuser came with lower pressure inside diffuser, when the pressure at the surface of outlet was higher  $x/L=0$  was at the inlet and  $x/L=1$  was the outlet.

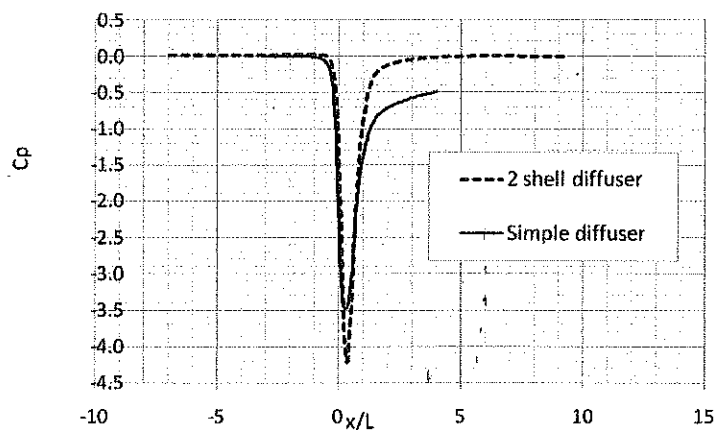
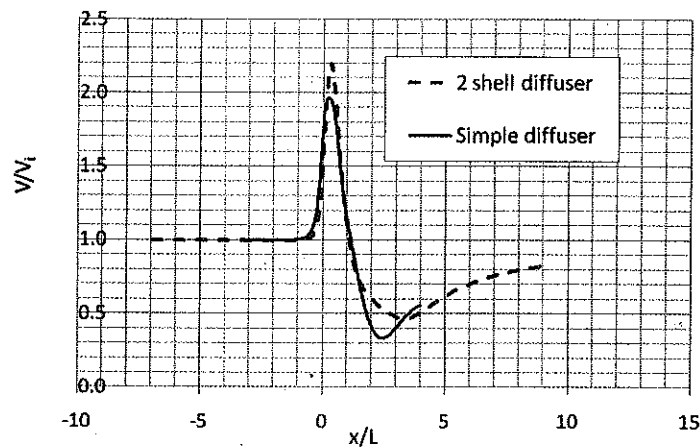


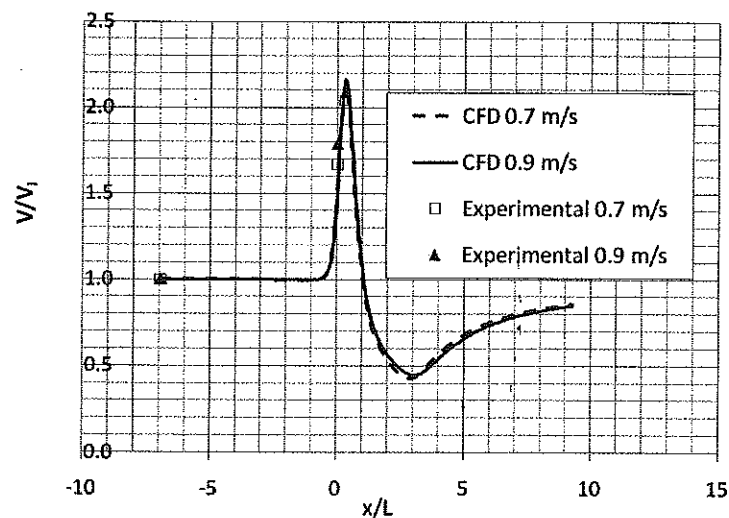
Figure 5.5 Pressure coefficients comparative.

Figure 5.6 Compared the axial velocity of the 2-shell diffuser and the simple diffuser. It shows that the velocity change was similar but not the maximum velocity. The 2-shell diffuser was able to increase the velocity 2.2 times, while the velocity in the simple diffuser increased only 1.9 times. At the outlet point ( $x/L=1$ ) the velocity of both types of diffuser was the same



**Figure 5.6** Shows ratio of diffuser velocity to free water velocity. The simple and 2-shell diffuser are on the same axis.

#### 5.1.4 2-shell diffuser model testing results



**Figure 5.7** CFD and testing velocity of the 2-shell diffuser.

According to the test results for the 2-shell diffuser as shown in Figure 5.7, it was found that the 2-shell diffuser could double the velocity, while the simulation was anticipated to be 2.2 (10% error). The simulation of the simple diffuser predicted the velocity would increase 1.9 times at the maximum velocity. The researcher decided to choose the simple diffuser because of its more simple construction and the expectation increase of 1.8 times of velocity.

### 5.1.5 Results of studying the diffuser angle effect

$Y^+$  check

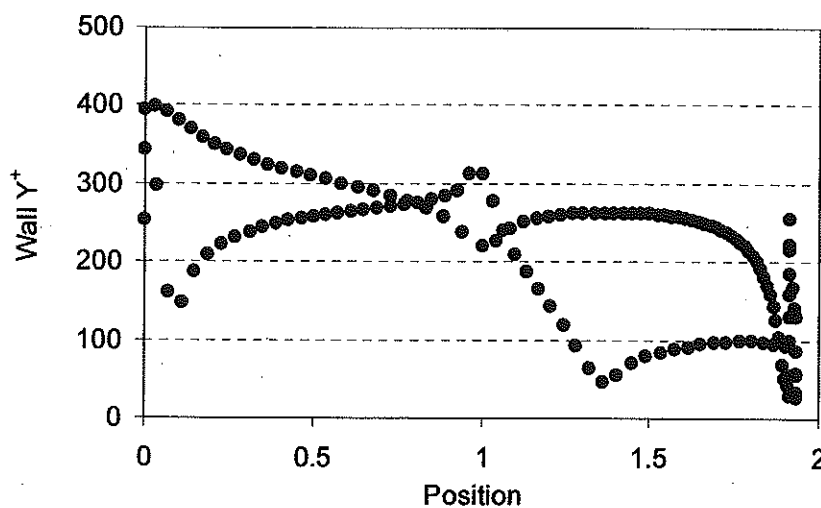


**Figure 5.8**  $Y^+$  of the simple diffuser wall values from 26 to 398.

To set the detail of the grid, the refinement factor equals 1, when  $Re > 100,000$ , the flow regime is turbulent, with standard wall functions. An  $Y^+$  is  $> 30$  and from Figure 5.8,  $Y^+$  values of the diffuser wall varied from 26 to 398.

The evaluation of the grid and the Reynolds number toward domain calculation was separated into 11,000 and 7,100 quadrilateral cells respectively and the Reynolds number was calculated at 1,800,000 and 2,400,000. The following outcomes were velocity ratio ( $V/V_0$ ) and pressure coefficient ( $C_p$ ) as indicated in figure 5.9 and 5.10 that will be cited later.

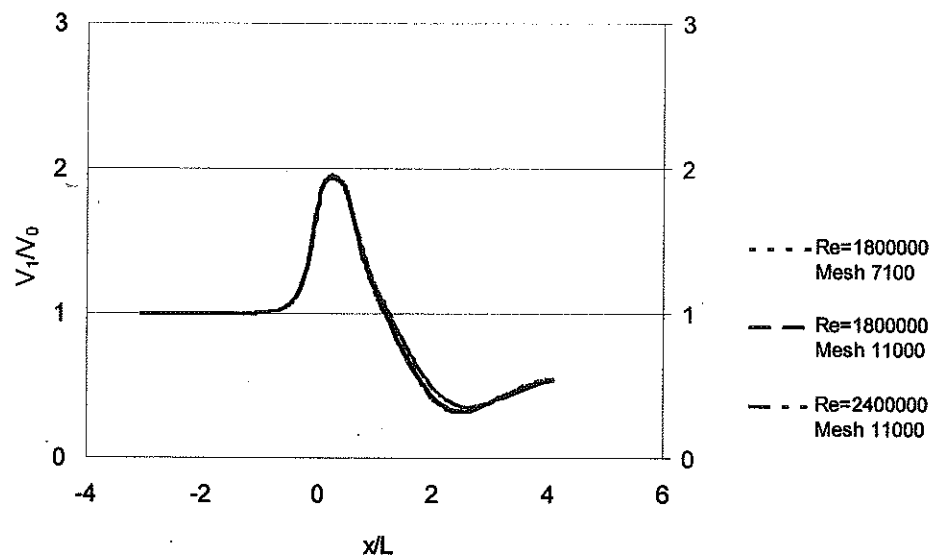


Figure 5.9 Shows  $V/V_0$  on the diffuser axis.

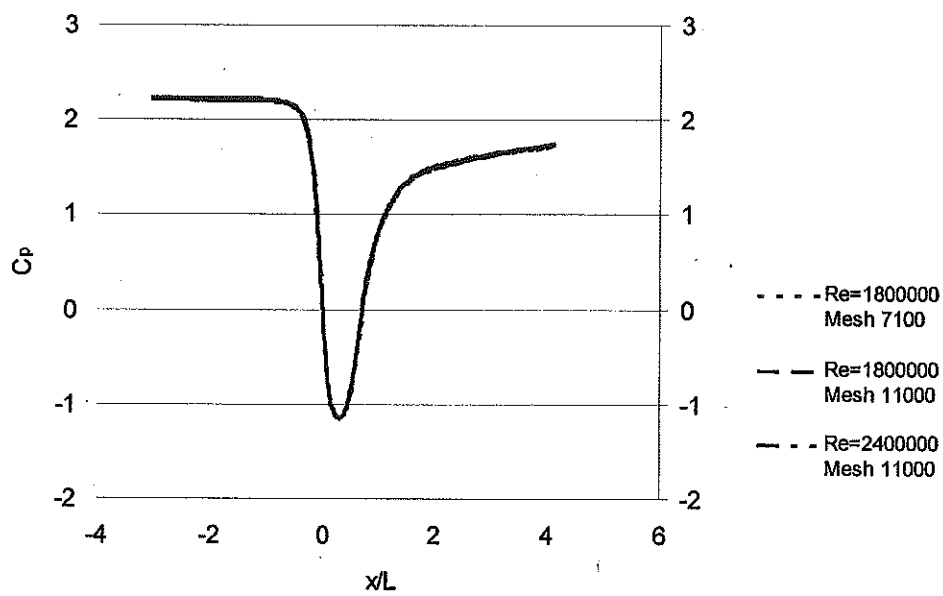
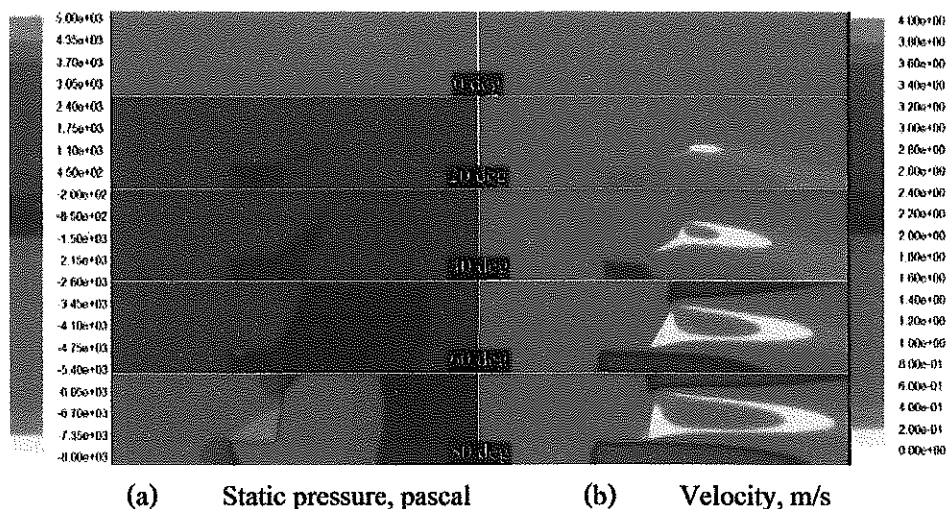


Figure 5.10 Shows  $C_p$  on the diffuser axis.



**Figure 5.11** (a) Results of the 2D simulation showing the pressure contour, (b) Showing the velocity contour when the diffuser angle was at 0, 20, 40, 60, and 80 degrees.

Figure 5.11 shows that the difference in pressure between upstream (in front of the diffuser) and downstream (at the end of the diffuser) increases when the diffuser angle is increased as shown in Figure 5.11(a). The velocity of the water at the throat therefore is increasing with the increased diffuser angle as shown in Figure 5.11(b). However, the flow pattern can be divided into two cases. The first case is when the diffuser angle is 0 and 20 degrees. In this case, the increasing velocity at the throat causes the pressure at the back of the diffuser to become negative. The fluid flow at the throat will try to maintain its flow condition and is accelerated through the diffuser and the maximum speed is in diffuser as shown in Figure 5.11 b. The other case is the case of wider angles (40, 60 and 80 degrees) Even though the axial exit velocity does not decrease but the recirculation occurred at the exit of the diffuser. This recirculation also caused a lower pressure, then the fluid in the diffuser tries to decrease the pressure to the exit value and the fluid is speeded up inside. All of these results agree with Ken-ichi Abe, Yuji Ohya (2004).

The relationship of the velocity inside the diffuser also shows in the results of the velocity plot on the x -axis with different diffuser angles as shown in Figure 5.12. These results confirm all previous results that the velocity inside the diffuser increases when the diffuser angle increases. Moreover, it was found that the wider the angle, the higher the velocity at the outlet ( $x/L=1$ ) where it nearly reaches the maximum velocity.



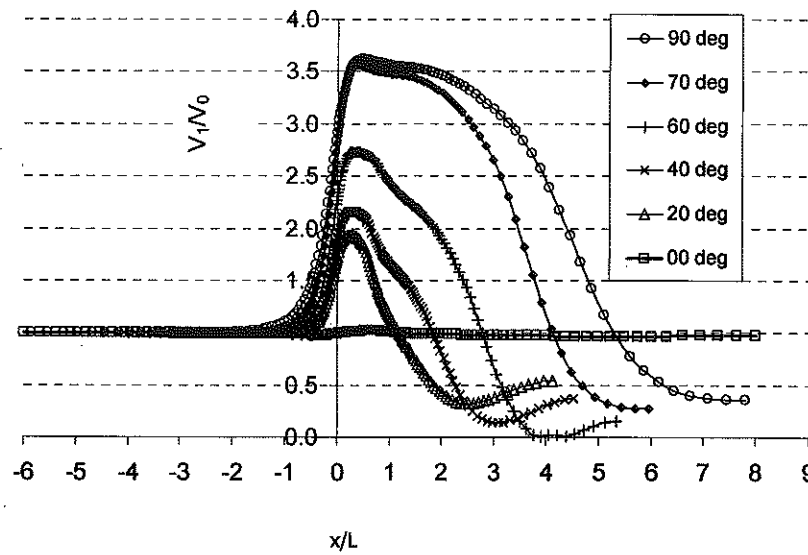


**Figure 5.12** The relation between  $V_1/V_0$  at different points on the x-axis direction and the angle of the empty diffuser.

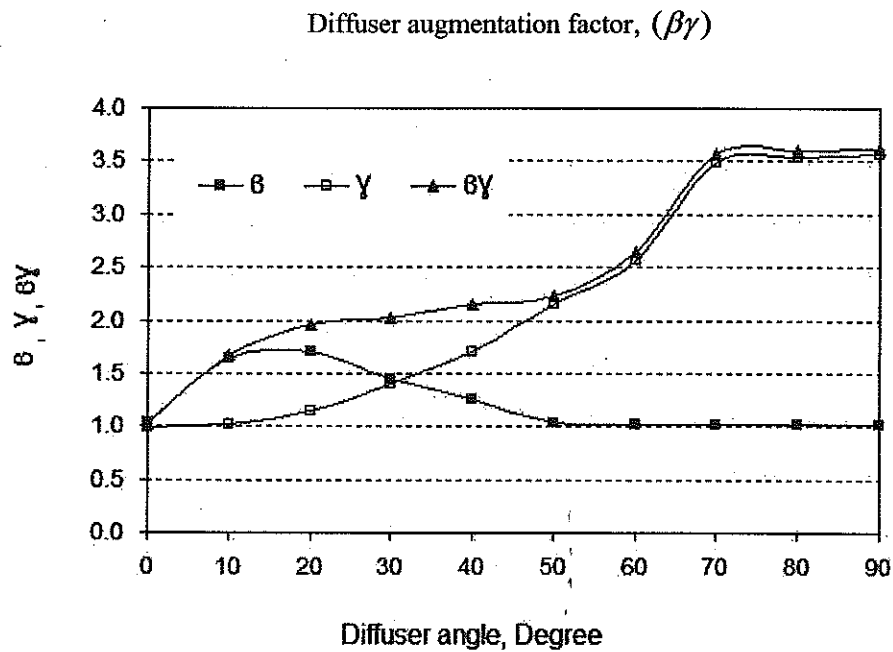


**Figure 5.13** The relationships of the diffuser area ratio ( $\beta$ ), back pressure velocity ratio ( $\gamma$ ), and the diffuser augmentation factor ( $\beta\gamma$ ) to the diffuser angle.

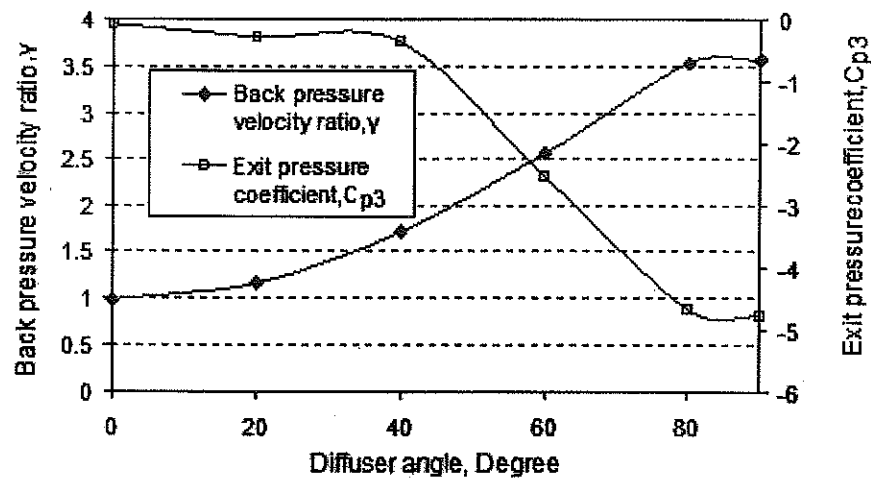


**Figure 5.14** The relationship of the back pressure velocity ratio ( $\gamma$ ) and the exit pressure coefficient  $C_{p,Exit}$  to the diffuser angle.

Figure 5.13 shows the diffuser area ratio ( $\beta$ ), the back pressure velocity ratio ( $\gamma$ ), the diffuser augmentation factor ( $\beta\gamma$ ), and the VS diffuser angle.  $\gamma$  increases if the angle of the diffuser is increased. This means that there is negative back pressure at the exit of the diffuser as seen in Figure 5.14. From Figure 5.14 the angle of the diffuser can be separated into four phases: 1) 0-20 degrees, 2) 20-50 degrees, 3) 50-70 degrees, and 4) 70-90 degrees. In phase one, both  $\beta$  and  $\gamma$  increase. In phase two,  $\beta$  looks to decrease but  $\beta\gamma$  values increase. In phase 3  $\beta$  is constant but  $\gamma$  and  $\beta\gamma$  are increasing. In the last phase,  $\beta$ ,  $\gamma$ , and  $\beta\gamma$  are all unchanged. When the angle is greater than 20°, the maximum velocity on axis of the diffuser is increasing, and the radial diffuseness of the velocity is sparse. This results in the ratio of  $V_1/V_3$  ( $\beta$ ) being lower and the value of  $\gamma$  ( $V_3/V_0$ ) being higher but the product of  $\beta$  and  $\gamma$  is up. Therefore, it can be said that  $\gamma$  significantly effects the diffuser augmentation factor ( $\beta\gamma$ ) while  $\beta$  alone will be important if the diffuser angle is less than 20°.

### Comparison of flow in the diffuser with and without 0.59 Cp of rotor turbine

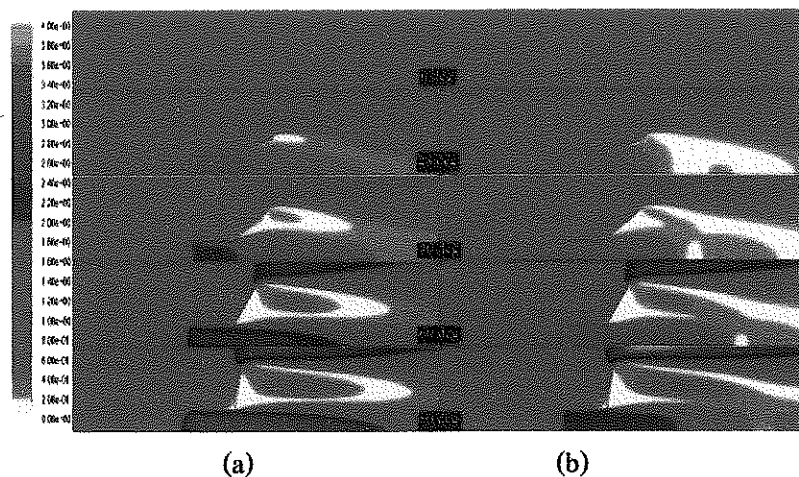


**Figure 5.15** The comparison of velocity contours between (a) an empty diffuser and (b) a diffuser with a 0.59 Cp rotor.

Figure 5.15 shows the velocity contours of an empty diffuser and a diffuser with a 0.59 Cp rotor. In the case with the installed rotor, the maximum velocity was decreased at every angle for the diffuser compared to an empty diffuser. This resulted because the rotor created an axial induction factor which caused the water speed in front of the rotor to decrease.

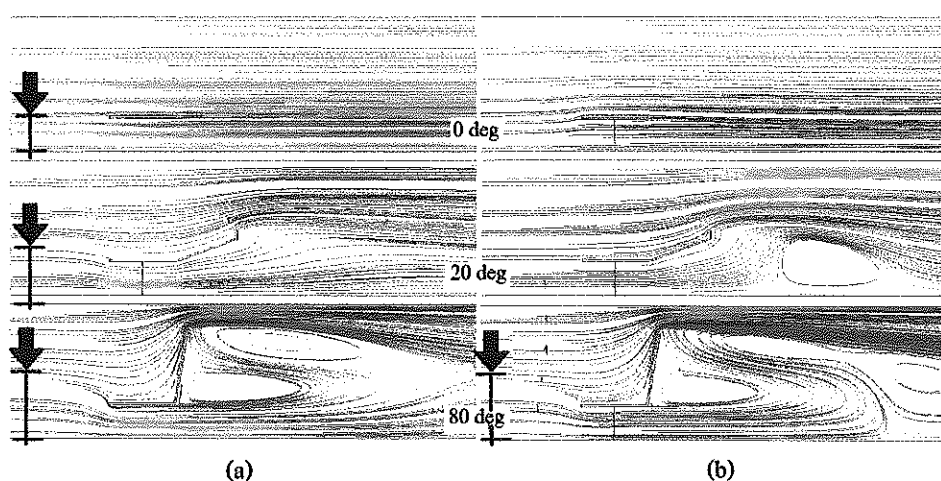


**Figure 5.16** Water streamlines of diffuser (a) without and (b) with 0.59 Cp of rotor turbine at 0, 20, 80 degrees.

The results of the 2D simulation show streamlines, for the diffuser at angles of  $0^\circ$ ,  $20^\circ$ , and  $80^\circ$ , for an empty diffuser and a diffuser with a  $0.59 \text{ Cp}$  rotor turbine as shown in Figure 5.16 (a) and 5.16 (b), respectively. The increasing angle of the diffuser shows the effects of the increasing effective area resulting in more recirculation.

This resulted even though when the rotor was installed, this area was not much changed. This is because the velocity increased in the diffuser. However when the rotor turbine is installed, the flow shows the increasing recirculation with increasing diffuser angle.

The results from Figure 5.17 also show that the water speed up strike to rotor with diffuser compared to the  $0^\circ$  degree diffuser with the rotor uninstalled or installed of installed of. When  $V_1/V_0$  increased according to angle of diffuser, the pressure drop across the rotor of the turbine increased as well. This shows that the system can produce more power when the angle of diffuser is increased with the installed rotor.

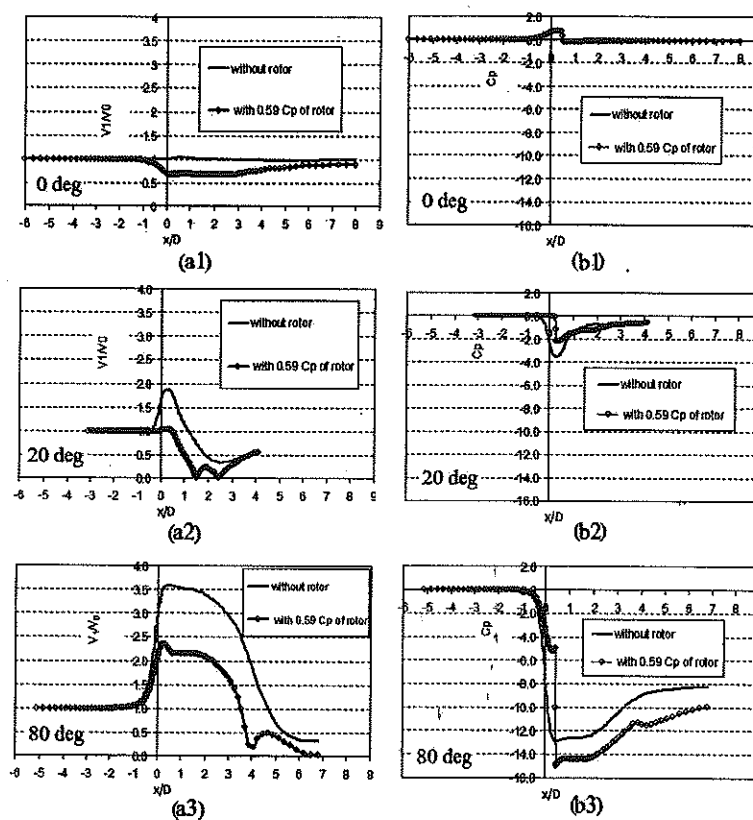


**Figure 5.17** (a) Velocity and (b) Pressure coefficients at the axis of the diffuser with and without the rotor turbine at 0, 20, 80 degree diffuser angles.

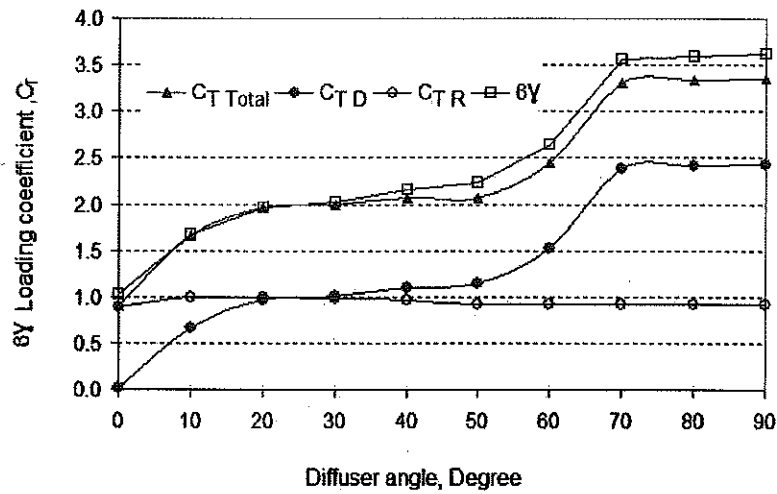


**Figure 5.18** Relationships of the disk loading coefficient,  $C_{T, Total}$ ,  $C_{T,D}$ ,  $C_{T,R}$ , and  $\beta\gamma$  to diffuser angle in degrees.

#### Thrust loading coefficient

Figure 5.18 shows that increasing the angle of diffuser causes the diffuser augmentation factor be higher; while the thrust toward the diffuser is obviously increasing between the phase of 0-20° and 50-70° there is only a slight influence on the thrust coefficient of the rotor. It can be seen that if we build the diffuser with a larger angle in order to generate the energy that we require, we will need to build a durable structure to compensate for the increasing thrust.

#### Power coefficient of diffuser augmentation water turbine (DAWT)

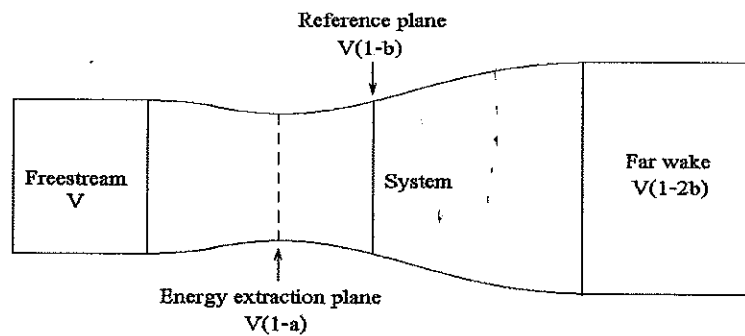


**Figure 5.19** Flow fields regions (P.M. Jamieson, 2009).

Wind turbine theory defines the axial induction factor of turbine as  $a = \frac{V_0 - V_1}{V_0}$ , where  $V_0$  is free stream wind velocity, and  $V_1$  use of blade velocity or energy extraction plane. In this study, the scope of study comprises the turbine and the diffuser (DAWT). So, the reference plane is set as shown in Figure 5.19 to find the axial induction factor of the system ( $b$ ) and the power coefficient ( $C_p$ ). that the results for the axial induction factor and the power coefficient are shown in Figures 5.20 and 5.21.

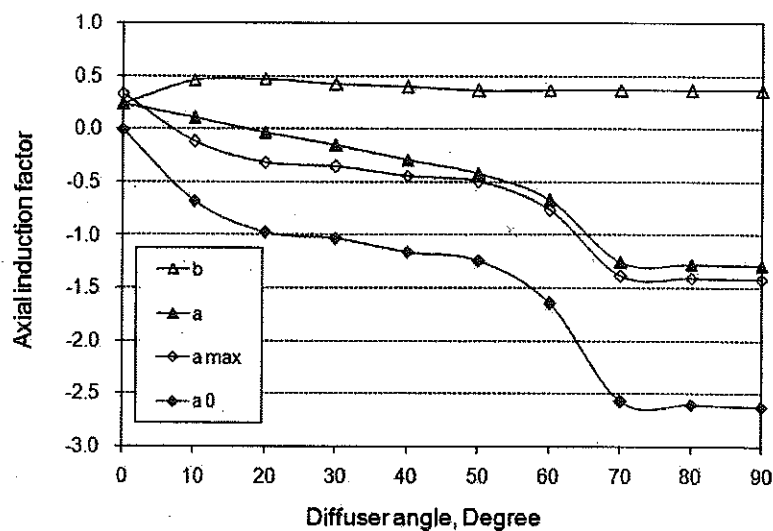


**Figure 5.20** The axial induction factor ( $b$ ) at the reference plane of the system, of the turbine ( $a$ ), of the turbine at the maximum power coefficient ( $a_{\max}$ ), and of the non-turbine diffuser ( $a_0$ )

Figure 5.20 indicates the axial induction factor at the reference plane ( $b$ ) of the system, of the turbine ( $a$ ), of the turbine at the maximum power coefficient ( $a_{\max}$ ), and of the non-turbine diffuser ( $a_0$ ) respectively. Without the turbine installed inside the diffuser, the value of the axial induction factor ( $a_0$ ) is minus and low regarding increasing the angle of the diffuser that shows capacity of additional velocity of the diffuser regarding increasing the angle of the diffuser. When the turbine was installed inside, the energy of the fluid flow would be extracted that decrease capacity of velocity of fluid flow. The value of the axial induction factor ( $a$ ) will be

higher than  $a_0$ . The value of the axial induction factor that causes the maximum power coefficient is  $a_{\max} = \frac{1+2a_0}{3}$  (Jamieson P., 2009). In the study, the power coefficient of the turbine was maximum set but the axial induction factor took place on turbine was higher than  $a_{\max}$  that reduce capacity of turbine, particularly between 0-40 degree of angle. It was likely to find that the study of parameter of diffuser by one dimension theory without considering perpendicular direction and match ideal fluid flow inside diffuser was different from the simulation results because it found in the simulation that fluid flow was perpendicular, particularly when angle was between 0-40 degree; meanwhile, there was slightly perpendicular flow when angle was between 40-90 degree and found there was a separation of.

The axial induction factor ( $b$ ) of the system that refers to the reference plane gave positive rates between 0.34-0.45. It means the fluid energy would be extracted that reduce velocity at the last stages of tide and efficiency of system would be less than Betz limits as in Figures 5.20 and 5.21.

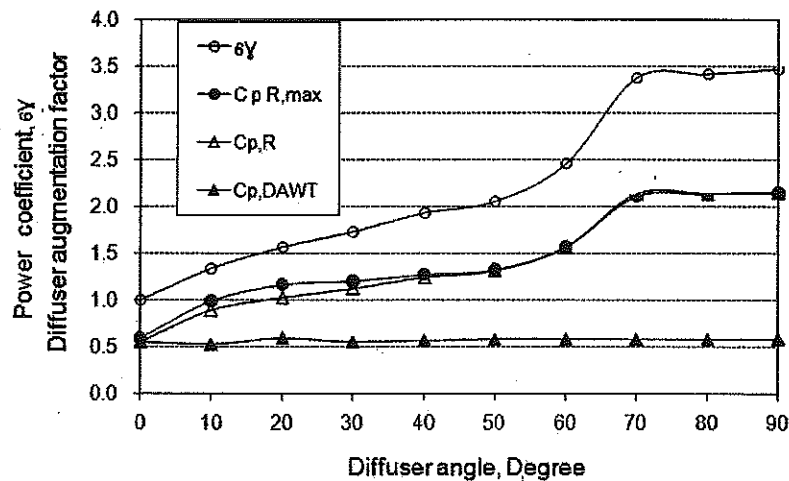


**Figure 5.21** Indicates the power coefficient ( $C_p$ ) and diffuser augmentation factor ( $\beta\gamma$ ).

From Figure 5.21 the power coefficient of the DAWT ( $C_{p,DAWT}$ ) assumed values between 0.59 when the angle was at 0 degrees and 2.14 when the angle was at 90 degrees. Whereas the power coefficient of the system showed ( $C_{p,system}$ ) values of 0.57 and 0.59, when the

angle was at 0 degree and 90 degree respectively. The ability to increase the capacity of the diffuser (Diffuser augmentation factor)  $\beta\gamma$  is about 1.0 when the angle was at 0 degrees and reached a maximum of 3.5 when the diffuser angle was at 90 degrees. When the diffuser angle was between 0-40 degrees,  $C_{P,DAWT}$  was lower than the maximum rate as mentioned in the previous paragraph.

### 5.1.6 3 Dimensional simulation results of the diffuser

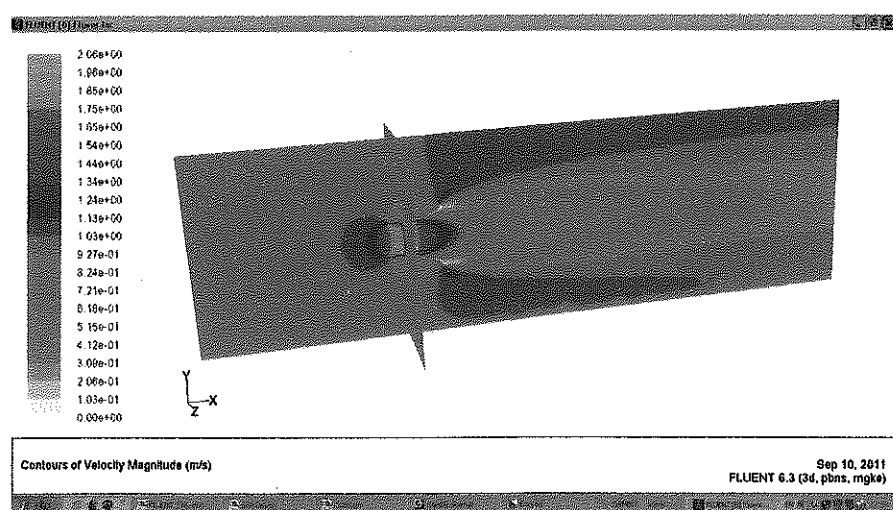


**Figure 5.22** The contour of the water velocity in the 3D diffuser.

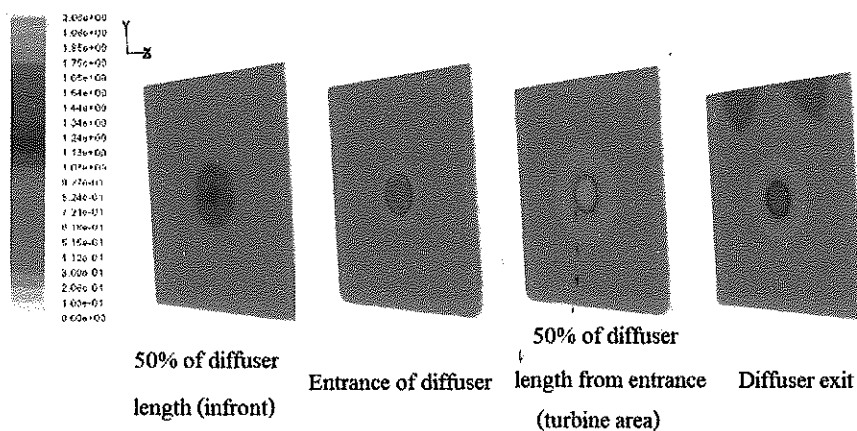


**Figure 5.23** Velocity contour inside the diffuser at different points.



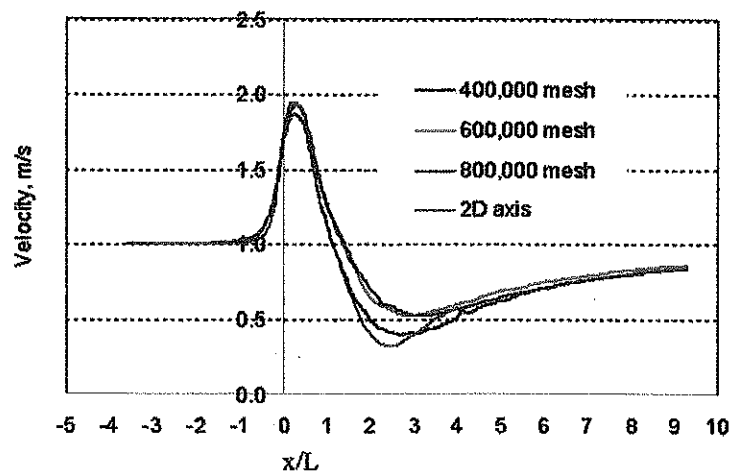


**Figure 5.24 (a)** The 3D water velocity on the diffuser axis; mesh 400,000; 600,000; and 800,000; and 2D axisymmetric respectively.

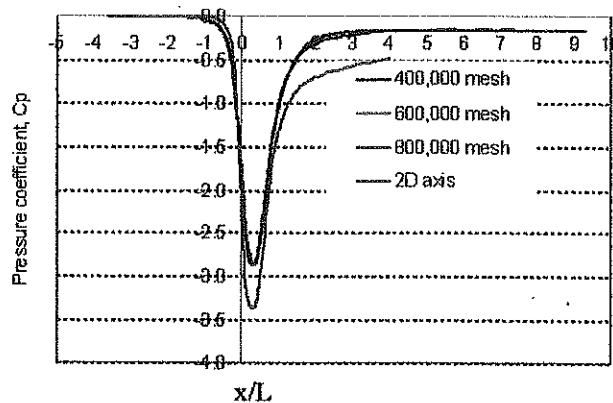


**Figure 5.24 (b)** The static pressure on the diffuser axis in 3D; mesh 400,000; 600,000; 800,000; and 2D axisymmetric.

The outcomes of the 3D modeling with the mesh's details at 400,000; 600,000; 800,000; and 2D axisymmetric as in Figure 5.22 (a) and 5.22 (b) demonstrated that both the 3D velocity and pressure in the diffuser (positions 0-1) did not differ much. The lowest rate of maximum velocity occurring for the cases where the mesh was at 600,000; 800,000; and 2D axisymmetric were 1.93, 1.92, and 1.94 m/s respectively. For the case of the pressure coefficient

(Cp), setting the scope of the problem in 2D axisymmetric style gave the lowest Cp value that matched the maximum velocity; meanwhile, details of the mesh only slightly influenced Cp.

#### Validation of the model

To validate the model simulation, a 1.1 meter diameter, 20 degree diffuser was constructed and tested in a natural flow channel. The velocity of the free upstream flow and the flow in the middle of the diffuser was collected every 2 seconds using a paddlewheel flow sensor, IP101 series. In the Figure 5.25 we showed the average velocity every a minute. It was found that with a mean free stream velocity of 0.90 m/s (in front of the diffuser) we got 1.55 m/s inside of the diffuser. We can say that the diffuser augmentation is 1.72 as seen in figure 5.23 whereas the maximum velocity in the diffuser was predicted to be 1.86, 1.93, 1.92, and 1.94 by 2D and 3D simulation with mesh at 400,000; 600,000; and 800,000.

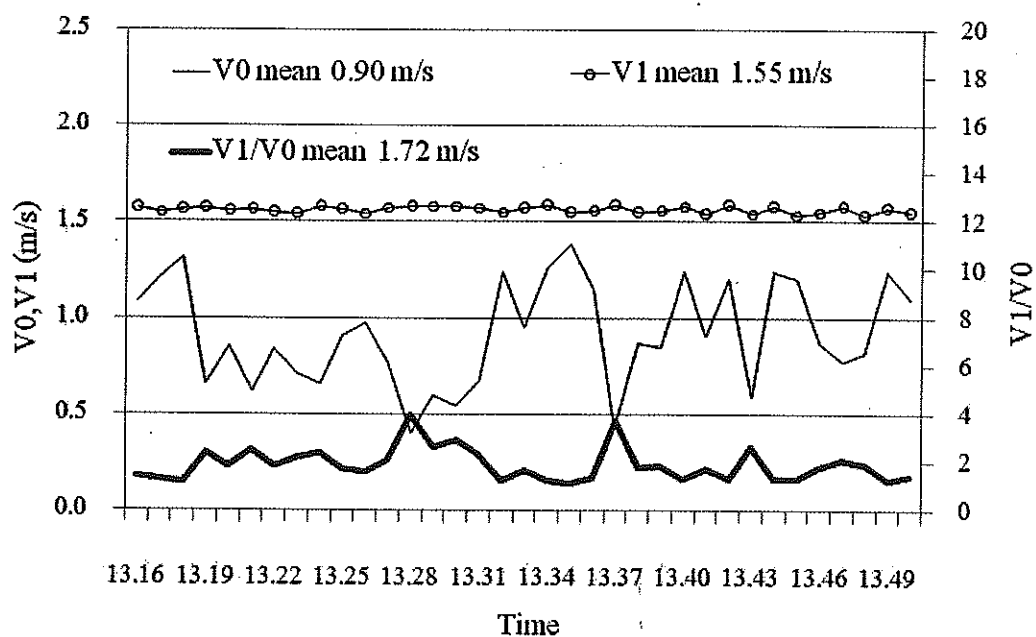


**Figure 5.25** The diffuser without the rotor turbine test results.

## 5.2 Design results of turbine blade

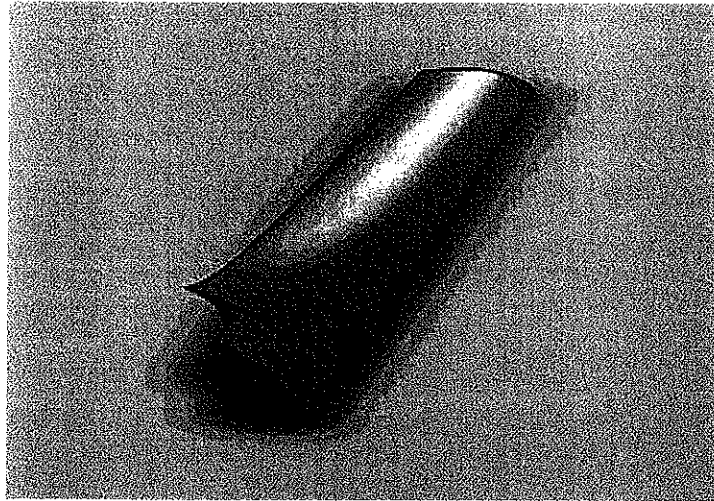


**Figure 5.26** Design result for the turbine blade based on blade element momentum theory.

**Table 5.1** Blade design results based on blade element momentum theory.

<b>Radius m</b>	<b>Chord m</b>	<b>Twist angle degrees</b>	<b>Attack angle degrees</b>	<b>Twist angle degrees</b>
0.05	0.1	25.00	13.15	64.19
0.10	0.095	48.00	10.60	43.28
0.20	0.090	72.00	6.98	18.36
0.25	0.085	77.00	6.94	12.25
0.30	0.080	80.20	7.04	8.94
0.35	0.075	82.50	7.05	7.38
0.40	0.070	84.20	7.01	6.51
0.45	0.065	85.60	7.04	5.26
0.50	0.060	86.70	7.05	5.00

### 5.3 Simulation results of a diffuser augmented water current turbine

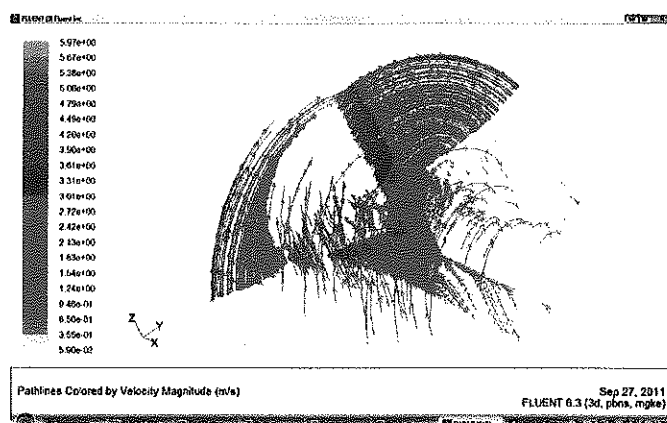


Figure 5.27 Water flows via turbine blade.

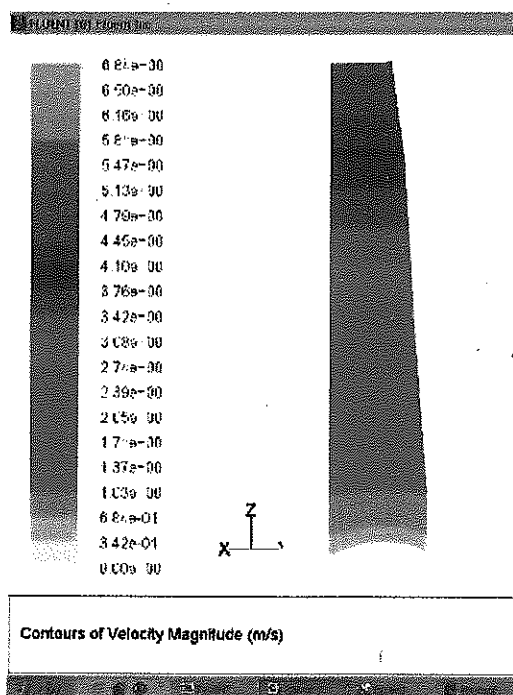


Figure 5.28 The velocity contour on the turbine blade.

Figure 5.27 shows the water flows over the turbine blades, the water surrounding the turbine rotated in the opposite way with the turbine. And velocity would be higher in regard to a radial turbine as indicated in Figure 5.27 and 5.28.

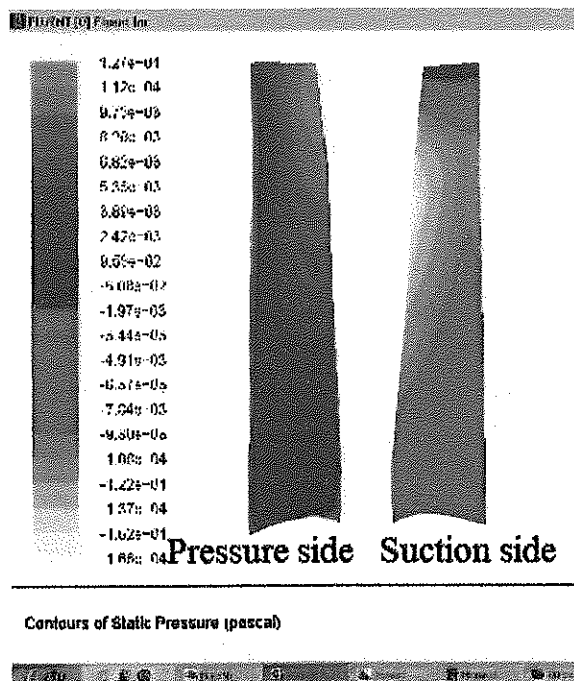


Figure 5.29 The pressure contour (1).

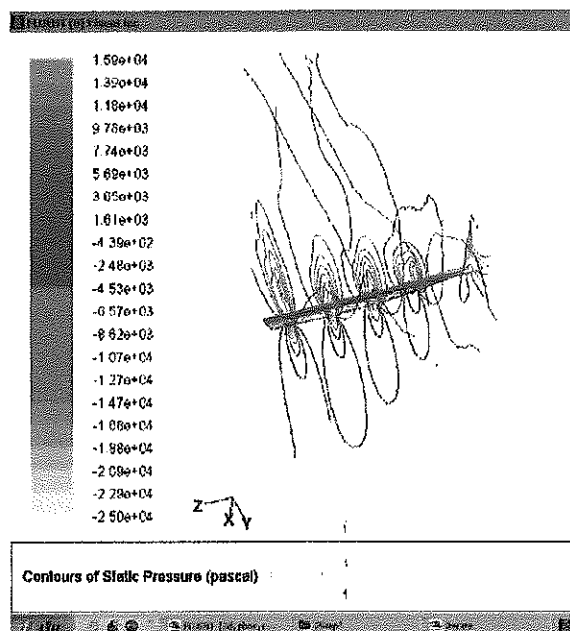


Figure 5.30 The pressure contour (2).

Figures 5.29 and 5.30 show the pressure contours on the pressure side and the suction side. The pressure on the suction side was lower than the pressure side that caused the lift force in

rotating the turbine; it a principal of the horizontal axis turbine. It was noticed that the pressure at the blade tip on the suction side is higher than other areas due to tip loss.

There were two designs of the turbine, a straight blade and a twisted blade. The simulation results were as below:

**Figure 5.2** Simulation results with the turbine installed inside the diffuser.

Types of turbine blade	Number of	Water speed	Torque (N*m)	Rotor speed rpm, rad/s	Power Watt	Power coefficient
Twisted blade	517,000	1.0	29.5	58, 6.1	180.2	38.6

#### 5.4 Examination of generating power

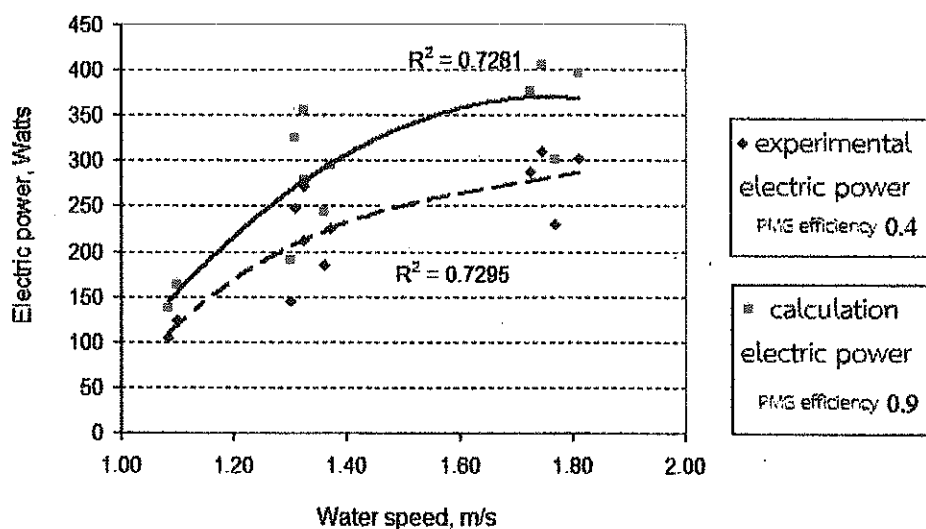


**Figure 5.31** Power (watts) vs velocity (m/s).

Figure 5.31 shows the electric power generated per unit of water velocity when the angle of blade was 35 degrees. The bold line and dotted line show the trend of the calculations and experiment data. At the average velocity of 1.1 m/s the experiment shows that the output power varied between 100-125 watts. If the efficiency of the permanent magnetic generator is 0.9, the

power will 140-160 watts Figure 5.30 shows that the experimental power coefficient or system coefficient at PMG efficiency 0.4 was 0.20 when the water velocity equaled 1.2 m/s and the average coefficient was 0.15 between 1.0-1.8 m/s. The calculated results for the power coefficient and average coefficient at PMG efficiency 0.9 were 0.28 and 0.33 respectively.

Figure 5.32 shows the power coefficient of the tip speed ratio (TSR) between 3.5 – 4.5. The power coefficient would increase to TSR but the study equipment had limited ability to collect the information when TSR greater than 4.5. If the trend lines were considered, it is possible to expect that the maximum coefficient of the turbine would be 15% when the TSR equaled 5.5.

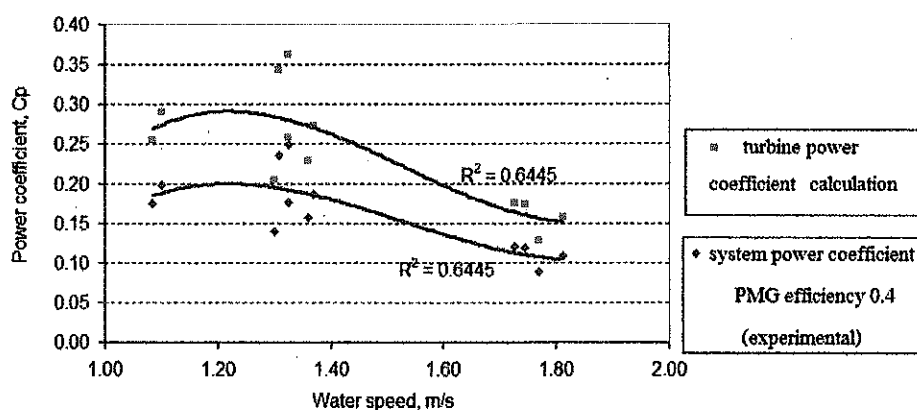


**Figure 5.32** The power coefficients at different velocities.

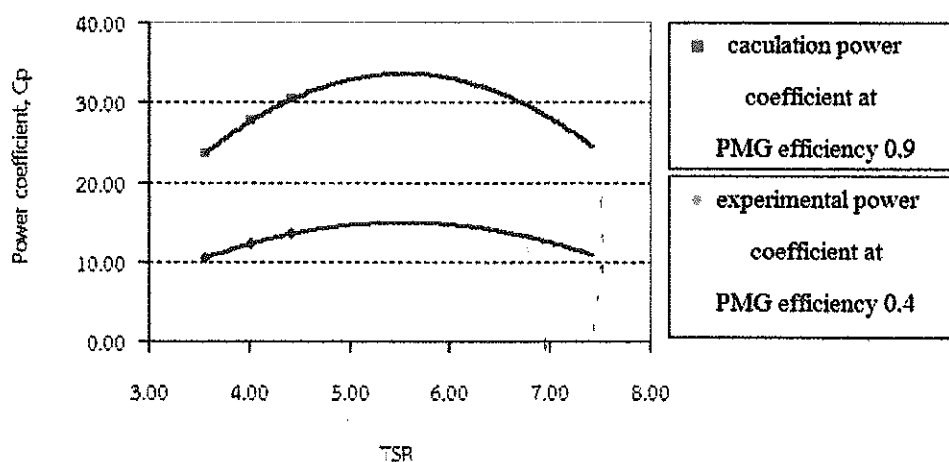


**Figure 5.33** The power coefficients as a function of variable TSR.

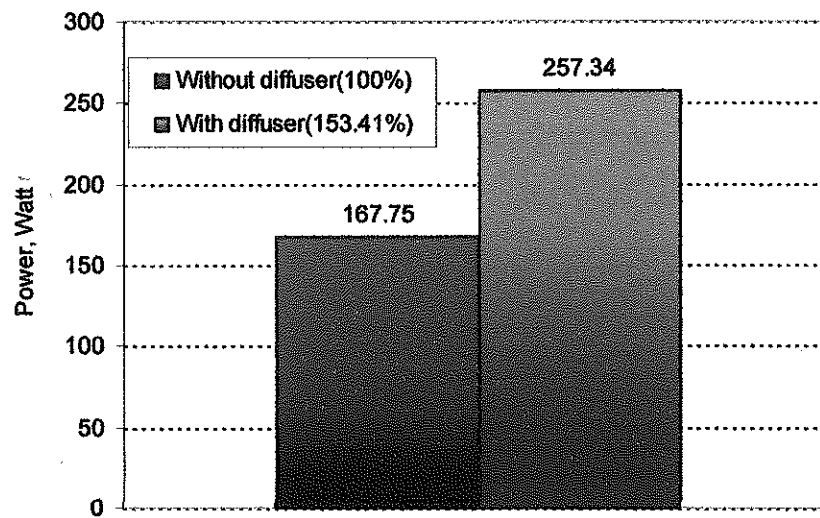


**Figure 5.34** Comparison of power before and after installing diffuser.

From Figure 5.34, when the diffuser was installed, the diffuser turbines generated 167.75 watts but the turbines could generate 257.43 watts (53.41% more) at a water velocity of 1.7 m/s. It can be said that the power coefficient of the diffuser augmentation turbine is 1.53 times that of a conventional water turbine, while the augmentation factor test of the diffuser showed a difference of 1.72 (12.4%).



## CHAPTER 6

### CONCLUSIONS

#### 6.1 Result of design and examination of diffuser

6.1.1 The two types of diffuser were modeled and examined, two types of diffusers: a 2-shell diffuser and a simple diffuser. The maximum velocity of the 2-shell diffuser appeared to be 2.1 times the velocity at the inlet but the simple diffuser had only 1.9 times (simulation results). What enabled the 2-shell diffuser to be faster was the curved inner space that was modified from the airfoil FX63-137. But the simple diffuser was chosen for construction instead because the construction was not so complicated and the capital cost was lower. The test of the simple diffuser indicated that it was able to increase the velocity 1.7 times or 9.5% error compare to simulation result.

6.1.2 Regarding to the angle of simple diffuser, the wider the diffuser's angle, the larger the increase in velocity inside the diffuser. The maximum value after calculating is at 3.5 when the angle is about  $90^\circ$ . That is similar to the value of the  $70^\circ$  angle and the  $80^\circ$  angle. Meanwhile, the designed  $20^\circ$  angle was able to increase velocity by a factor of 1.9. The factors influencing the capability of the diffuser were the diffuser area ratio ( $\beta$ ) and the back pressure velocity ratio ( $\gamma$ ).  $\beta$  Would increase when the diffuser angle was less than  $20^\circ$ , decreased when the angle was between  $20^\circ$ - $50^\circ$ , and remained constant when the angle was between  $50^\circ$ - $90^\circ$ .  $\gamma$  Would be increase in relation to the angle of the diffuser until it remained constant when the angle was about  $70^\circ$ - $90^\circ$ . This would lower in pressure coefficient at the outlet of diffuser. Though a wider angle on the diffuser distinctively caused the velocity inside diffuser to increase, when the angle was at  $0^\circ$ - $20^\circ$  and  $50^\circ$ - $70^\circ$  it was found that the diffuser disk loading coefficient and total loading coefficient would quickly increase the as same as the power coefficient. Thus, to construct a diffuser depended on several components: the required maximum velocity, the construction cost, the stability of the material, etc.

6.1.3 When the diffuser angle increased, more recirculation was found that at outlet. This recirculation caused lower pressure at outlet, and that resulted in an increase in the velocity at the inlet. In addition to the ratio of the inlet area to the outlet, designing the diffuser with recirculation at the outlet is significant in order to augment the velocity in the diffuser.

6.1.4 In studying system performance, it indicated that when the turbine was set as a bare ideal turbine with an axial induction factor of  $1/3$  or power coefficient of 0.59, we found that the power coefficient of the system was close to 0.59 at any size angle on the diffuser. This probably said that the performance of the diffuser augmentation water turbine (DAWT) depends greatly on efficiency of the turbine and would not be over the Betz limit. The power coefficient of the turbine would be 1 and 3.5 if the angle was at 0 degrees and 90 degrees respectively when compared to the non-diffuser turbine.

## 6.2 Electricity generating test

6.2.1 Based on Blade Element Momentum Theory, the turbine was designed and employed as a fluid model with numerical calculations, which enabled us to know the capability of the system and the fluid behavior inside the turbine. As such, its design was revised appropriately before construction. After calculating at 1.0 m/s speed of water, it provided 180.2 watts and a power coefficient of 38.6%. But after examination at 1.1 m/s, it provided only 112.5 watts with a power coefficient of 17.8% and an average power coefficient of 15% which was lower than the specific target. So, it came to the following factors:

6.2.1.1 The blade surface was rough and malfunctioned because of indelicate molding. As for that reason, the blade was bent by the water pressure.

6.2.1.2 The turbine's blade weighed too much because it was molded from fiberglass reinforced plastic (FRP) and strengthened with a steel plate.

6.2.1.3 With regards to the numerical calculation results system fluid model, the trash strainer, chain bumper, and turbine supportive structure were not applied in the calculation in order to reduce the complication of the simulation.

6.2.1.4 This research mainly focused on the turbine and diffuser design but did not studied in detail of Permanent Magnetic Generator (PMG). The 3 phase motor was modified to

a Permanent Motor Generator (PMG) type. After examining the efficiency at 115-278 rpm. It had average efficiency of 40% which meant that the efficiency of the turbine and diffuser to transform kinetic energy from hydropower to mechanical energy was 37% ( $15 \times 100 / 40$ ). If considering only the efficiency of the non-installed diffuser turbine, it would be  $37\% / 1.7$  (1.7 was defined as the diffuser's value that increased the velocity 1.7 times that of the incoming water stream.) or 22% that was similar to specified value, 25%.

6.2.2 In the test of power generation of the installed diffuser type and non-diffuser one, with a water velocity of 1.7 m/s when the diffuser was not installed, the turbines generated 167.7 watts and 257.4 watts with diffuser installing. It can be said that the power coefficient of the diffuser augmented turbine is 1.53 times that of the non-diffuser water turbine.

### 6.3 Application

After configuring the diffuser, it was constructed in a metal forming process using steel plate strengthened with Stiffeners-type steel. It was then painted with coal tar epoxy to withstand rust when using it in water.

The model of the turbine blade was wooden set up by a CNC machine, then molded with fiberglass reinforced plastic and internal strengthened with a steel plate. After revising the plastic admixture it was found to be well-functioning, durable, and with a decreased cost (important when making a lot of blades). For long-term application and in a high velocity context other lighter and more durable materials need to be investigated.

Chain transmission gave high efficiency, but its disadvantages were noisiness and rust formation on the chain.

To apply this hydro turbine for commercial purposes, its effectiveness, strength, and construction cost will need to be improved. Through this research it was anticipated to be able to apply this model with continued development in forthcoming commercial applications.

#### 6.4 Suggestions

To summarize the obstacles mentioned above, development of a hydro turbine for low speed water will require finding out how to make the turbine blade lighter but stronger. The materials might be changed to molded aluminum or aluminum milling by a CNC machine. Additionally, appropriate formation of the generator needs deep studying order to generate the most efficient electricity.

Since rivers and canals in general are not wide enough or deep enough, it will be impossible to construct such huge turbine to generate electricity. The practical way would be increasing the number of turbines, set and installed like a tidal fence that will allow convenient passer-by travel.

## REFERENCES

## REFERENCES

- Bahaj, A. S. and et al. Power and thrust measurements of marine current turbines under various hydrodynamic flow conditions in cavitations tunnel and towing tank.  
<http://www.sciencedirect.com>. February, 2006.
- Bahaj, A. S. and Myers, L. E. "Fundamentals applicable to the utilization of marine current turbines for energy production", Renewable energy. 28(14): 2205-2211; November 2003.
- Batten, W. M. J. and et al. "Hydrodynamics of marine current turbines", Renewable Energy. 31(2): 249-256; February, 2006.
- . "Experimentally validated numerical method for the hydrodynamic design of horizontal axis tidal turbines", Sustainable Energy Research Group, School of Civil Engineering and the Environment, University of Southampton, UK, Ocean Engineering. 34(7): 1013-1020; May, 2007.
- Bayondor, J., Abanteriba, S. and Bates, I. "An advance zero head hydro-propulsion", Renewable Energy. 24(3-4): 475-484; November, 2001.
- Bryden, I. G. and et al. "The utilization of short term energy storage with tidal current generation systems", Energy. 25(9): 893-907; September, 2000.
- Coiro D.P. and et al. "Horizontal Axis Tidal Current Turbine: Numerical and Experimental Investigations", in Department of Aeronautical Engineering (DPA), University of Naples "Federico II" - Naples, Italy, Offshore Wind and Other Marine Renewable Energy in Mediterranean and European Seas Conference. Italy: Civitavecchia; April 20-22, 2006.
- Energy Policy and Planning Office. Energy to understand, Used to value, Sustainable development. <http://www.eppo.go.th/doc/doc/doc-energy.html#17>. June, 2011.
- Fraelkel, P. Tidal Current Energy Technologies. UK: Marine Current Turbines Limited, 2006.
- Foreman, K. M. and Grumman, R. A. "Advantages of the Diffuser-Augmented Wind Turbine", Research Department Grumman Aerospace Corporation. New York: Bethpage, 1999.

## REFERENCES (CONTINUED)

- Gaden, D. L. F. and Bibeau, E. L. "Increasing power density of kinetic turbines for cost-effective distributed power generation", in POWER-GEN Renewable Energy Conference. pp.10-12. Las Vegas: NV; April, 2008.
- Garret, C. and Cummins, P. "The efficiency of a turbine in a tidal channel", Journal of Fluid Mechanics. 558: 243-251, 2007.
- Gorlov, A. and Silantyev, T. "Limits of the Turbine Efficiency for Free Fluid Flow", Journal of Energy Resources Technology. 123(4): 311-317; 2001.
- Jamieson, P. M. "Beating Betz: Energy Extraction Limits in a Constrained Flow Field", Journal of Solar Energy Engineering. 131(3): 031008; August, 2009.
- Juma, Y. A. "Modeling and dynamic analysis of the performance of diffuser augmented wind turbine", The Islamic University Journal (Series of natural studies and engineering). 8(2): 85-110, 2010.
- Ken-ichi, A. and Yiji, O. "An investigation of flow fields around flanged diffusers using CFDE", Journal of Wind Engineering and Industrial Aerodynamics, 92(3-4): 315-330; March, 2004.
- Kibicho, K. and Sayers, A. "Experimental Measurements of the Mean FlowField in Wide-Angled Diffusers: A Data Bank Contribution", Proceedings of World Academy of Science, Engineering And Technology. 33; September, 2008.
- Kiho, S. and et al. "The power generation from tidal currents by Darrieus turbine", Renewable Energy. 9(4): 1242-1245; December, 1996.
- Kirke, B. Development in ducted water current turbines. www.cyberiad.net. December, 2005.
- Lee, J. H. and et al. "Computational and Experimental Analysis for Horizontal Axis Marine Current Turbine Design", in Second International Symposium on Marine Propulsors smp'11. pp. 51-60. Germany: Hamburg. June, 2011.
- Matsushima, T., Takagi, S. and Muroyama, S. "Characteristics of a highly efficient propeller type small wind turbine with a diffuser" Renewable Energy. 31(9): 1343-1354; July, 2006.

## REFERENCES (CONTINUED)

- O'Doherty, T. and et al. "Experimental and Computational Analysis of a Model Horizontal Axis Tidal Turbine", Proceedings of the 8th European Wave and Tidal Energy Conference. Sweden: Uppsala, 2009.
- Ohya, Y. and et al. "Development of a shrouded wind turbine with a flanged diffuser", Journal of Wind Engineering and Industrial Aerodynamics. 96(5): 524–539; May, 2008.
- Ohya, Y. and Karasudani, T. "A shrouded wind turbine generating high output power with wind-lens technology", Energies. 3(4): 634–649, 2010.
- Phillips, D. G., Richards, P. J., and Flay, R. G. J. "CFD modeling and the development of the diffuser augmented wind turbine", Wind and Structure. 5(2-4): 267–276, 2002.
- . Diffuser development for a diffuser augmented wind turbine using computational fluid dynamics. [http://www.cham.co.uk/PUC/PUC\\_Luxembourg/Presentations/AucklandU\\_Phillips.doc](http://www.cham.co.uk/PUC/PUC_Luxembourg/Presentations/AucklandU_Phillips.doc). December, 2008.
- Ponta, F. and Dutt, G. S. "An improved vertical-axis water-current turbine incorporating a channeling device, ISEP Group, Electrotechnical Department, School of Engineering, University of Buenos Aires, Paseo Colon 850, 1064 Capital Federal, Buenos Aires, Argentina", Renewable Energy. 20(2): 223–241; June, 2000.
- Ponta, F. L. and Jacovkis, P. M. "Marine-current power generation by diffuser-augmented floating hydro-turbines", Renewable Energy. 33(4): 665–673; April, 2008.
- Sale, D., Jonkman, J. and Musial, W. "A Hydrodynamic Optimization Method and Design Code for Stall-Regulated Hydrokinetic Turbine Rotors, presented at the ASME 28<sup>th</sup>", in International Conference on Ocean, Offshore, and Arctic Engineering. OMAE: Honolulu, Hawaii. May 31 - June 5, 2009.
- Sullerey, R. K., Chandra, B. and Muralidhar, V. "Performance Comparison of Straight and Curved Diffusers", Defence Science Journal. 33(3): 203; July, 1983.
- Sun, X., Chick, J. P. and Bryden, I. G. "Laboratory-scale simulation of energy extraction from tidal currents", Renewable Energy. 33(6): 1267–1274; June, 2008.



## REFERENCES (CONTINUED)

- VanZieten, J. and Driscoll, F. R. "Design of a prototype ocean current turbine-Part 1: mathematical modeling and dynamics simulation", Ocean Engineering. 33(11-12): 1485-1521; August, 2006.
- Visser, K. D. "Wind Tamer turbine performance report, 1-15 kw performance predictions", Department of mechanical and aeronautical engineering. New York: Clarkson University Potrdam, 2009.
- Wang, L. B., Zhang, L. and Zeng, N. D. "A potential flow 2-D vortex panel model: applications to vertical axis straight blade tidal turbine", Energy conversion and management. 48(2): 454-461; February, 2007.

## APPENDIX

**APPENDIX**  
**A: PUBLICATION**



Songklanakarin J. Sci. Technol.  
34 (1), 61-67, Jan. - Feb. 2012

**SJST** SONGKLANAKARIN  
JOURNAL OF SCIENCE  
AND TECHNOLOGY  
<http://www.sjst.psu.ac.th>

*Original Article*

## A study of diffuser angle effect on ducted water current turbine performance using CFD

Palapum Khunthongjan\* and Adun Janyalertadun

*Department of Mechanical Engineering, Faculty of Engineering,  
Ubon Ratchathani University, Mueang, Ubon Ratchathani, 34190 Thailand.*

Received 9 March 2011; Accepted 26 October 2011

### Abstract

The water current has used as the energy resource for long time however its velocity is very low therefore there are not found in wide range of uses. This study purposes accelerate water velocity by installing diffuser. The problems were analyzed by one dimension analysis and computational fluid dynamics (CFD); the domain covers the diffuser and turbine which substituted by porous jump condition is install inside. The flow was identified as axisymmetric steady flow, the inlet boundary is identified as uniform flow, all simulation use the same size of diffuser, only the diffuser angles are vary. The results show that velocities of water current in diffuser are increase when the diffuser angle are widen. The angle of diffuser is  $20^\circ$ , the velocity is increase to 1.96 times, compared to free stream velocity. If the angle was about  $0-20^\circ$  and  $50-70^\circ$  the force toward diffuser became high instantly, where as the force toward the rotor will be still and the maximum rate of diffuser augmentation possibly was 3.62 and rotor power coefficient was 2.14.

**Keywords:** water current turbine, diffuser, computational fluid dynamics, power augmentation, ducted water turbine

### 1. Introduction

The uses of kinetic energy of water current for generating electricity or pumping has been studied for a long times, which mainly aims to use in remote areas (Fraenkel, 2006; Ponta and Jacovki, 2008; Ponta and Dutt, 2000; Myers and Bahaj, 2006; Bahaj and Myers 2003; Khan *et al.*, 2008; Kiho *et al.*, 1999; G MacPherson-Grant, 2005). According to the kinetic energy use from water current, commercial wind turbine-based knowledge can appropriately be applied where its capacity of energy distribution is as Betz limit. The wind turbine has its maximum power coefficient,  $C_p = 0.59$ , defined as energy produced by wind turbine per total energy available of wind. Although its capacity was 45% developed, it still challenges the researcher to continue strengthen the effectiveness.

A setup of diffuser is a choice to increase the efficiency that can be with both wind and water turbines as found in the wind turbine study by Phillips *et al.* (2002) from the University of Auckland, New Zealand, Toshio Matsushima *et al.* (2006) and Yuji Ohya *et al.* (2008). The study of Gerald and Van Bassel (2007) however indicates no any power augmentation factor was more than 3, while as in the theory the power coefficient probably was 2.5; but the price of a diffuser is somewhat high.

David *et al.* (2008) were applying diffusers to water turbine that points to a 1.3 times increase of the output power of the bare turbine by installing a duct. Kirke (2005) shows in the examination of the axial flow turbine that a slotted duct installed in a towing tank tells to increase 70% of the output power if compared to a bare turbine. Grant (2005) reported that the ducted turbine was capable to pay a double load of the duct uninstalled turbine.

In addition, several countries, Canada, Ireland, England, U.S.A., Australia, and Portugal, have been developing water turbines for electricity, which are all in process, for

\* Corresponding author:  
Email address: [pakhunthongjan@gmail.com](mailto:pakhunthongjan@gmail.com)

examining the model mechanics, and for commercial use.

Although the capacity of water current at low flow velocity, to be used as the energy source, is seldom applied to a water turbine, this article means to study functions and performance of a diffuser as to be the output power accelerator of horizontal axis water current turbine at low flow velocity, in order to be applied in the Northeast of Thailand that has two main rivers, the Moon and the Chii. The velocity of the water current is between 0-1.3 m/s, which is transformed into a two dimensional system by computational fluid dynamic (CFD). The attractive factors are the effect of diffuser angle, maximum augmentation factor, and rotor power coefficient due to the use of the diffuser design for a water current turbine.

## 2. Materials and Methods

### 2.1 One dimensional analysis

The one dimensional analysis is based on van Bassel (2007)

#### 1) Empty diffuser case

From Figure 1 the surface of the diffuser outlet will be the reference point, front and back space of diffuser equals atmospheric pressure ( $P_0$ ). The Bernoulli equation shows that the total pressure equals

$$P_{tot} = P_0 + \frac{1}{2} \rho V_0^2 = P_1 + \frac{1}{2} \rho V_1^2 = P_2 + \frac{1}{2} \rho V_2^2 = P_3 + \frac{1}{2} \rho V_3^2 \quad (1)$$

From the continuity equation the coherence between the inlet velocity ( $V_0$ ), outlet velocity ( $V_3$ ), and diffuser area ratio ( $\beta$ ) is

$$V_1 = \beta V_0 \quad (2)$$

$$V_3 = \gamma V_0 \quad (3)$$

#### 2) In terms of installed the rotor turbine:

$$V_1 = \gamma(1-a)V_0 \quad (4)$$

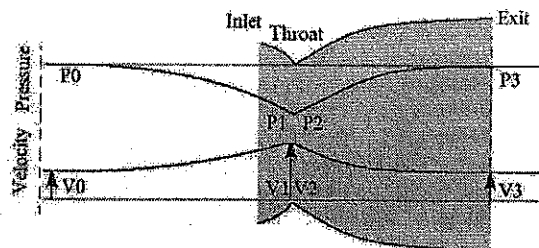


Figure 1. Relationship between pressure and velocity within the empty diffuser

$$V_1 = \beta \gamma (1-a) V_0 \quad (5)$$

The axial induction factor  $a$  is defined as  $a = (V_0 - V_1)/V_0$ , rotor power coefficient  $C_{P,R}$  is defined as  $C_{P,R} = \beta \gamma 4a(1-a)^2$ , power coefficient at diffuser exit  $C_{P,exit}$  is defined as  $C_{P,exit} = \gamma 4a(1-a)^2$ , total thrust coefficient  $C_{T,T}$  is defined as  $C_{T,T} = \beta \gamma 4a(1-a)$ , and thrust coefficient of diffuser  $C_{T,D}$  is defined as  $C_{T,D} = C_{T,T} - C_{T,R} = (\beta \gamma - 1) 4a(1-a)$ .

### 2.2 Computational fluid dynamics

Computational Fluid Dynamics (CFD) is a branch of fluid mechanics that uses numerical methods and algorithms to solve and analyze problems that involve fluid flows. Computers are used to perform the calculations required to simulate the interaction of liquids or gases with surfaces defined by boundary conditions. There are three main processes – pre-processing, calculation processing, and post-processing. Here the Fluent 6.3 commercial code 2 dimensions with the finite volume method was used.

#### Governing equations

In this study, the Reynolds-Average Naviaers-Stokes (RANS) equation is considered with renormalization group  $k-\epsilon$  turbulence model, which are indicated in Equation 6 to 11.

Continuity:

$$\frac{\partial}{\partial x_i} (\rho u_i) = 0 \quad (6)$$

Momentum:

$$\frac{\partial}{\partial x_j} (\rho u_i u_j) = \frac{\partial \bar{p}}{\partial x_i} + \frac{\partial}{\partial x_j} \left[ \mu_t \left( \frac{\partial u_i}{\partial x_j} + \frac{\partial u_j}{\partial x_i} - \frac{2}{3} \delta_{ij} \frac{\partial u_k}{\partial x_k} \right) \right] + \frac{\partial}{\partial x_j} (\rho u_i' u_j') \quad (7)$$

In Equations 6 and 7  $\bar{p}$  is the mean pressure,  $\bar{u}$  is the mean velocity,  $\mu$  is the molecular viscosity, and  $-\rho u_i' u_j'$  denotes the Reynolds stress. To correctly account for turbulence, Reynolds stress is modeled utilizing the Boussineq hypothesis to relate the Reynolds stress to mean velocity gradients within the flow. The Reynolds stress is defined as:

$$-\rho u_i' u_j' = \mu_t \left( \frac{\partial u_i}{\partial x_j} + \frac{\partial u_j}{\partial x_i} \right) - \frac{2}{3} \left( \rho k + \mu_t \frac{\partial u_k}{\partial x_k} \right) \delta_{ij} \quad (8)$$

where  $\mu_t$  is the turbulent viscosity and  $k$  is the turbulent kinetic energy. For  $k-\epsilon$  in the turbulence model the turbulent viscosity is computed through the solution of two transport equations for turbulent kinetic energy and turbulence dissipation rate  $\epsilon$ . The RNG transport equations are

$$\frac{\partial}{\partial t} (\rho k) + \frac{\partial}{\partial x_j} (\rho k u_j) = \frac{\partial}{\partial x_j} \left[ \alpha_k \mu_t \frac{\partial k}{\partial x_j} \right] + G_k + G_b - \rho \epsilon - Y_M + S_k \quad (9)$$

$$\frac{\partial}{\partial t} (\rho \epsilon) + \frac{\partial}{\partial x_j} (\rho \epsilon u_j) = \frac{\partial}{\partial x_j} \left[ \alpha_\epsilon \mu_t \frac{\partial \epsilon}{\partial x_j} \right] + C_{\epsilon 1} \frac{\epsilon}{k} (G_k + G_b) - C_{\epsilon 2} \rho \frac{\epsilon^2}{k} + S_\epsilon \quad (10)$$

$$R_k = \frac{C_\mu \rho \eta^+ (1 - \eta/\eta_0) \epsilon^2}{1 + \beta \eta^+} \frac{\epsilon^2}{k} \quad (11)$$

### Computational conditions

The domain of the flow problem will cover diffuser and turbine area that are specified as wall and porous jump condition. The inlet boundary is set as the uniform flow velocity; the outlet boundary is set as outflow; top wall is as moving (slip) wall instead of volume of fluid (VOF) model, because of less time for calculation and acceptable accuracy, and the bottom wall is set as axisymmetric shown in Figure 2 and 3. Domains will be drawn in the Gambit program before been computerized by Fluent 6.3. Problem domains will be separated by quadrilateral grids into approximately 11,000 cells. Anyhow, grids will be dense around diffuser wall and turbine area.

The study sets the flow as axisymmetric steady flow it is segregated solver, whereas the turbulence model is a RNG  $k-\epsilon$  model. The standard near wall function was chosen for the near wall treatment method with  $10^{-6}$  of the convergence criterion. Sizes of the diffuser are unchanged but the diffuser angle shown in Figure 3 was changed from 0-90°. The porous medium will be from Darcy's Law and an additional inertial loss term with the equation as follows:

$$\Delta p = \left( \frac{\mu}{\alpha} v + C_2 \frac{1}{2} \rho v^2 \right) \quad (12)$$

where  $\mu$  is the laminar fluid viscosity,  $\alpha$  is the permeability of the medium,  $C_2$  is the pressure jump coefficient,  $v$  is the velocity normal to the porous face, and  $\Delta p$  is the thickness of the medium.

## 3. Results and Discussion

### 3.1 Simulation results

#### $Y^+$ checks

In order to set the fineness of partition of the grid the refinement factor equals and when  $Re > 100,000$ , the flow regime is turbulent and for the standard wall functions the proper  $Y^+$  value is  $> 30$ . From Figure 4  $Y^+$  of the diffuser wall values are from 26 to 398.

The evaluation of grid and Reynolds numbers per domain is split into 11,000 and 7,100 quadrilateral cells and the calculated Reynolds number is at 1,800,000 and 2,400,000, respectively. The Reynolds number was defined as  $VD/\nu$  where  $V$  is the axial velocity in m/s,  $D$  is the diameter of the diffuser and  $\nu$  is the kinematic viscosity of water. Its result are an increased velocity ( $V_1/V_0$ ) and a pressure coefficient ( $C_p$ ) that is slightly different as shown in Figure 5 and 6, which will be cited later.

#### Flow inside the Diffuser

The results show that the differential pressure between upstream, in front of the diffuser, and downstream,

at the end of the diffuser, increase when the diffuser angle is increased as shown in Figure 6a. The velocity of the water at the throat therefore is increasing varying with an increase of

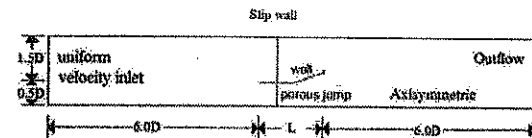


Figure 2. Domain of the problem

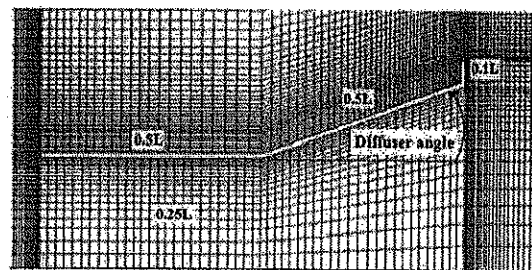


Figure 3. Diffuser dimension and grid system

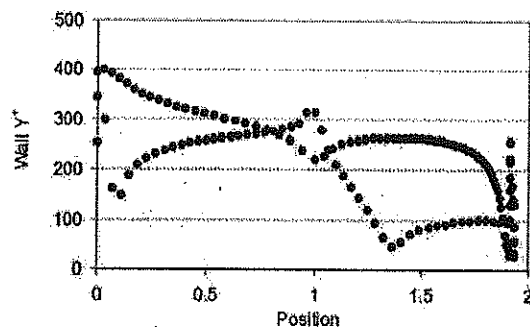


Figure 4.  $Y^+$  of diffuser wall.

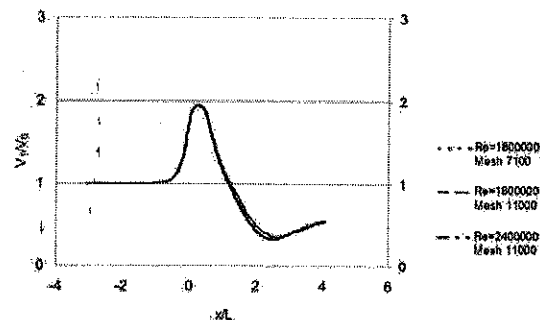


Figure 4.1  $V_1/V_0$  at axial diffuser.

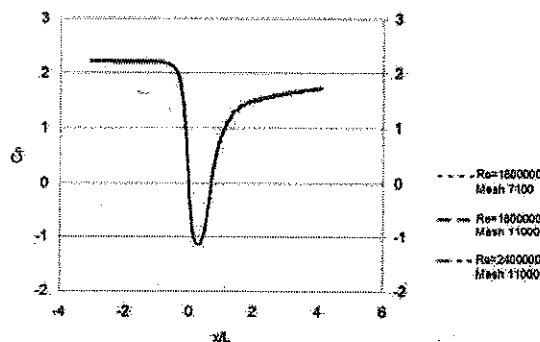
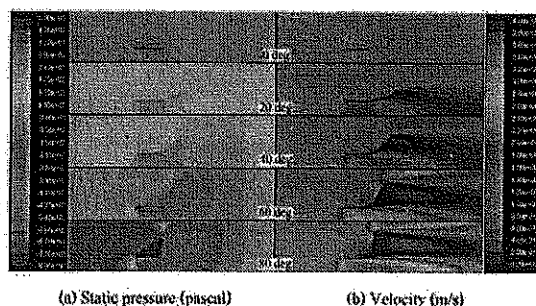
Figure 5. Value of  $C_p$  at axial diffuser.

Figure 6. Velocity (a) and pressure contour (b) of the empty diffuser.

the diffuser angle as shown in Figure 6b. However, the flow pattern can be divided into two cases: the first group is when the diffuser angles are between 0 and 20 degrees, which are the reasons for the increase in velocity at the throat because the pressure at the back of the diffuser becomes negative pressure due to the diffuser angle as shown in Figure 6a. The fluid flow at the throat will try to maintain its flow condition and accelerated through diffuser and the maximum speed is in the diffuser as shown in Figure 6b. The other group is the case of higher degrees, 40, 60 and 80 degree, even though the axial exit velocity does not decrease but the recirculation occurred at the exit of the diffuser. This recirculation also caused of lower pressure, then fluid in diffuser try to decrease pressure to exit value and fluid is speed up inside. That all results agree with Abe, Ohya, 2004

When rotor turbine was installed in diffuser. Equation (12) was used to find out load of rotor. The  $1^{\text{st}}$  term is assumed to be zero. Maximum turbine power coefficient from Betz theory is 0.59 when induction factor ( $a$ ) is  $1/3$ , then  $C_p$  equals 1333/m at porous medium of 0.0015 m thickness.

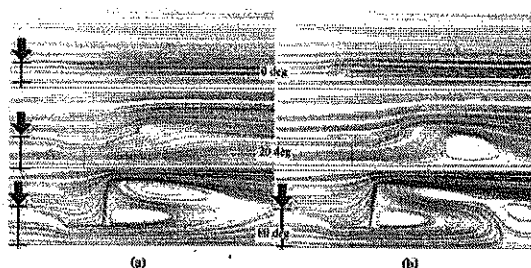
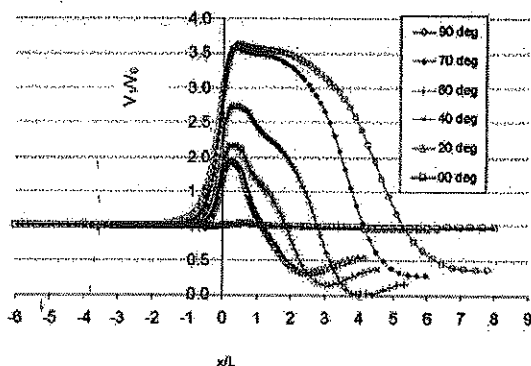
The results of 2D Simulation show the streamline, at the angle of diffuser at 0°, 20°, and 80°, of empty diffuser and diffuser with 0.59  $C_p$  of rotor turbine as shown in Figure 7a) and 7b), respectively. The increasing angle of diffuser shows the increasing of effective area. Even though when the rotor

was installed, this area is not much changed. This is the reason the velocity increased in the diffuser and there was more recirculation at exit of duct. However when the rotor turbine is installed, the flow shows the increase of recirculation with increasing diffuser angle.

The relation of velocity inside diffuser also show in the results of velocity plot on x-axis with different diffuser angle as shown in Figure 8. These results confirm all previous results that the velocity inside diffuser increases when the diffuser angle increases.

### 3) Diffuser augmentation, $\beta\gamma$

The results show diffuser area ratio, ( $\beta$ ) Back pressure velocity ratio, ( $\gamma$ ), Diffuser augmentation ( $\beta\gamma$ ), VS Diffuser angle.  $\beta$  increases up to approximately 1.75 at 20 degree and then decreases to 1.0 at 50 degree, while  $\gamma$  gets increasing when the angle of diffuser increases as shown in Figure 9. It means that there is negative back pressure at the exit of the diffuser as seen in Figure 10. But the multiplication of  $\beta$  and  $\gamma$  is up. Therefore, it can be defined as  $\gamma$  significantly effects on diffuser augmentation ( $\beta\gamma$ ) while  $\beta$  will be important if its angle is less than 20°

Figure 7. Water streamlines of diffuser (a) without and (b) with 0.59  $C_p$  of rotor turbine at 0, 20, and 80 degree.Figure 8. Relation between  $V/V_0$  at different points on the x-axis direction to angle of the empty diffuser

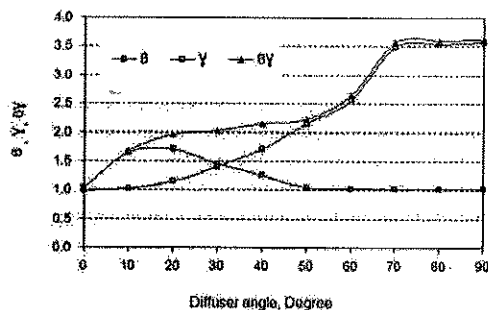


Figure 9. Relation of the diffuser area ratio, ( $\beta$ ), back pressure velocity ratio, ( $\gamma$ ), and diffuser augmentation, ( $\beta\gamma$ ) to diffuser angle.

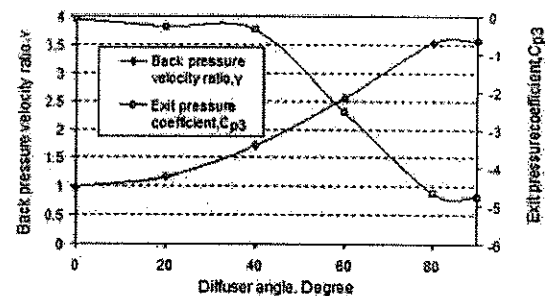


Figure 10. Relation of back pressure velocity ratio, ( $\gamma$ ), and exit pressure coefficient,  $C_{p3}$ , to diffuser angle.

#### 4) Axial flow

The results also show From Figure 11 we can see that water speed up strike to rotor with diffuser compare to un-install or installation of 0 degree diffuser. When  $V_1/V_0$  increased according to angle of diffuser, pressure drop across rotor of turbine increased too. This show system can produce more power when more angle of diffuser was installed to rotor.

#### 5) Thrust loading coefficient

Figure 12: to widen angle of diffuser causes diffuser augmentation be higher; while thrust forced toward diffuser is obviously getting up between the phase of 0-20° and 50-70° but slightly influence on thrust coefficient of rotor. It can be defined as if we build diffuser with the more degree in order to keep energy as much as we require, durable structure is needed for the increasing thrust.

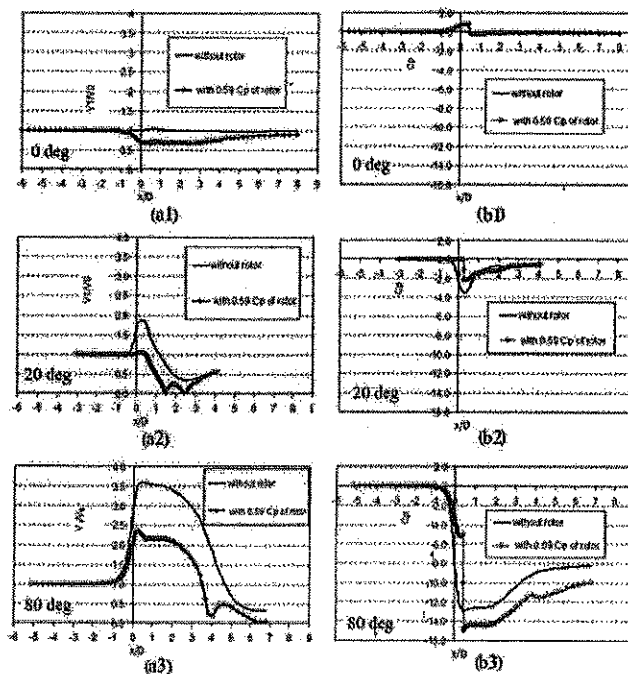


Figure 11. Velocity (a) and pressure coefficient (b) at axis of diffuser with and without rotor turbine with 0, 20, and 80 degree of the diffuser.



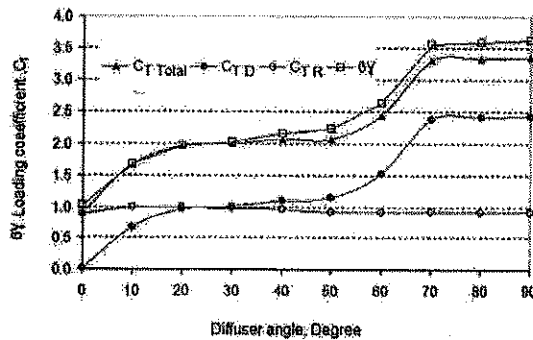


Figure 12. Relation of disk loading coefficient,  $C_{TD}$ ,  $C_{TR}$ ,  $C_p$  and  $\beta\gamma$  to diffuser angle, in degree.

#### 6) Rotor power coefficient

Figure 13: It shows the Rotor power coefficient and diffuser augmentation,  $\beta\gamma$  in case of axial induction factor,  $a = 1/3$ . We will see that the Maximum rotor power coefficient is 2.14 at 90 degree, and the minimum is 0.59 at 0 degree (we supposed it is the ideal turbine). We can say that the diffuser augmented rotor power 3.62 times compared to the system without the diffuser

#### 7) Validation of model

To validate the model simulation, 1.1 meter diameter 20 degree of diffuser was constructed and test in natural flow channel. Velocity of free upstream and middle of diffuser was collected every 20 second by paddlewheel flow sensor IP101 series. It was found that at mean free stream in front of diffuser 0.90 m/s we got 1.55 m/s inside of diffuser. We can say that Diffuser augmentation is 1.72 compare to the simulation result 1.96 or 14% different.

#### 4. Concluding remarks

Widening degree of diffuser causes more augmentation of  $V_1/V_0$  which will be rapidly growing during the phase 0-20° and 50-70°. If the degree approximately equals 20°-50°, the augmentation will not change much; while the angle is about 70°-90°  $V_1/V_0$  will be fixed. Thrust toward rotor will be steady if the augmentation is increased; where as thrust toward diffuser will be higher similarly. So, before contouring it's necessary to evaluate thrust. The effective factors towards  $V_1/V_0$  include Diffuser area ratio, ( $\beta$ ) and Back pressure velocity ratio ( $\gamma$ ) that the latter one indicates it's increasing according to degree of diffuser which is good to performance of diffuser angle. At the same time  $\beta$  will be lower if the angle degree is more than 20° and will 1 as approximation when the degree is up to 50°. Via the study the diffuser augmentation will reach the maximum rate at 3.62 when the angle degree

equals 90° and when the angle degree is about 20°- 50° the maximum rotor power coefficient will be about 2.14

The above study aims at studying single factor that is diffuser angle. Still, there are many important factors needed further studying such as height of flange, length of diffuser and installing technique and etc.

#### Acknowledgment

The authors thank the Electricity Generating Authority of Thailand for funding this research.

#### References

- Bahaj, A.S. and Myers, L.E. 2003, Fundamentals applicable to the utilization of marine current turbine for energy production, *Renewable Energy* 28, 2205-2211.
- Kirke, B. 2005. Development in ducted water current turbines available online at [www.Cyberiad.net](http://www.Cyberiad.net)
- David, L. F., Gaden and Eric L. Bibeau. 2008. Increasing Power Density of inetic Turbines for Cost-effective Distributed Power Generation. Department of Mechanical and Manufacturing Engineering, University of Manitoba.

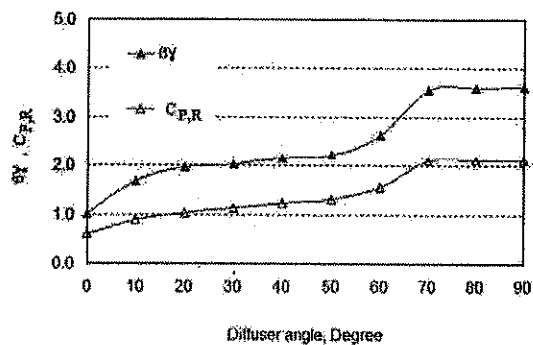


Figure 13. Relation of rotor power coefficient,  $C_{p,R}$  and diffuser augmentation,  $\beta\gamma$ , to diffuser angle, in degree, in case of  $a = 1/3$ .

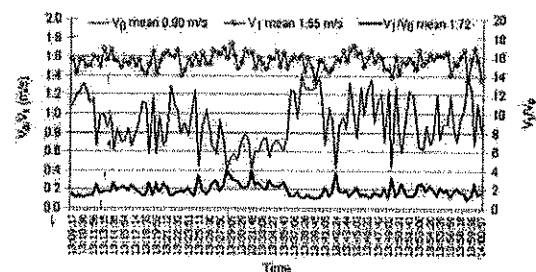


Figure 14. Diffuser without rotor turbine test result.

- Canada.
- Fernando Ponta and Gautam Shankar Dutt, An improved vertical-axis water-current turbine incorporating a channeling device, *Renewable energy* 20 (2000), 223-241.
- Final Report on Preliminary Works Associated with IMW Tidal Turbine Project Reference: T/06/00233/00/00 URN 06/2046 Contractors Sea Generation Ltd Prepared by David Ainsworth, Jeremy Thake Marine Current Turbines Ltd.
- Gerard, J.W. van bassel. 2007. The science of making more torque from wind: Diffuser experiments and revisited. *Journal of physics: conference series* 75(2007) 012010 IOP Publishing doi: 10.1088/1742-6596/75/1/012010.
- G Mac Pherson-Grant. 2005. (17) The Advantages of Ducted over Unducted Turbines. 6th European Wave & Tidal Energy Conference Glasgow, September 2005.
- G Mac Pherson-Grant, The Advantages of Ducted over Unducted Turbines Rotec Engineering Ltd. 6th European Wave & Tidal Energy Conference Glasgow, September 2005.
- Ken-ichi Abe, Yuji Ohya. 2004. An investigation of flow field around flange diffuser using CFD, *Journal of Wind Engineering and Industrial Aerodynamics* 92, 315-330.
- Khan M.J., Iqbal M.T. and J.E. Qualicoe. 2008. River current energy conversion system: Progress, prospects and challenges, *Renewable and sustainable energy reviews* 12, 2177-2193.
- Kiho, S., Shiono, M. and Suzuki, K. The power generation from tidal currents by Darrieus turbine, Department of Electric Engineering, College of Science & Technology, Nihon University Tokyo, Japan.
- Myers, L., Bahaj, A.S. 2006. Power output performance characteristics of horizontal axis marine current turbine, *Renewable energy* 31, 197-208.
- Fraenkel, P. 2006. Tidal current energy technologies, Marine current turbine limited, the green, stoke gifford, Bristol. BS 34 8PD, UK. Ibis 148, 145-151.
- Phillips, D.G., Richards, P.J., Flay, R.G.J. 2002. CFD modeling and the Development of the diffuser augmented wind turbine, *Wind and Structure*, 5(2-4), 267-276.
- Ponta, F.L and Jacovki, P.M. 2008. Marine current power generation by diffuser- augmented floating hydro turbines, *Renewable energy* 33, 665-673.
- Phillips, D.G., Richards, P.J., Flay, R.G.J. 2008. Diffuser development for a diffuser augmented wind turbine using computational fluid dynamics. Department of Mechanical Engineering the University of Auckland, New Zealand.
- Matsushima, T., Takagi, S., Muroyama, S. 2006. Characteristics of a highly efficient propeller type small wind turbine with a diffuser. *Renewable Energy*, 31, 1343-1354.
- Ohya, Y., Karasudania, T., Sakurai, A., Abek, K., Inoue, M. 2008. Development of a shrouded wind turbine with a flanged diffuser. *Journal of wind Engineering and Industrial aerodynamics*, 96, 524-539.

# Symbols:

$\alpha$	Axial induction factor
$\alpha_e, \alpha_s$	Inverse effective Prandtl numbers of $k$ and $\epsilon$ consequently
$\beta$	Diffuser area ratio
$\beta\gamma$	Diffuser augmentation
$C_p$	Pressure coefficient
$C_p^i$	Pressure coefficient at location $i$
$C_{PR}$	Rotor power coefficient
$C_{P,exit}$	Power coefficient at diffuser exit
$C_{T,D}$	Thrust coefficient of diffuser
$C_{T,T}$	Total thrust coefficient of diffuser plus rotor
$C_{T,R}$	Thrust coefficient of rotor
$C_{1a}, C_{2a}, C_{3a}$	Constant values
$\epsilon$	Dissipation rate
$G_i$	Kinematic energy of mean velocity flow
$G_b$	Kinematic energy of buoyancy flow
$\gamma$	Back pressure velocity ratio
$k$	Turbulence kinetic energy
$P_i$	Pressure at location $i$
$\mu$	Molecular viscosity
$V_i$	Velocity at location $i$
$\bar{x}$	Mean of $x$
$Y_M$	Contribution of the fluctuating dilatation in compressible turbulence to the overall dissipation rate

**APPENDIX**  
**B: PRESENTATIONS**

Reference no. GMSARN-2009-097

### Duct design for water current turbine application

P.Khunthongjan\* and U.Teeboonma

Mechanical Engineering Department, Faculty of Engineering,  
Ubon Ratchathni University, Ubon Ratchathni Thailand

\*Corresponding author email [palapum.k@egat.co.th](mailto:palapum.k@egat.co.th)

### Abstract

The water turbine is the mechanical tool that changes the kinetic energy of water current to be useful with environmental influence slightly, since it's unnecessary to build a dam. Somehow, water current in rivers probably was not about to use as the energy resource because its velocity was quite slow. This research, so, studied and designed duct worked as Diffuser in order to be the augmentation factor and CFD Simulation for the water diffuser with Fluent commercial code program. The Field test resulted that they were consistent each other well and the designed diffuser was able to two times increase velocity of water.

**Keyword:** Water duct, Diffuser, Duct, Augmentation factor, CFD Simulation

### 1. Introduction

The function of water turbine is similar to wind turbine that is it gets the kinetic energy of fluid and lower its velocity as said by Betz that if we want to maintain the energy capacity while the velocity is lower, we have to broaden space of the water duct (the limitation of kinetic energy usage from fluid is the specific energy per unit of fluid will be function of velocity<sup>3</sup>) Anyway, if the velocity of fluid is lower, the more complicated of usages its energy. In order to maintain the power it's either need bigger size of turbine or add number of turbine or can be both. If we decide to increase size of the turbine the speed of blade tip may cause the Cavitations and also the location problem. Adding number of turbine was other alternative but it came together with high cost of the project in the inefficient way or the system would be more complicate if we tried to connect several sets of Impeller to the single shaft. Therefore, the possible way of kinetic energy usage from fluid with low velocity was to use Diffuser in order to widen Effective area of the duct; meanwhile, it's to speed up inlet water current. There are some diffuser application with windmill, for example, D.G. Phillips and others (1,2) from the University of Auckland, New Zealand studied and revised DAWT model called Vortec 7 that was built and designed by Foreman and Grumman. The External air jet was used to prevent fluid disperse and control the

Boundary layer in Diffuser from building model by CFD method and Visualization test and found that the Power coefficient factor was four times increase. Toshio Matsushima et al.(3) studied the Frustum-shape Diffuser that was incentive capacity of small windmill from the model system by I-DEAS Frustum-shape Diffuser program and found Power coefficient factor was 1-7 times increase. Yuji Ohya et al.(4) studied and developed Diffuser-installed windmill. It's basically studied Nozzle type, Cylindrical type, and Diffuser type and found the latest one came with 1.8 times as the maximum speed. Not only the windmill, diffuser was applied with the water current turbine, David L. et al.(5) studied result of Diffuser of the energy from water turbine by the model system with the program of ANSYS CFX-5.7 Brian (6) installed 1.2\*1.2 meters slot duct (2 sides Airfoil section slats) with the Cross flow turbine type. However, other additional details of diffuser were not mentioned. Karanja Kibicho and Anthony Sayers (7) studied the fluid flow in Wide angel diffuser since the disperse of pressure in Wide angel diffuser was irregular; one found it's flowing while another one not that called Stalling. It effected to overall flow in Diffuser and without efficiency. R. K. Sullerey et at. (8) had the comparative study the capacity between Straight and Curve and diffuser at Reynolds number  $7.8 \times 10^5 - 1.29 \times 10^6$ . The fluid flow in Diffuser depended on Divergence angle, length and width Throat and the vicissitudes of Inlet free stream.

This study aimed to design diffuser using Computational Fluid Dynamics (CFD) Fluent commercial code for horizontal axis water turbine application and also proposed the field test result at different circumstance.

## 2. Material and Method

Water speed simulation in diffuser would use the program of Fluent commercial code. The simulation would regularly set the speed of fluid flow from the inlet boundary to the outlet (Fig.1) Domain was separated into quadrilateral cells total 30,194 cells as in Table 1

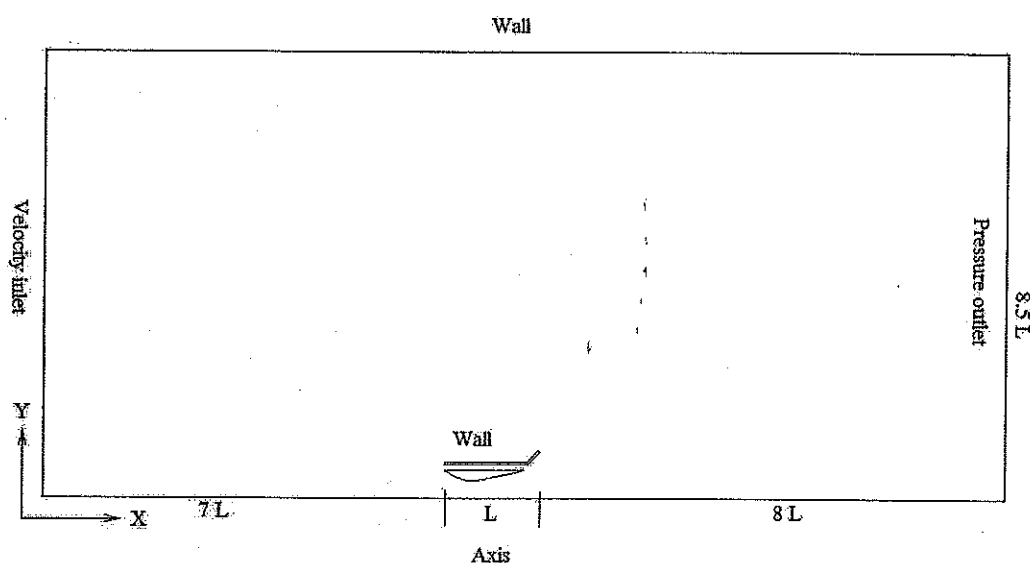


Fig.1 Boundary condition

Table. 1 Computational parameters

Solver	Axisymmetric, steady
Viscous model	K-epsilon RNG, Standard wall function
Turbulent kinetic energy $k(m^2/s^2)$	0.5
Turbulent dissipation rate $(m^2/s^3)$	0.5
Pressure velocity coupling	simple
Under relaxation factor	0.3 for pressure, 0.7 for momentum
Discretization	
Pressure	standard
Convergence criteria	$10^{-4}$

Duct would be set with a rafting and was pulled with a small boat and test in a reservoir. The pressure of inlet boundary, nozzle, and external of Diffuser would be measured by Manometer principal, using 3 mm diameter transparent plastic pipe.

### 3. Result and Discussion

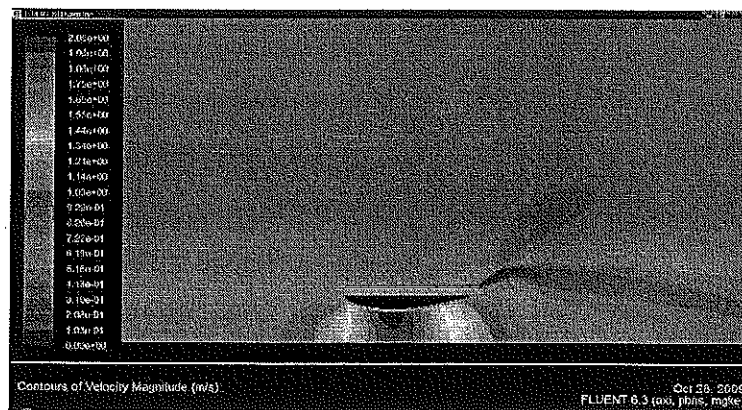


Fig.2 Velocity contour

Fig.2 showed Velocity contour of the simulation. Diffuser effected water speed if the inlet velocity was set at 0.9 m/s, the maximum velocity in diffuser was 1.8 (a double increase) that was happened around the nozzle and lower part, in particular, behind Flange and came about the whirlpool as in Fig.3

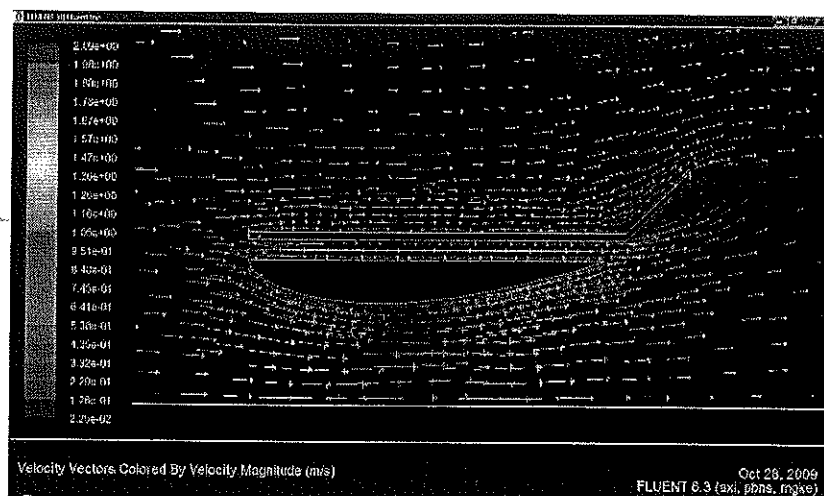


Fig.3 Velocity vector

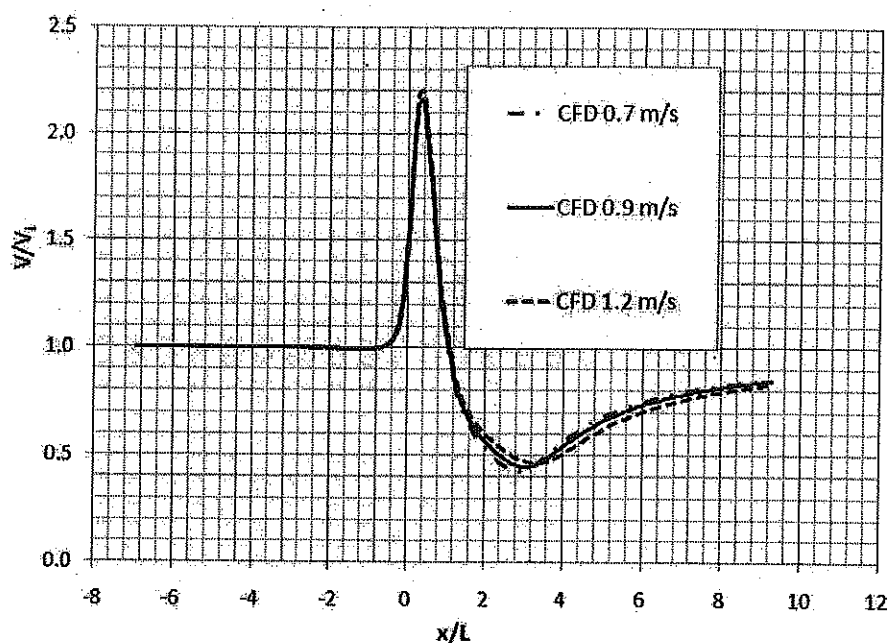


Fig.4 Velocity rate change

Fig.4 at the inlet velocity between 0.7 to 1.2 found the velocity at in front of diffuser ( $x/L = -0.5$ ) started to increase, at the entrance ( $x/L = 0$ ) velocity was 1.3 times and at the exit was 1.0 time of velocity at inlet boundary. At the nozzle of diffuser ( $x/L = 0.3$ ) maximum velocity increasing 2.2 times. Considering effect of velocity inlet to local velocity rate change, from inlet boundary ( $x/L = -7$ ) to exit of diffuser, there were no effect. From exit ( $x/L = 1$ ) to pressure outlet boundary ( $x/L = 9$ ) inlet velocity was a little effect on the rate change of local velocity.

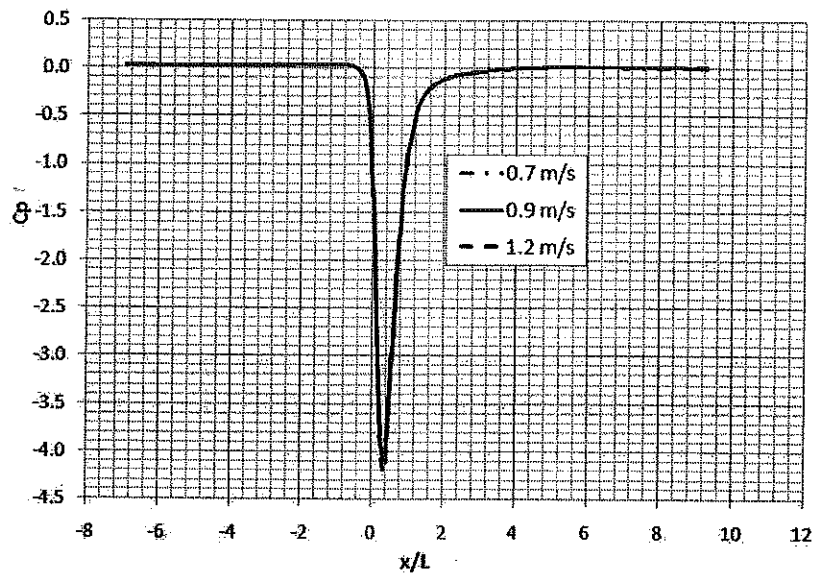


Fig.5 Pressure coefficient comparative

The fig.5 showed Pressure coefficient on the Diffuser axis. At the inlet ( $x/L=0$ ) and outlet of Diffuser ( $x/L=1$ ) the pressure coefficient was lower than zero, which the fluid flow through the Diffuser was higher and not differ even the inlet velocity change.

Fig.6 Velocity line graph from the water speed simulation. It shows three different speed experimental at three different points, external side, inlet and at the nozzle of the Diffuser. Bernoulli's equation was used to calculate the velocity. Experimental velocity at the inlet of diffuser ( $x/L=0$ ) was faster than the external one ( $x/L=-7$ ) same as simulation.

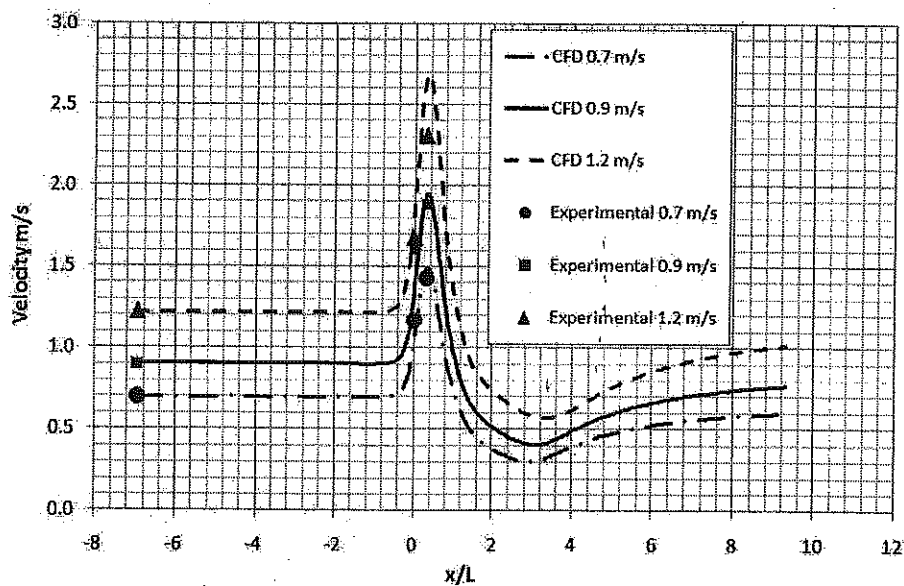


Fig.6 Simulation and Experimental results



#### 4. Conclusions

1. The simulation result with Fluent commercial code program was consistent with Field test result, the diffuser designed doubled velocity of inlet water. Somehow, the case of the internal turbine installed in the Diffuser needs additional study.

2. The hypothesis of simulation was that the velocity was stable and regular. The test get done at deep water if compared to size of diffuser. If the diffuser designed was used or tested in different circumstance, such as shallow water, strong wind and wave etc., probably the results would be different.

3. The installment of duct with water turbine in order to increase velocity of fluid flow was another alternative of water turbine application, particularly in the area of low velocity of water e.g. rivers and canals in Thailand.

#### 5. Acknowledgement

The authors would like to thank The EGAT (Electricity Generating Authority of Thailand) and Ubon ratchathani supported the fund.

#### 6. References

1. Phillips, D.G., Richards, P.J., Flay, R.G.J., 2008, "Diffuser development for a diffuser augmented wind turbine using computational fluid dynamics", Department of Mechanical Engineering the University of Auckland, New Zealand.
2. Phillips, D.G., Richards, P.J., Flay, R.G.J., 2002, "CFD modeling and the development of the diffuser augmented wind turbine", *Wind and Structure*, Vol.5, No.2-4, pp. 267-276.
3. Toshio Matsushima, Shinya Takagi, Seiichi Muroyama, 2006, "Characteristics of a highly efficient propeller type small wind turbine with a diffuser", *Renewable Energy*, Vol. 31, pp. 1343-1354.
4. Yuji Ohya, Takashi Karasudania, Akira Sakuraib, Ken-ichi Abeb, Masahiro Inouec, 2008, "Development of a shrouded wind turbine with a flanged diffuser", *Journal of Wind Engineering and Industrial Aerodynamics*, Vol. 96, pp. 524-539.
5. David L. F. Gaden and Eric L. Bibeau, 2008, "Increasing Power Density of Kinetic Turbines for Cost-effective Distributed Power Generation", Department of Mechanical and Manufacturing Engineering, University of Manitoba, Canada.
6. Brian Kirke, 2005, "Development in ducted water current turbines" available online at [www.Cyberiad.net](http://www.Cyberiad.net)
7. Karanja Kibicho and Anthony Sayers, 2008, "Experimental Measurements of the Mean Flow Field in Wide-Angled Diffusers: A Data Bank Contribution, Proceedings of world academy of science, engineering and technology, Vol.33, September 2008.
8. Sullerey, R. K., Chandra, B. and Muralidhar, V., 1983, "Performance Comparison of Straight and Curved Diffusers", *Def Science Journal*, Vol. 33, No 3, pp. 195-203.

**APPENDIX**  
**C: TEST RESULTS**

Table C1 Electricity generating test results at vary water speed

Water speed m/s	RPM(Rotor)	Power, watts	Power coefficient, Cp
1.08	98.29	104.36	0.18
1.30	112.94	145	0.14
1.32	168.32	212	0.18
1.37	186.01	225.11	0.19
1.31	195.23	248.06	0.24
1.32	200.13	271.46	0.25
1.10	95.01	124.1	0.2
1.36	125.81	185.2	0.16
1.77	139.35	229.8	0.09
1.73	142.66	288	0.12
1.75	152.37	309.9	0.12
1.81	161.61	301.7	0.11

Table C2 Test results at water speed

1.1 m/s

MM/DD/YY 24/6/2011

RPM (PMG)	RPM (Rotor)	Volt, V	Amp., A	Power, Watts	Power coefficient, Cp
198	92.4	18	8	144	0.23
191	89.13	16	7	112	0.18
175	81.67	17	7	119	0.19
233	108.73	17	7	119	0.19
181	84.47	18	7	126	0.2
229	106.87	17	7	119	0.19
201	93.8	16	7	112	0.18
221	103.13	18	7	126	0.2
198	92.4	17	8	136	0.22
209	97.53	16	8	128	0.21
Average	95.01	17	7.3	124.1	0.2

Table C3 Test results at water speed

1.36 m/s

MM/DD/YY 24/6/2011

RPM (PMG)	RPM (Rotor)	Volt,V	Amp., A	Power, watts	Power coefficient, Cp
289	134.87	21	8	168	0.14
286	133.47	20	9	180	0.15
277	129.27	22	9	198	0.17
267	124.6	21	8	168	0.14
288	134.4	21	8	168	0.14
265	123.67	20	8	160	0.14
254	118.53	28	9	252	0.21
243	113.4	21	8	168	0.14
225	105	24	8	192	0.16
302	140.93	22	9	198	0.17
Average	125.81	22	8.4	185.2	0.16

Table C4 Test results at water speed

1.77 m/s

MM/DD/YY 24/6/2011

RPM (PMG)	RPM (Rotor)	Volt,V	Amp., A	Power, watts	Power coefficient, Cp
289	134.87	24	10	240	0.09
311	145.13	23	10	230	0.09
292	136.27	20	10	200	0.08
296	138.13	20	10	200	0.08
288	134.4	24	10	240	0.09
301	140.47	26	10	260	0.1
312	145.6	20	10	200	0.08
278	129.73	20	10	200	0.08
310	144.67	26	11	286	0.11
309	144.2	22	11	242	0.09
Average	139.35	22.50	10.2	229.8	0.09

Table C5 Test results at water speed

1.73 m/s

MM/DD/YY 24/6/2011

RPM (PMG)	RPM (Rotor)	Volt,V	Amp., A	Power, watts	Power coefficient, Cp
310	144.67	25	11	275	0.11
296	138.13	24	11	264	0.11
288	134.4	31	11	341	0.14
286	133.47	28	12	336	0.14
322	150.27	25	10	250	0.1
279	130.2	20	12	240	0.1
295	137.67	30	9	270	0.11
329	153.53	27	12	324	0.13
318	148.4	31	10	310	0.13
334	155.87	30	9	270	0.11
Average	142.66	27.1	10.7	288	0.12

Table C6 Test results at water speed

1.75 m/s

MM/DD/YY 24/6/2011

RPM (PMG)	RPM (Rotor)	Volt,V	Amp., A	Power, watts	Power coefficient, Cp
332	154.93	30	12	360	0.14
341	159.13	31	12	372	0.15
304	141.87	31	11	341	0.14
315	147	30	11	330	0.13
328	153.07	28	11	308	0.12
360	168	29	10	290	0.12
302	140.93	27	10	270	0.11
308	143.73	26	10	260	0.1
340	158.67	28	11	308	0.12
335	156.33	26	10	260	0.1
Average	152.37	28.6	10.8	309.9	0.12

Table C7 Test results at water speed

1.81 m/s

MM/DD/YY 24/6/2011

RPM (PMG)	RPM (Rotor)	Volt,V	Amp., A	Power, watts	Power coefficient, Cp
373	174.07	25	12	300	0.11
382	178.27	29	12	348	0.12
321	149.8	28	11	308	0.11
345	161	23	10	230	0.08
297	138.6	23	10	230	0.08
304	141.87	26	11	286	0.1
353	164.73	30	11	330	0.12
362	168.93	35	11	385	0.14
365	170.33	33	10	330	0.12
361	168.47	27	10	270	0.1
Average	161.61	26	11	301.7	0.11

Table C8 Test results at water speed

1.08 m/s

MM/DD/YY 22/6/2011

RPM (PMG)	RPM (Rotor)	Volt,V	Amp., A	Power, watts	Power coefficient, Cp
251	117.26	33	3	99	0.17
229	106.66	33	3	99	0.17
209	97.72	37	3	111	0.19
202	94.37	36	3	108	0.18
217	101.07	39	3	117	0.2
196	91.58	36	3	108	0.18
190	88.79	38	3	114	0.19
209	97.72	35	3	105	0.18
207	96.6	31	2	62	0.1
239	111.68	37	3	111	0.19
167	77.78	38	3	114	0.19
Average	98.29	35.73	2.91	104.36	0.18

Table C9 Test results at water speed

1.3 m/s

MM/DD/YY 22/6/2011

RPM (PMG)	RPM (Rotor)	Volt,V	Amp., A	Power, watts	Power coefficient, Cp
240	111.88	36	5	180	0.17
259	120.83	32	6	192	0.19
253	118.28	27	6	162	0.16
204	95.26	31	5	155	0.15
240	111.88	26	5	130	0.13
247	115.08	24	5	120	0.12
266	124.03	26	5	130	0.13
219	102.29	26	6	156	0.15
269	125.31	25	6	150	0.14
288	112.99	30	6	180	0.17
289	113.09	25	5	125	0.12
301	112.38	25	6	150	0.14
271	111.85	4	6	24	0.02
273	113.36	25	5	125	0.12
256	113.49	25	6	150	0.14
Average	112.94	26.06	5.59	145	0.14

Table C10 Test results at water speed

1.32 m/s

MM/DD/YY 22/6/2011

RPM (PMG)	RPM (Rotor)	Volt,V	Amp., A	Power, watts	Power coefficient, Cp
399	186	26	8	208	0.19
355	165.62	27	8	216	0.2
382	178.36	35	8	280	0.26
368	171.57	23	8	184	0.17
357	166.47	29	7	203	0.19
360	168.17	28	8	224	0.21
357	166.47	29	8	232	0.21

Table C10 (Cont.) Test results at water speed

1.32 m/s

MM/DD/YY 22/6/2011

RPM (PMG)	RPM (Rotor)	Volt,V	Amp., A	Power, watts	Power coefficient, Cp
349	163.07	25	8	200	0.18
335	156.28	25	6	150	0.14
360	168.17	25	7	175	0.16
335	168.32	30	9	270	0.25
		26	7	182	0.17
		22	7	154	0.14
		32	8	256	0.23
		30	7	210	0.19
Average	168.32	27.56	7.67	212	0.19

Table C11 Test results at water speed

1.37 m/s

MM/DD/YY 22/6/2011

RPM (PMG)	RPM (Rotor)	Volt,V	Amp., A	Power, watts	Power coefficient, Cp
424	197.89	26	8	208	0.17
340	158.57	27	8	216	0.18
423	197.25	35	8	280	0.23
462	215.62	23	8	184	0.15
317	147.94	29	9	261	0.22
541	252.36	28	8	224	0.19
358	167.27	29	8	232	0.19
332	154.83	25	8	200	0.17
477	222.39	28	8	224	0.19
326	186.01	30	9	270	0.22
		26	9	234	0.19
		25	8	200	0.17
		25	8	200	0.17



Table C11 (Cont.) Test results at water speed

1.37 m/s

MM/DD/YY 22/6/2011

RPM (PMG)	RPM (Rotor)	Volt,V	Amp., A	Power, watts	Power coefficient, Cp
		31	8	248	0.21
		32	8	256	0.21
		30	8	240	0.2
Average	186.01	27.72	8.11	225.11	0.19

Table C12 Test results at water speed

1.31 m/s

MM/DD/YY 22/6/2011

RPM (PMG)	RPM (Rotor)	Volt,V	Amp., A	Power, watts	Power coefficient, Cp
376	175.47	25	10	250	0.24
382	178.04	24	12	288	0.27
352	164.34	28	10	280	0.27
398	185.74	21	11	231	0.22
405	189.16	21	10	210	0.2
440	205.43	25	10	250	0.24
471	219.98	20	8	160	0.15
387	180.6	25	9	225	0.21
		24	11	264	0.25
		20	10	200	0.19
		25	10	250	0.24
		26	10	260	0.25
		26	11	286	0.27
		22	11	242	0.23
		26	9	234	0.22
		25	9	225.11	0.21
Average	195.23	24.37	10.16	248.06	0.24

Table C13 Test results at water speed

1.48 m/s

MM/DD/YY 22/6/2011

RPM (PMG)	RPM (Rotor)	Volt,V	Amp., A	Power, watts	Power coefficient, Cp
374	174.53	31	9	279	0.26
408	190.24	25	9	225	0.21
355	165.81	24	7	168	0.15
380	177.15	30	9	270	0.25
333	155.33	27	9	243	0.22
520	242.6	30	10	300	0.28
563	262.67	30	11	330	0.3
449	209.44	34	10	340	0.31
638	297.58	27	11	297	0.27
350	163.19	33	13	429	0.39
342	159.7	21	11	231	0.21
436	203.33	30	10	300	0.28
		33	9	297	0.27
		30	9	270	0.25
		20	10	200	0.18
		28	10	280	0.26
		25	12	300	0.28
		22	10	220	0.2
		24	9	225.11	0.21
		30	9	225.11	0.21
Average	200.13	27.7	9.85	271.46	0.25

Table C14 Water speed data at Sirindhorn hydropower operation 10 mw

MM/DD/YY 24/6/2011

Average water speed 1.10m/s

Time	Flow rate m3/hr	Speed m/s	Time	Flow rate m3/hr	Speed m/s
12:07:02	451.61	1.77	12:08:07	255.27	1
12:07:07	255.3	1	12:08:12	255.27	1
12:07:12	255.3	1	12:08:17	255.27	1
12:07:17	439.46	1.73	12:08:22	279.57	1.1
12:07:22	439.46	1.73	12:08:27	279.57	1.1
12:07:27	439.46	1.73	12:08:32	205.61	0.81
12:07:32	363.22	1.43	12:08:37	205.61	0.81
12:07:37	363.22	1.43	12:08:42	205.61	0.81
12:07:42	235.65	0.93	12:08:47	471.23	1.85
12:07:47	235.65	0.93	12:08:52	471.23	1.85
12:07:52	284.72	1.12	12:08:57	147.24	0.58
12:07:57	284.72	1.12	12:09:02	147.24	0.58
12:08:02	284.72	1.12	12:09:07	206.15	0.81
12:09:12	206.15	0.81	12:10:37	210.96	0.83
12:09:17	206.15	0.81	12:10:42	210.96	0.83
12:09:22	323.4	1.27	12:10:47	166.89	0.66
12:09:27	323.4	1.27	12:10:52	166.89	0.66
12:09:32	323.4	1.27	12:10:57	382.88	1.5
12:09:37	343.56	1.35	12:11:02	382.88	1.5
12:09:42	343.56	1.35	12:11:07	382.88	1.5
12:09:47	373.02	1.47	12:11:12	165.44	0.65
12:09:52	373.02	1.47	12:11:17	165.44	0.65
12:09:57	186.58	0.73	12:11:22	165.44	0.65
12:10:02	186.58	0.73	12:11:27	103.37	0.41
12:10:07	186.58	0.73	12:11:32	103.37	0.41
12:10:12	443.01	1.74	12:11:37	323.97	1.27
12:10:17	443.01	1.74	12:11:42	323.97	1.27

Table C14 (Cont.) Water speed data at Sirindhorn hydropower operation 10 mw

MM/DD/YY 24/6/2011

Average water speed 1.10m/s

Time	Flow rate m3/hr	Speed m/s	Time	Flow rate m3/hr	Speed m/s
12:10:22	288.29	1.13	12:11:47	323.97	1.27

Table C15 Water speed data at Sirindhorn hydropower operation 15 mw

MM/DD/YY 24/6/2011

Average water speed 1.36 m/s

Time	Flow rate m3/hr	Speed m/s	Time	Flow rate m3/hr	Speed m/s
11:50:02	353.64	1.39	11:51:52	417.15	1.64
11:50:07	353.64	1.39	11:51:57	417.15	1.64
11:50:12	433.91	1.7	11:52:02	172.24	0.68
11:50:17	433.91	1.7	11:52:07	172.24	0.68
11:50:22	433.91	1.7	11:52:12	172.24	0.68
11:50:32	337.45	1.33	11:52:22	450.02	1.77
11:50:37	141.07	0.55	11:52:27	417.93	1.64
11:50:42	141.07	0.55	11:52:32	417.93	1.64
11:50:47	141.07	0.55	11:52:37	417.93	1.64
11:50:52	259.08	1.02	11:52:42	417.82	1.64
11:51:17	510.76	2.01	11:53:07	192.56	0.76
11:51:22	510.76	2.01	11:53:12	192.56	0.76
11:51:27	289.31	1.14	11:53:17	530.31	2.08
11:51:32	289.31	1.14	11:53:22	530.31	2.08
11:51:37	289.31	1.14	11:53:27	530.31	2.08
11:51:42	626.82	2.46	11:53:32	157.99	0.62
11:51:47	626.82	2.46	11:53:37	157.99	0.62
11:53:42	191.51	0.75	11:54:12	322.81	1.27
11:53:47	191.51	0.75	11:54:17	322.81	1.27
11:53:52	191.51	0.75	11:54:22	358.12	1.41

Table C15 (Cont.) Water speed data at Sirindhorn hydropower operation 15 mw

MM/DD/YY 24/6/2011

Average water speed 1.36 m/s

Time	Flow rate m3/hr	Speed m/s	Time	Flow rate m3/hr	Speed m/s
11:53:57	265.19	1.04	11:54:27	358.12	1.41
11:54:02	265.19	1.04	11:54:32	515.51	2.03
11:54:07	322.81	1.27	11:54:37	515.51	2.03
11:54:42	515.51	2.03	11:55:37	193.7	0.76
11:54:47	306.99	1.21	11:55:42	193.7	0.76
11:54:52	306.99	1.21	11:55:47	188.38	0.74
11:55:07	530.33	2.08	11:56:02	350.75	1.38
11:55:12	257.12	1.01	11:56:07	350.75	1.38
11:55:17	257.12	1.01	11:56:12	498.22	1.96
11:55:22	336.52	1.32	11:56:17	498.22	1.96
11:55:27	336.52	1.32	11:56:22	406.32	1.6
11:55:32	193.7	0.76	11:56:27	406.32	1.6
11:56:32	406.32	1.6	11:57:37	185.31	0.73
11:56:37	414.44	1.63	11:57:42	185.31	0.73
11:56:42	414.44	1.63	11:57:47	185.31	0.73
11:56:47	560.84	2.2	11:57:52	609.55	2.39
11:57:12	305.33	1.2	11:58:17	337.59	1.33
11:57:17	305.33	1.2	11:58:22	337.59	1.33
11:57:22	305.33	1.2	11:58:27	433.91	1.7
11:57:27	183.75	0.72	11:58:32	433.91	1.7
11:57:32	183.75	0.72	11:58:37	453.18	1.78
11:58:42	453.18	1.78	11:59:47	321.45	1.26
11:58:47	453.18	1.78	11:59:52	530.35	2.08
11:58:52	328.77	1.29	11:59:57	530.35	2.08
11:58:57	328.77	1.29	12:00:02	530.35	2.08
11:59:02	328.77	1.29	11:59:22	385.69	1.52
11:59:07	380.33	1.49	11:59:27	145.44	0.57

Table C15(Cont.) Water speed data at Sirindhorn hydropower operation 15 mw

MM/DD/YY 24/6/2011

Average water speed 1.36 m/s

Time	Flow rate m3/hr	Speed m/s	Time	Flow rate m3/hr	Speed m/s
11:59:12	380.33	1.49	11:59:32	145.44	0.57

Table C16 Water speed data at Sirindhorn hydropower operation 20 mw

MM/DD/YY 24/6/2011

Average water speed 1.77 m/s

Time	Flow rate m3/hr	Speed m/s	Time	Flow rate m3/hr	Speed m/s
10:42:02	490.93	1.93	10:43:52	466.76	1.83
10:42:07	466.9	1.83	10:43:57	454.8	1.79
10:42:12	466.9	1.83	10:44:02	454.8	1.79
10:42:17	466.53	1.83	10:44:07	342.92	1.35
10:42:22	466.53	1.83	10:44:12	342.92	1.35
10:42:27	466.53	1.83	10:44:17	342.92	1.35
10:42:32	421.7	1.66	10:44:22	481.13	1.89
10:42:37	421.7	1.66	10:44:27	481.13	1.89
10:42:42	234.64	0.92	10:44:32	481.13	1.89
10:42:47	234.64	0.92	10:44:37	383.02	1.5
10:42:52	234.64	0.92	10:44:42	383.02	1.5
10:42:57	435.76	1.71	10:44:47	466.59	1.83
10:43:02	435.76	1.71	10:44:52	466.59	1.83
10:43:07	517.24	2.03	10:44:57	484.33	1.9
10:43:12	517.24	2.03	10:45:02	484.33	1.9
10:43:17	517.24	2.03	10:45:07	484.33	1.9
10:43:22	459.24	1.8	10:45:12	426.24	1.67
10:43:27	459.24	1.8	10:45:17	426.24	1.67
10:43:32	460.2	1.81	10:45:22	451.84	1.77
10:43:37	460.2	1.81	10:45:27	451.84	1.77

Table C16 (Cont.) Water speed data at Sirindhorn hydropower operation 20 mw

MM/DD/YY 24/6/2011

Average water speed 1.77 m/s

Time	Flow rate m3/hr	Speed m/s	Time	Flow rate m3/hr	Speed m/s
10:43:42	460.2	1.81	10:45:32	451.84	1.77
10:43:47	466.76	1.83	10:45:37	452.67	1.78
10:45:42	452.67	1.78	10:48:02	524.02	2.06
10:45:47	465.87	1.83	10:48:07	388.06	1.52
10:45:52	465.87	1.83	10:48:12	388.06	1.52
10:45:57	465.87	1.83	10:48:17	477.76	1.88
10:46:02	568.5	2.23	10:48:22	477.76	1.88
10:46:07	568.5	2.23	10:48:27	462.99	1.82
10:46:12	379.01	1.49	10:48:32	462.99	1.82
10:46:17	379.01	1.49	10:48:37	462.99	1.82
10:46:22	379.01	1.49	10:48:42	568.07	2.23
10:46:27	477.51	1.88	10:48:47	568.07	2.23
10:46:32	477.51	1.88	10:48:52	438.5	1.72
10:46:37	441.06	1.73	10:48:57	438.5	1.72
10:46:42	441.06	1.73	10:49:02	438.5	1.72
10:46:47	441.06	1.73	10:49:07	398.04	1.56
10:46:52	568.52	2.23	10:49:12	398.04	1.56
10:46:57	568.52	2.23	10:49:17	408.64	1.61
10:47:07	458.7	1.8	10:49:27	408.64	1.61
10:47:12	482.51	1.9	10:49:32	402.2	1.58
10:47:17	482.51	1.9	10:49:37	402.2	1.58
10:47:22	482.51	1.9	10:49:42	410.66	1.61
10:47:27	502.1	1.97	10:49:47	410.66	1.61
10:47:32	502.1	1.97	10:49:52	410.66	1.61
10:47:37	502.1	1.97	10:49:57	431.28	1.69
10:47:42	479.44	1.88	10:47:52	524.02	2.06
10:47:47	479.44	1.88	10:47:57	524.02	2.06

Table C17 Water speed data at Sirindhorn hydropower operation 25 mw

MM/DD/YY 24/6/2011

Average water speed 1.73 m/s

Time	Flow rate m3/hr	Speed m/s	Time	Flow rate m3/hr	Speed m/s
11:02:22	388	1.52	11:04:12	469.22	1.84
11:02:27	431.98	1.7	11:04:17	469.22	1.84
11:02:32	431.98	1.7	11:04:22	511.95	2.01
11:02:37	431.98	1.7	11:04:27	511.95	2.01
11:02:42	343.49	1.35	11:04:32	523.34	2.06
11:02:47	343.49	1.35	11:04:37	523.34	2.06
11:02:52	451.86	1.77	11:04:42	523.34	2.06
11:02:57	451.86	1.77	11:04:47	511.59	2.01
11:03:02	451.86	1.77	11:04:52	511.59	2.01
11:03:07	532.4	2.09	11:04:57	505.32	1.98
11:03:12	532.4	2.09	11:05:02	505.32	1.98
11:03:17	496.6	1.95	11:05:07	569.57	2.24
11:03:22	496.6	1.95	11:05:12	569.57	2.24
11:03:27	496.6	1.95	11:05:17	569.57	2.24
11:03:32	352.81	1.39	11:05:22	494.26	1.94
11:03:37	352.81	1.39	11:05:27	494.26	1.94
11:03:42	381.09	1.5	11:05:32	344.71	1.35
11:03:47	381.09	1.5	11:05:37	344.71	1.35
11:03:52	484.74	1.9	11:05:42	344.71	1.35
11:03:57	484.74	1.9	11:05:47	501.79	1.97
11:04:02	484.74	1.9	11:05:52	501.79	1.97
11:06:02	180.5	0.71	11:08:22	342.21	1.34
11:06:07	180.5	0.71	11:08:27	439.17	1.73
11:06:12	306.84	1.21	11:08:32	439.17	1.73
11:06:17	306.84	1.21	11:08:37	416.36	1.64
11:06:22	449.5	1.77	11:08:42	416.36	1.64
11:06:27	449.5	1.77	11:08:47	416.36	1.64



Table C17(Cont.) Water speed data at Sirindhorn hydropower operation 25 mw

MM/DD/YY 24/6/2011

Average water speed 1.73 m/s

Time	Flow rate m3/hr	Speed m/s	Time	Flow rate m3/hr	Speed m/s
11:06:32	449.5	1.77	11:08:52	445.84	1.75
11:06:37	532.55	2.09	11:08:57	445.84	1.75
11:06:42	532.55	2.09	11:09:02	279.76	1.1
11:07:07	306.82	1.21	11:09:27	451.16	1.77
11:07:17	385.34	1.51	11:09:37	451.16	1.77
11:07:22	385.34	1.51	11:09:42	550.46	2.16
11:07:27	434.15	1.71	11:09:47	550.46	2.16
11:07:32	434.15	1.71	11:09:52	514.33	2.02
11:07:37	295.53	1.16	11:09:57	514.33	2.02
11:07:42	295.53	1.16	11:10:02	514.33	2.02
11:07:47	295.53	1.16	11:10:07	459.39	1.8
11:07:52	564.26	2.22	11:10:12	459.39	1.8
11:07:57	564.26	2.22	11:10:17	568.47	2.23
11:08:02	397.57	1.56	11:10:22	568.47	2.23
11:08:07	397.57	1.56	11:10:27	568.47	2.23
11:08:12	342.21	1.34	11:10:32	285.06	1.12
11:08:17	342.21	1.34	11:10:37	285.06	1.12
11:10:42	532.4	2.09			
11:10:47	532.4	2.09			
11:10:52	532.4	2.09			
11:10:57	487.3	1.91			

Table C18 Water speed data at Sirindhorn hydropower operation 30 mw

MM/DD/YY 24/6/2011

Average water speed 1.75 m/s

Time	Flow rate m3/hr	Speed m/s	Time	Flow rate m3/hr	Speed m/s
11:15:22	252.42	0.99	11:17:12	437.25	1.72
11:15:27	421.84	1.66	11:17:17	318.64	1.25
11:15:32	421.84	1.66	11:17:22	318.64	1.25
11:15:37	475.67	1.87	11:17:27	318.64	1.25
11:15:42	475.67	1.87	11:17:32	504.82	1.98
11:15:47	475.67	1.87	11:17:37	504.82	1.98
11:15:52	456.6	1.79	11:17:42	582	2.29
11:15:57	456.6	1.79	11:17:47	582	2.29
11:16:02	312.08	1.23	11:17:52	582	2.29
11:16:07	312.08	1.23	11:17:57	475.65	1.87
11:16:32	203.86	0.8	11:18:22	339.79	1.33
11:16:37	203.86	0.8	11:18:27	339.79	1.33
11:16:42	436.89	1.72	11:18:32	640.69	2.52
11:16:47	436.89	1.72	11:18:37	640.69	2.52
11:16:52	413.77	1.63	11:18:42	442.77	1.74
11:16:57	413.77	1.63	11:18:47	442.77	1.74
11:17:02	413.77	1.63	11:18:52	442.77	1.74
11:17:07	437.25	1.72	11:18:57	262.14	1.03
11:19:02	262.14	1.03	11:21:22	611.59	2.4
11:19:07	572.74	2.25	11:21:27	558.71	2.19
11:19:12	572.74	2.25	11:21:32	558.71	2.19
11:19:17	572.74	2.25	11:21:37	485.33	1.91
11:19:22	252.41	0.99	11:21:42	485.33	1.91
11:19:27	252.41	0.99	11:21:47	349.51	1.37
11:19:32	431.82	1.7	11:21:52	349.51	1.37
11:19:37	431.82	1.7	11:21:57	349.51	1.37
11:19:42	431.82	1.7	11:22:02	281.53	1.11

Table C18(Cont.) Water speed data at Sirindhorn hydropower operation 30 mw

MM/DD/YY 24/6/2011

Average water speed 1.75 m/s

Time	Flow rate m3/hr	Speed m/s	Time	Flow rate m3/hr	Speed m/s
11:19:47	232.99	0.92	11:22:07	281.53	1.11
11:19:52	232.99	0.92	11:22:12	320.32	1.26
11:19:57	467.65	1.84	11:22:17	320.32	1.26
11:20:02	467.65	1.84	11:22:22	320.32	1.26
11:20:07	467.65	1.84	11:22:27	433.88	1.7
11:20:12	495.08	1.94	11:22:32	433.88	1.7
11:20:17	495.08	1.94	11:22:37	454.16	1.78
11:20:22	331.16	1.3	11:22:42	454.16	1.78
11:20:27	331.16	1.3	11:22:47	454.16	1.78
11:20:52	592.17	2.33	11:23:12	611.58	2.4
11:20:57	592.17	2.33	11:23:17	475.71	1.87
11:21:02	472.25	1.86	11:23:22	475.71	1.87
11:21:07	472.25	1.86	11:23:27	610.81	2.4
11:21:12	611.59	2.4	11:23:32	610.81	2.4
11:21:17	611.59	2.4	11:23:37	610.81	2.4
11:23:42	368.88	1.45	11:23:52	436.87	1.72
11:23:47	368.88	1.45	11:23:57	436.87	1.72
11:24:02	436.87	1.72	11:25:07	519.01	2.04
11:24:07	479.64	1.88	11:25:12	519.01	2.04
11:24:12	479.64	1.88	11:25:17	446.37	1.75
11:24:17	495.04	1.94	11:25:22	446.37	1.75
11:24:22	495.04	1.94	11:25:27	446.37	1.75
11:24:27	495.04	1.94	11:25:32	489.08	1.92
11:24:32	252.44	0.99	11:25:37	489.08	1.92
11:24:37	252.44	0.99	11:25:42	489.08	1.92
11:24:42	563.04	2.21	11:25:02	621.28	2.44
11:24:47	563.04	2.21	11:25:47	563.53	2.21

Table C18(Cont.) Water speed data at Sirindhorn hydropower operation 30 mw

MM/DD/YY 24/6/2011

Average water speed 1.75 m/s

Time	Flow rate m3/hr	Speed m/s	Time	Flow rate m3/hr	Speed m/s
11:24:52	621.28	2.44	11:25:52	563.53	2.21
11:24:57	621.28	2.44	11:25:57	271.82	1.07

Table C19 Water speed data at Sirindhorn hydropower operation 35 mw

MM/DD/YY 24/6/2011

Average water speed 1.81 m/s

Time	Flow rate m3/hr	Speed m/s	Time	Flow rate m3/hr	Speed m/s
11:32:22	574.28	2.26	11:34:12	614.36	2.41
11:32:27	574.28	2.26	11:34:17	614.36	2.41
11:32:32	347.25	1.36	11:34:22	681.11	2.68
11:32:37	347.25	1.36	11:34:27	681.11	2.68
11:32:42	353.2	1.39	11:34:32	414	1.63
11:32:47	353.2	1.39	11:34:37	414	1.63
11:32:52	353.2	1.39	11:34:42	414	1.63
11:32:57	624.87	2.45	11:34:47	414.07	1.63
11:33:02	624.87	2.45	11:34:52	414.07	1.63
11:33:52	314.22	1.23	11:35:42	494.08	1.94
11:33:57	614.29	2.41	11:35:47	427.35	1.68
11:34:02	614.29	2.41	11:35:52	427.35	1.68
11:34:07	614.29	2.41	11:35:57	427.35	1.68
11:36:02	160.37	0.63	11:38:22	383.66	1.51
11:36:07	160.37	0.63	11:38:27	240.4	0.94
11:36:12	160.37	0.63	11:38:32	240.4	0.94
11:36:17	291.66	1.15	11:38:37	240.4	0.94
11:36:22	291.66	1.15	11:38:42	587.62	2.31
11:36:27	247.94	0.97	11:38:47	587.62	2.31

Table C19(Cont.) Water speed data at Sirindhorn hydropower operation 35 mw

MM/DD/YY 24/6/2011

Average water speed 1.81 m/s

Time	Flow rate m3/hr	Speed m/s	Time	Flow rate m3/hr	Speed m/s
11:36:32	247.94	0.97	11:38:52	908.11	3.57
11:36:37	483.81	1.9	11:38:57	908.11	3.57
11:36:42	483.81	1.9	11:39:02	908.11	3.57
11:36:47	483.81	1.9	11:39:07	414.1	1.63
11:36:52	388.4	1.53	11:39:12	414.1	1.63
11:36:57	388.4	1.53	11:39:17	414.1	1.63
11:37:02	307.13	1.21	11:39:22	293.79	1.15
11:37:07	307.13	1.21	11:39:27	293.79	1.15
11:37:12	307.13	1.21	11:39:32	400.61	1.57
11:37:17	367.35	1.44	11:39:37	400.61	1.57
11:37:22	367.35	1.44	11:39:42	454.02	1.78
11:37:27	400.75	1.57	11:39:47	454.02	1.78
11:37:52	625.76	2.46	11:38:17	383.66	1.51
11:37:57	625.76	2.46	11:38:07	454.03	1.78
11:38:02	625.76	2.46			

Table C20 Water speed data at Sirindhorn hydropower operation 11 mw

MM/DD/YY 22/6/2011

Average water speed 1.08 m/s

Time	Flow rate m3/hr	Speed m/s	Time	Flow rate m3/hr	Speed m/s
14:31:32	214.83	0.84	14:41:37	208.29	0.82
14:31:32	214.83	0.84	14:41:37	208.29	0.82
14:32:17	226.38	0.89	14:41:42	208.29	0.82
14:33:12	204.75	0.8	14:41:52	324.87	1.28
14:33:17	204.75	0.8	14:41:57	378.99	1.49
14:33:42	204.75	0.8	14:42:02	243.6	0.96

Table C20(Cont. Water speed data at Sirindhorn hydropower operation 11 mw

MM/DD/YY 22/6/2011

Average water speed 1.08 m/s

Time	Flow rate m3/hr	Speed m/s	Time	Flow rate m3/hr	Speed m/s
14:34:52	312.81	1	14:42:22	243.6	0.96
14:35:07	199.8	0.78	14:42:27	243.6	0.96
14:35:17	292.47	1.15	14:42:42	335.19	1.32
14:36:27	242.97	0.95	14:43:02	292.71	1.15
14:36:57	270.69	1.06	14:43:12	243.69	0.96
14:37:42	313.53	1.23	14:43:17	243.69	0.96
14:37:52	374.28	1	14:43:22	379.02	1.49
14:37:57	374.28	1.47	14:43:27	210.03	0.83
14:38:17	270.69	1.06	14:43:32	335.25	1.32
14:38:22	270.69	1.06	14:43:37	290.73	1.14
14:39:02	206.76	0.81	14:43:42	214.92	0.84
14:39:47	206.76	0.81	14:43:47	214.92	0.84
14:40:32	206.76	0.81	14:43:52	514.95	2.02
14:41:02	206.76	0.81	14:43:57	313.62	1.23
14:44:02	364.74	1.43	14:47:27	438.12	1.72
14:44:07	364.74	1.43	14:47:32	438.12	1.72
14:44:12	363.03	1.43	14:47:37	314.76	1.24
14:44:27	243.6	0.96	14:47:42	348.12	1.37
14:44:42	406.02	1.59	14:47:47	270.3	1.06
14:44:47	199.8	0.78	14:47:52	270.3	1.06
14:45:02	215.07	0.84	14:48:02	297.36	1.17
14:45:07	280.59	1.1	14:48:12	514.29	2.02
14:45:12	270.48	1.06	14:48:17	514.29	2.02
14:45:17	460.17	1.81	14:48:22	311.67	1.22

Table C21 Water speed data at Sirindhorn hydropower operation 15 mw

MM/DD/YY 22/6/2011

Average water speed 1.3 m/s

Time	Flow rate m3/hr	Speed m/s	Time	Flow rate m3/hr	Speed m/s
15:20:17	481.48	1.89	15:22:02	337.92	1.33
15:20:22	481.48	1.89	15:22:07	236.75	0.93
15:20:27	341.55	1.34	15:22:12	275.09	1.08
15:20:32	341.55	1.34	15:22:17	275.09	1.08
15:20:37	150.51	0.59	15:22:22	576.96	2.27
15:20:42	269.45	1.06	15:22:27	195.64	0.77
15:20:47	269.45	1.06	15:22:32	260.25	1.02
15:20:52	271.18	1.07	15:22:37	260.25	1.02
15:20:57	271.18	1.07	15:22:42	260.25	1.02
15:21:02	424.78	1.67	15:22:47	152.74	0.6
15:21:07	314.42	1.24	15:22:52	259.85	1.02
15:21:12	339.7	1.33	15:22:57	506.67	1.99
15:21:17	359.08	1.41	15:23:02	506.67	1.99
15:21:22	251.19	0.99	15:23:07	422.19	1.66
15:21:27	251.19	0.99	15:23:12	422.19	1.66
15:21:32	307.56	1.21	15:23:17	378.25	1.49
15:21:37	251.99	0.99	15:23:22	372.47	1.46
15:21:42	422.44	1.66	15:23:27	324.74	1.28
15:21:47	422.44	1.66	15:23:32	324.74	1.28
15:21:52	464.65	1.83	15:23:37	273.1	1.07
15:21:57	267.09	1.05	15:23:42	258.75	1.02
15:23:47	213.41	0.84	15:26:02	256.06	1.01
15:23:52	394.61	1.55	15:26:07	283.38	1.11
15:23:57	394.61	1.55	15:26:12	280.36	1.1
15:24:02	349.46	1.37	15:26:17	280.36	1.1
15:24:07	378.67	1.49	15:26:22	485.83	1.91
15:24:12	274.58	1.08	15:26:27	485.83	1.91

Table C21(Cont.) Water speed data at Sirindhorn hydropower operation 15 mw

MM/DD/YY 22/6/2011

Average water speed 1.3 m/s

Time	Flow rate m3/hr	Speed m/s	Time	Flow rate m3/hr	Speed m/s
15:24:17	654.82	2.57	15:26:32	485.83	1.91
15:24:22	654.82	2.57	15:25:42	364.28	1.43
15:24:32	297.68	1.17	15:25:52	302.17	1.19
15:24:37	183.82	0.72	15:25:57	302.17	1.19
15:24:42	236.65	0.93	15:26:37	528.04	2.07
15:24:47	236.65	0.93	15:26:42	270.34	1.06
15:24:52	311.16	1.22	15:26:47	270.34	1.06
15:24:57	315.98	1.24	15:26:52	246.88	0.97
15:25:07	244.08	0.96	15:27:02	271.25	1.07
15:25:12	244.08	0.96	15:27:07	281.04	1.1
15:25:17	377.15	1.48			
15:25:22	377.15	1.48			
15:25:27	296.63	1.17			
15:25:32	296.63	1.17			
15:25:37	359.03	1.41			

Table C22 Water speed data at Sirindhorn hydropower operation 20 mw

MM/DD/YY 22/6/2011

Average water speed 1.32 m/s

Time	Flow rate m3/hr	Speed m/s	Time	Flow rate m3/hr	Speed m/s
15:35:22	533.92	2.1	15:37:12	462.42	1.82
15:35:27	309.63	1.22	15:37:17	354.96	1.39
15:35:32	309.63	1.22	15:37:22	372.67	1.46
15:35:37	438.84	1.72	15:37:27	272.16	1.07
15:35:42	406.95	1.6	15:37:32	591.98	2.33
15:35:47	388.56	1.53	15:37:37	591.98	2.33



Table C22 (Cont.) Water speed data at Sirindhorn hydropower operation 20 mw

MM/DD/YY 22/6/2011

Average water speed 1.32 m/s

Time	Flow rate m3/hr	Speed m/s	Time	Flow rate m3/hr	Speed m/s
15:35:52	388.56	1.53	15:37:42	295.1	1.16
15:35:57	219	0.86	15:37:47	307.38	1.21
15:36:02	351.41	1.38	15:37:52	185.18	0.73
15:36:07	150.08	0.59	15:37:57	185.18	0.73
15:36:12	333	1.31	15:38:02	326.36	1.28
15:36:17	333	1.31	15:38:07	371.91	1.46
15:36:27	355.78	1.4	15:38:17	250	0.98
15:36:32	269.33	1.06	15:38:22	285.52	1.12
15:36:37	261.72	1.03	15:38:27	285.52	1.12
15:36:42	257.46	1.01	15:38:32	343.13	1.35
15:36:47	257.46	1.01	15:38:37	335.79	1.32
15:39:02	172.55	0.68	15:41:22	351.45	1.38
15:39:07	156.66	0.62	15:41:27	293.83	1.15
15:39:12	156.66	0.62	15:41:32	170.25	0.67
15:39:17	443.97	1.74	15:41:37	304.84	1.2
15:39:22	358.4	1.41	15:41:42	304.84	1.2
15:39:27	198.09	0.78	15:41:47	278.57	1.09
15:39:32	246.64	0.97	15:41:52	301.99	1.19
15:39:37	274	1.08	15:41:57	757.76	2.98
15:39:42	274	1.08	15:42:02	440.48	1.73
15:39:47	417.89	1.64	15:42:07	440.48	1.73
15:39:52	272.63	1.07	15:42:12	548.38	2.15
15:39:57	425.44	1.67	15:42:17	226.46	0.89
15:40:02	425.44	1.67	15:42:22	259.04	1.02
15:40:07	205.49	0.81	15:42:27	418.06	1.64

Table C22(Cont.) Water speed data at Sirindhorn hydropower operation 20 mw

MM/DD/YY 22/6/2011

Average water speed 1.32 m/s

Time	Flow rate m <sup>3</sup> /hr	Speed m/s	Time	Flow rate m <sup>3</sup> /hr	Speed m/s
15:40:12	434.54	1.71	15:42:32	316.83	1.24
15:40:17	389.73	1.53	15:42:37	316.83	1.24
15:40:22	329.52	1.29	15:42:42	306.13	1.2
15:40:27	337.12	1.32	15:42:47	266.58	1.05
15:40:32	337.12	1.32	15:42:52	138.05	0.54
15:40:37	332.94	1.31	15:42:57	138.05	0.54
15:40:42	554.91	2.18	15:43:02	369.94	1.45
15:40:52	162.09	0.64	15:43:12	219.45	0.86
15:40:57	223.53	0.88	15:43:17	426.71	1.68
15:41:02	480.95	1.89	15:43:22	406.95	1.6
15:41:07	278.7	1.09	15:43:27	406.95	1.6
15:43:52	146.53	0.58	15:45:02	192.74	0.76
15:43:57	406.82	1.6	15:45:07	307.15	1.21
15:44:02	316.15	1.24	15:45:12	314.45	1.24
15:44:07	399.32	1.57	15:45:17	372.36	1.46
15:44:12	186.45	0.73	15:45:22	573.45	2.25
15:44:17	186.45	0.73	15:45:27	573.45	2.25
15:44:22	302.17	1.19	15:45:32	233.11	0.92
15:44:27	331.4	1.3	15:45:37	296.04	1.16
15:44:32	331.4	1.3	15:45:42	281.49	1.11
15:44:37	1308.62	5.14	15:45:47	440.96	1.73
15:44:42	517.91	2.03	15:45:52	440.96	1.73
15:44:47	428.76	1.68	15:45:57	260.19	1.02

Table C23 Water speed data at Sirindhorn hydropower operation 25 mw

MM/DD/YY 22/6/2011

Average water speed 1.37 m/s

Time	Flow rate m3/hr	Speed m/s	Time	Flow rate m3/hr	Speed m/s
15:52:22	297.81	1.17	15:53:37	318.14	1.25
15:52:27	297.81	1.17	15:53:42	218.37	0.86
15:52:32	253.09	0.99	15:53:47	218.37	0.86
15:52:37	253.09	0.99	15:53:52	218.37	0.86
15:52:42	253.09	0.99	15:53:57	496.3	1.95
15:52:47	278.01	1.09	15:54:02	416.86	1.64
15:52:52	337.44	1.33	15:54:07	416.86	1.64
15:52:57	337.44	1.33	15:54:12	281.41	1.11
15:53:02	347.84	1.37	15:54:17	337.46	1.33
15:53:07	435.71	1.71	15:54:22	337.46	1.33
15:53:12	263.14	1.03	15:54:27	226.2	0.89
15:53:17	263.14	1.03	15:54:32	326.2	1.28
15:53:22	375.32	1.47	15:54:37	226.2	0.89
15:55:02	595.56	2.34	15:56:07	225.7	0.89
15:55:07	496.28	1.95	15:56:12	325.7	1.28
15:55:12	418.02	1.64	15:56:17	485.45	1.91
15:55:17	358.67	1.41	15:56:22	357.32	1.4
15:55:22	358.67	1.41	15:56:27	476.37	1.87
15:55:27	714.65	2.81	15:56:32	278.01	1.09
15:55:32	450.87	1.77	15:56:37	258.08	1.01
15:55:37	436.7	1.72	15:56:42	258.08	1.01
15:55:42	436.72	1.72	15:56:47	201.08	0.79
15:55:47	222.09	0.87	15:56:52	574.02	2.25
15:55:52	222.09	0.87	15:56:57	258.06	1.01
15:57:02	258.06	1.01	15:58:32	271.41	1.07
15:57:07	396.84	1.56	15:58:37	276.01	1.08
15:57:12	205.39	0.81	15:58:42	377.7	1.48

Table C23(Cont.) Water speed data at Sirindhorn hydropower operation 25 mw

MM/DD/YY 22/6/2011

Average water speed 1.37 m/s

Time	Flow rate m3/hr	Speed m/s	Time	Flow rate m3/hr	Speed m/s
15:57:17	205.39	0.81	15:58:47	377.7	1.48
15:57:22	423.94	1.67	15:58:52	377.19	1.48
15:57:27	398.46	1.57	15:58:57	377.19	1.48
15:57:32	398.46	1.57	15:59:02	297.75	1.17
15:57:37	416.88	1.64	15:59:07	297.75	1.17
15:57:42	446.32	1.75	15:59:12	258.17	1.01
15:57:47	158.86	0.62	15:59:17	399.19	1.57
15:57:52	158.86	0.62	15:59:22	258.81	1.02
15:57:57	297.84	1.17	15:59:27	364.12	1.43
15:58:02	297.84	1.17	15:59:32	232.76	0.91
15:58:07	354.82	1.39	15:59:37	232.76	0.91
15:59:52	170.83	0.67	16:00:52	575.65	2.26
15:59:57	170.83	0.67	16:00:57	496.3	1.95
16:00:02	170.83	0.67			
16:00:07	218.48	0.86			
16:00:12	241.96	0.95			
16:00:17	241.96	0.95			
16:00:22	416.01	1.63			
16:00:27	416.01	1.63			
16:00:32	285.52	1.12			
16:00:37	694.83	2.73			
16:00:42	694.83	2.73			
16:00:47	454.65	1.79			

Table C24 Water speed data at Sirindhorn hydropower operation 31 mw

MM/DD/YY 22/6/2011

Average water speed 1.31 m/s

Time	Flow rate m3/hr	Speed m/s	Time	Flow rate m3/hr	Speed m/s
16:15:22	433.47	1.7	16:16:27	567.89	2.23
16:15:27	248.15	0.97	16:16:32	289.1	1.14
16:15:37	379	1.49	16:16:42	268.8	1.06
16:15:42	324.04	1.27	16:16:47	340.72	1.34
16:15:47	183.01	0.72	16:16:52	318.25	1.25
16:15:52	183.01	0.72	16:16:57	127.62	0.5
16:15:57	586.43	2.3	16:17:02	127.62	0.5
16:16:02	231.93	0.91	16:17:07	363.92	1.43
16:16:07	231.93	0.91	16:17:12	152.31	0.6
16:16:12	454.38	1.78	16:17:17	340.76	1.34
16:17:42	492.19	1.93	16:19:07	511.09	2.01
16:17:47	511.05	2.01	16:19:12	511.09	2.01
16:17:52	511.05	2.01	16:19:17	189.32	0.74
16:17:57	378.61	1.49	16:19:22	347.45	1.36
16:18:02	214.35	0.84	16:19:27	347.45	1.36
16:18:07	171.6	0.67	16:19:32	302.87	1.19
16:18:12	171.6	0.67	16:19:37	155.06	0.61
16:18:17	490.13	1.93	16:19:42	302.87	1.19
16:18:22	336.67	1.32	16:19:47	752.59	2.96
16:18:27	961.35	3.78	16:19:52	752.59	2.96
16:18:32	200.9	0.79	16:19:57	174.47	0.69
16:18:37	611.84	2.4	16:20:02	279.56	1.1
16:18:42	611.84	2.4	16:20:07	246.1	0.97
16:18:47	374.79	1.47	16:20:12	154.27	0.61
16:18:52	170.42	0.67	16:20:17	154.27	0.61
16:20:22	386.24	1.52	16:21:47	461.94	1.81
16:20:27	549.05	2.16	16:21:52	244.08	0.96

Table C24(Cont.) Water speed data at Sirindhorn hydropower operation 31 mw

MM/DD/YY 22/6/2011

Average water speed 1.31 m/s

Time	Flow rate m3/hr	Speed m/s	Time	Flow rate m3/hr	Speed m/s
16:20:32	646.52	2.54	16:21:32	318.06	1.25
16:20:37	162.72	0.64	16:21:37	318.06	1.25
16:20:42	397.53	1.56	16:21:42	362.53	1.42
16:20:47	397.53	1.56	16:21:17	316.5	1.24
16:20:52	340.86	1.34	16:21:22	200.3	0.79
16:20:57	170.46	0.67	16:21:27	204.66	0.8

Table C25 Water speed data at Sirindhorn hydropower operation 35 mw

MM/DD/YY 22/6/2011

Average water speed 1.48 m/s

Time	Flow rate m3/hr	Speed m/s	Time	Flow rate m3/hr	Speed m/s
16:30:27	288.71	1.13	16:31:32	340.77	1.34
16:30:32	851.83	3.35	16:31:37	375.28	1.47
16:30:37	851.83	3.35	16:31:42	289.6	1.14
16:30:42	605.22	2.38	16:31:47	528.11	2.07
16:30:47	214.85	0.84	16:31:52	528.11	2.07
16:30:52	233.21	0.92	16:31:57	528.11	2.07
16:30:57	206.45	0.81	16:32:02	255.64	1
16:31:02	359.06	1.41	16:32:07	293.26	1.15
16:31:07	359.06	1.41	16:32:12	413.76	1.63
16:31:12	610.14	2.4	16:32:17	494.05	1.94
16:31:17	248.5	0.98	16:32:22	494.05	1.94
16:31:22	258.52	1.02	16:32:27	213.78	0.84
16:31:27	340.77	1.34	16:32:32	408.85	1.61
16:32:37	300.06	1.18	16:34:02	442.96	1.74
16:32:42	300.06	1.18	16:34:07	415.21	1.63

Table C25(Cont.) Water speed data at Sirindhorn hydropower operation 35 mw

MM/DD/YY 22/6/2011

Average water speed 1.48 m/s

Time	Flow rate m3/hr	Speed m/s	Time	Flow rate m3/hr	Speed m/s
16:32:47	476.46	1.87	16:34:12	169.11	0.66
16:32:52	272.08	1.07	16:34:17	386.44	1.52
16:32:57	579.22	2.28	16:34:22	238.57	0.94
16:33:02	562.23	2.21	16:34:27	238.57	0.94
16:33:07	238.53	0.94	16:34:32	562.19	2.21
16:33:12	238.53	0.94	16:34:37	363.27	1.43
16:33:17	498.96	1.96	16:34:42	1138.88	4.47
16:33:22	148.06	0.58	16:34:47	249.8	0.98
16:33:27	388.1	1.52	16:34:52	249.8	0.98

Table C26 Water speed data at Sirindhorn hydropower operation 35 mw

MM/DD/YY 22/6/2011

Average water speed 1.48 m/s

Time	Flow rate m3/hr	Speed m/s	Time	Flow rate m3/hr	Speed m/s
16:33:32	388.1	1.52	16:34:57	365.14	1.43
16:33:37	243.04	0.95	16:35:02	190.08	0.75
16:35:27	213.97	0.84	16:36:52	352.85	1.39
16:35:32	270.06	1.06	16:36:57	352.85	1.39
16:35:37	270.06	1.06	16:37:02	455.39	1.79
16:35:57	341.48	1.34	16:37:22	255.56	1
16:36:02	409.41	1.61	16:37:27	379.15	1.49
16:36:07	409.41	1.61	16:37:32	374.96	1.47
16:36:12	494.01	1.94	16:37:37	442.89	1.74
16:36:17	459.97	1.81	16:37:42	340.56	1.34
16:36:22	415.78	1.63	16:37:47	340.56	1.34
16:36:27	415.78	1.63	16:37:52	271.59	1.07

Table C26 (Cont.) Water speed data at Sirindhorn hydropower operation 35 mw

MM/DD/YY 22/6/2011

Average water speed 1.48 m/s

Time	Flow rate m <sup>3</sup> /hr	Speed m/s	Time	Flow rate m <sup>3</sup> /hr	Speed m/s
16:36:32	303.02	1.19	16:37:57	187.5	0.74
16:36:37	272.61	1.07			
16:36:42	242.15	0.95			
16:36:47	476.98	1.87			

Table C27.1 Power coefficient at 82.6 RPM

Water speed 1.29 m/s

Load Level 1	RPM(PMG)	RPM(Rotor)	Volt,V	Amp., A	Power, Watts
1	189	88.2	15	2	60.0
2	173	80.7	18	3	108.0
3	177	82.6	19	3	114.0
4	186	86.8	16	3	96.0
5	188	87.7	21	3	126.0
6	187	87.3	17	3	102.0
7	204	95.2	16	3	96.0
8	189	88.2	17	3	102.0
9	146	68.1	20	4	160.0
10	187	87.3	21	4	168.0
11	163	76.1	20	3	120.0
12	196	91.5	19	3	114.0
13	177	82.6	20	3	120.0
14	167	77.9	20	3	120.0
15	179	83.5	14	1	28.0
16	167	77.9	19	3	114.0



Table C27.1 (Cont.) Power coefficient at 82.6 RPM

Water speed 1.29 m/s

Load Level 1	RPM(PMG)	RPM(Rotor)	Volt, V	Amp., A	Power, Watts
17	188	87.7	16	2	64.0
18	164	76.5	15	3	90.0
19	176	82.1	15	3	90.0
Average, RPM		82.6			105.3
TSR		3.6			
Cp		10.5			

Table C7.2 Power coefficient at 93.3 RPM

Water speed 1.29 m/s

Load Level 2	RPM(PMG)	RPM(Rotor)	Volt, V	Amp., A	Power, Watts
1	183	85.4	14	3	84.0
2	207	96.6	15	3	90.0
3	200	93.3	13	3	78.0
4	192	89.6	18	3	108.0
5	179	83.5	20	4	160.0
6	192	89.6	18	4	144.0
7	195	91.0	18	4	144.0
8	186	86.8	19	4	152.0
9	188	87.7	14	3	84.0
10	271	126.5	16	4	128.0
11	179	83.5	15	3	90.0
12	193	90.1	14	3	84.0
13	203	94.7	18	4	144.0
14	223	104.1	15	3	90.0
15	198	92.4	16	3	96.0

Table C27.2 (Cont.) Power coefficient at 93.3 RPM

Water speed 1.29 m/s

Load Level 2	RPM(PMG)	RPM(Rotor)	Volt,V	Amp., A	Power, Watts
16	209	97.5	18	4	144.0
17	198	92.4	17	4	136.0
18	201	93.8	19	4	152.0
19	198	92.4	24	5	240.0
20	205	95.7	16	4	128.0
	Average, RPM	93.3			123.8
	TSR	4.0			
	Cp	12.3			

Table C27.3 Power coefficient at 102.8 RPM

Water speed 1.29 m/s

Load Level 3	RPM(PMG)	RPM(Rotor)	Volt,V	Amp., A	Power, Watts
1	215	100.3	17	4	136.0
2	191	89.1	21	3	126.0
3	220	102.7	24	4	192.0
4	256	119.5	19	4	152.0
5	207	96.6	17	3	102.0
6	210	98.0	20	4	160.0
7	213	99.4	18	3	108.0
8	196	91.5	25	4	200.0
9	217	101.3	19	4	152.0
10	257	119.9	18	4	144.0
11	255	119.0	15	3	90.0
12	233	108.7	19	3	114.0



**VITAE**

<b>NAME</b>	Mr. Palapum Khunthongjan
<b>BIRTHDATE</b>	July 27, 1967
<b>EDUCATION</b>	Bachelor's degree in Mechanical Engineering, Ubon Ratchathani University (1992) Master's degree in Mechanical Engineering, Ubon Ratchathani University (2005)
<b>EMPLOYER</b>	Sirindhorn Hydropower Department, Electricity Generating Authority of Thailand
<b>POSITION</b>	Engineer
<b>WORK EXPERIENCE</b>	2006-Present Sirindhorn Hydropower Department, Electricity Generating Authority of Thailand 2002-2005 Lan Krabue Thermal Power Construction Project, Electricity Generating Authority of Thailand 1997-2001 Krabi Thermal Power Construction Project, Electricity Generating Authority of Thailand 1996-1997 Wang Noi Thermal Power Construction Project, Electricity Generating Authority of Thailand 1992-1996 Mae Moh Thermal Power Construction Project, Electricity Generating Authority of Thailand
<b>HOME ADDRESS</b>	223 Moo 9 Thumbon Non-Phuang, Warin Chamrap District Ubon Ratchathani Province 34190
<b>TELEPHONE</b>	(66)45-267658; (66)81-9994396
<b>E-MAIL</b>	palapum.k@egat.co.th, pakhunthongjan@gmail.com